

Fundamentally Structural Characteristics of Integral Bridges

メタデータ	言語: eng 出版者: 公開日: 2017-10-05 キーワード (Ja): キーワード (En): 作成者: メールアドレス: 所属:
URL	http://hdl.handle.net/2297/9646

Fundamentally Structural
Characteristics of Integral Bridges

Hiroshi AKIYAMA

January 2008

D i s s e r t a t i o n

Fundamentally Structural
Characteristics of Integral Bridges

Graduate School of
Natural Science & Technology
Kanazawa University

Major Subject:

Environmental Science & Engineering

Course:

Environment Creation Course

School Registration No. 0523142401

Name: Hiroshi AKIYAMA

Chief Advisor: Prof. Yasuo KAJIKAWA

CONTENTS

Chapter 1 Introduction

1.1 Integral Bridge Concept	-----	1
1.2 Contents of Dissertation	-----	4
1.3 Definitions of Terms Related to Integral Bridge	-----	5
References	-----	11

Chapter 2 State of Art of Integral Bridge Construction

2.1 Introduction	-----	13
2.2 State of Art of Integral Bridges in Japan	-----	13
2.3 State of Art of Integral Bridges in the U.K.	-----	21
2.4 State of Art of Integral Bridges in U.S.A.	-----	23
2.5 State of Art of Integral Bridges in Canada	-----	15
2.6 State of Art of Integral Bridges in Europe	-----	30
2.7 Conclusion	-----	35
References	-----	36

Chapter 3 Static Characteristics of Integral Bridges

3.1 Introduction	-----	39
3.2 Temperature Effects	-----	39
3.3 Shrinkage Effects	-----	42
3.4 Creep Effects	-----	43
3.5 Earth Pressure	-----	45
3.6 Soil Structure Interaction of Integral Abutment	-----	47
3.7 Case study on Static Behaviour of Single Span Integral Bridge - A Study on the Long Span Integral Bride for Longitudinal Movement, Constraint Stress and Prestressing Efficiency -	-----	49
3.8 Case Study on Static Behaviour of Multiple Spanned Integral Bridge with Curvature in Plan	-----	55
3.9 Conclusion	-----	68
References	-----	69

Chapter 4 Seismic Design of Integral Bridges

4.1 Introduction	-----	71
4.2 Displacement Based Design Concept	-----	73
4.3 Case Study on Single Span Integral Bridge	-----	82
4.4 Conclusion	-----	88
References	-----	87

Chapter 5 Vibrational Serviceability of Integral Bridges

5.1 Introduction	-----	89
5.2 General Description of the Numerical Study	-----	92
5.3 Static Analysis	-----	96
5.4 Eigen-value Analysis	-----	97
5.5 Dynamic Response Analysis		
- Serviceability for Pedestrians -	-----	101
5.6 Dynamic Response Analysis		
- Infrasound -	-----	105
5.7 Dynamic Response Analysis		
- Ground Vibration -	-----	107
5.8 Conclusion	-----	109
References	-----	111

Chapter 6 Application of High Performance Lightweight Aggregate Concrete to Integral Bridge

6.1 Introduction	-----	113
6.2 Fundamental Properties of HLA and HLAC	-----	115
6.3 Confining Effect of HLAC under Axial Pressure Load	-----	125
6.4 Serviceability of HLAC Single Span Bridges with different types of structural systems	-----	136
6.5 Conclusion	-----	156
References	-----	158

Chapter 7 Conclusion

7.1 Conclusion ----- 161

7.2 Vista ----- 163

7.3 Feature Assignment ----- 163

EPILOGUE ----- 165

ACKNOWLEDGEMENT ----- 167

Chapter 1 Introduction

1. Integral Bridge Concept

1.1 Need for Integral Bridge Study

Needless to say, the function of bridge is crossing the departed sides. Mankind has been constructed numerous bridges; bridge engineering has been developing along with their history. Even ancient age, a number of large scale structures were constructed without modern structural engineering. Some remarkable structures have served against aging, environmental effects and turbulences as wars for thousands of years (*Photo 1. 1*) [1-1] .



Photo 1. 1: Pont du Gard (Gard département, France)

Modern and recent development in structural engineering have accomplished various form of structural design, mile-scale span, hybrid structure, sophisticated seismic design e.g. isolation design etc. The development in structural engineering is urged by numerical approach, industrialised fabrication and developments in construction materials. In particular, structural mechanics and numerical analysis made it possible to conduct various structural analyses; even highly complex phenomena can be simulated by the technology of structural analysis.

By the way, structural analysis is conducted by idealising actual structures into simplified structural models. In a sense, the achievement of structural engineering in design has developed with simplified modelling of the structural systems; in this way, bearings and expansion joints have been essential to implement the assumed behaviour of simplified and idealised structural models.

In spite of the development of the analytical technology that enables complex structural design, however conventional simplified structural systems, e.g. simply supported bridges with bearings and expansion joints at both abutments, are still employed to numerous bridges in accustomed manner of practice (*Fig. 1.1*).



Fig. 1.1: Simply supported bridge

These kinds of modern bridges with simplified structural system have been ironically suffered from maintenance issues for their modernised bridge accessory devices. Failed expansion joints by fatigue, leaked expansion joints and corroded bearings are representative phenomena for maintenance problems of modernised form of bridge systems. These kinds of problems are increasingly loading the cost and effort for the maintenance of bridges along with the stock of infrastructure in the aging society with declining birth rate. Because approximately the same amount of money spent on bridge construction is required to maintain it during its lifetime. The issue is recognised among many people concerned with infrastructure.

Thus, the rationalisation and sophistication of bridge maintenance is essential to resolve the issue. In these circumstances, a simple idea to eliminate the modernised accessory devices so far as possible would be reasonable as a countermeasure for the issue. Integral bridge solution would be supposed an answer for the problems. It is also focused in European countries and North America over recent years for same reasons. Integral bridge is characterised by a monolithic articulation between deck and abutment (*Fig. 1.2*). Bearings and expansion joints can be

therefore eliminated or reduced to the minimum and the superstructure acts as a single structural unit. This gives a remarkably increased redundancy with improved response towards seismic and other extreme events.

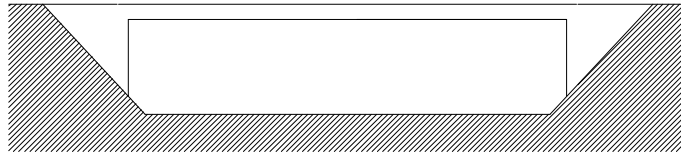
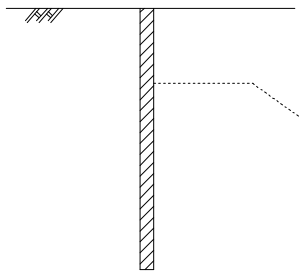
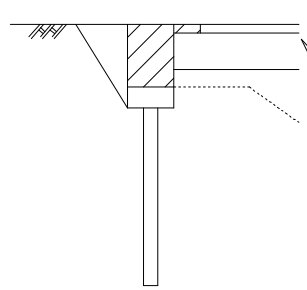


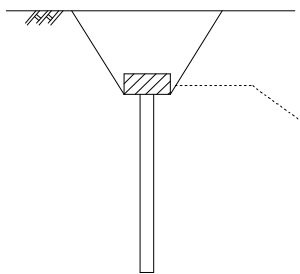
Fig. 1.2: Integral bridge



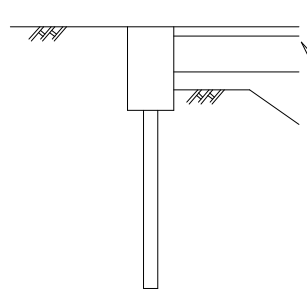
Step1: Drive Piles



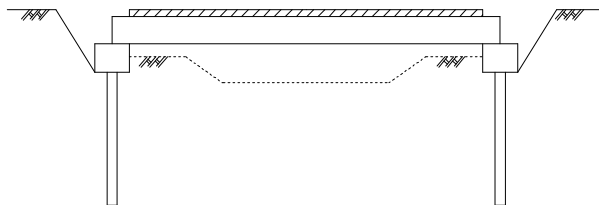
Step4: Cast upper part of pile caps



Step2: Cast lower part of pile caps



Step5: Earth works



Step3: Place steel/precast beams and cast deck

Fig. 1.3: Construction procedure of integral bridge using steel/precast prestressed concrete beams

Steel and prestressed concrete beams are usually employed for integral bridge construction in the U.K., U.S.A and Canada. The industrialised manner of construction with prefabricated beams enables the popularisation of integral bridge construction for its economical aspect and short construction period.

The standard integral bridge construction procedure using steel/prestressed concrete beams is shown in *Fig. 1.3*.

Since integral bridge constrains the longitudinal movement of temperature change, shrinkage, creep etc., the range of applicable bridge length is limited to short and middle long bridges. However, majority of the bridges are such short and middle long bridges; integral bridge diffusion would give eminent benefits to the society.

Thus, the study on integral bridge is highly beneficial for bridge engineering. The supreme aim of this study is wide diffusion of integral bridges.

The scope of the study on this dissertation is to grasp the fundamentally structural characteristics in comprehensive fields to urge the wide range of studies as a clue. The study was conducted on following aspects.

- state of art
- static characteristics
- seismic design (toward displacement based design)
- vibrational serviceability
- application of high performance lightweight aggregate concrete to extend the range of integral bridge solution

1.2 Contents of Dissertation

This dissertation comprises seven chapters. It comprehensively discusses the fundamentally structural characteristics of integral bridges.

State of art of integral bridge construction is described in Chapter 2 with the information of foreign countries.

Static behaviour of integral bridges is discussed in Chapter 3 for primary load with case study on single span integral bridge and multiple spans continuous curved bridge.

Seismic design of integral bridge is discussed in Chapter 4, mainly for

the approach toward displacement based design for integral bridge. Vibrational serviceability under traffic load on single span integral bridge is discussed with comparison among four different types of structural systems by numerical approach in Chapter 5. The compared structural systems are conventionally simply supported bridge, extended deck bridge, semi-integral bridge and integral bridge. Desirable extended deck length for vibrational control is also discussed.

The approach toward the extension of the range of integral bridge application by high performance lightweight concrete is discussed in Chapter 6. The fundamental material properties, e.g. creep and shrinkage, of high performance lightweight aggregate (HLA) and high performance lightweight aggregate concrete (HLAC) are discussed with experimental approach. The confining effects of HLAC are discussed with the experiments. Novel numerical model to estimate the stress-strain relationship of confined HLAC is proposed. Vibrational serviceability of integral bridges with HLAC is also discussed with comparison to the counterparts of normal concrete.

The conclusion, vista and feature assignment of the studies are discussed in Chapter 7.

1.3 Definitions of Terms Related to Integral Bridge

The follows are the definitions of the terms related with integral bridges.

- (1) Asphaltic Plug Joint
An in situ joint in the pavement, comprising a band of specially formulated flexible material which may also form the surfacing.
- (2) Abutment
The part of a bridge structure that abuts the roadway pavement and formation at the end of a bridge.
- (3) Bank Pad Abutment
Bank seat end support for bridge constructed internally with deck, acting as a shallow foundation for end span as a shallow retaining wall for adjoining pavements and embankment (*Fig. 1.4*).

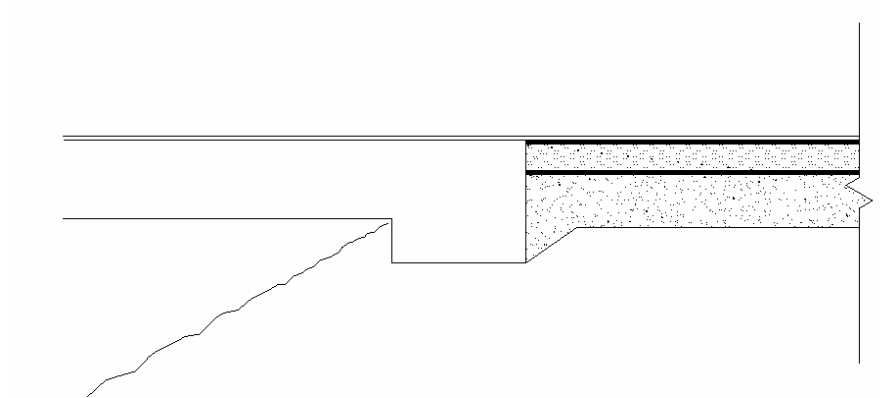


Fig. 1.4: Bank pad abutment

(4) Embedded Abutment

End support for bridge comprising a diaphragm wall (including contiguous, or secant or sheet pile walls) with toe embedded in ground below lower ground surface (*Fig. 1.5*).

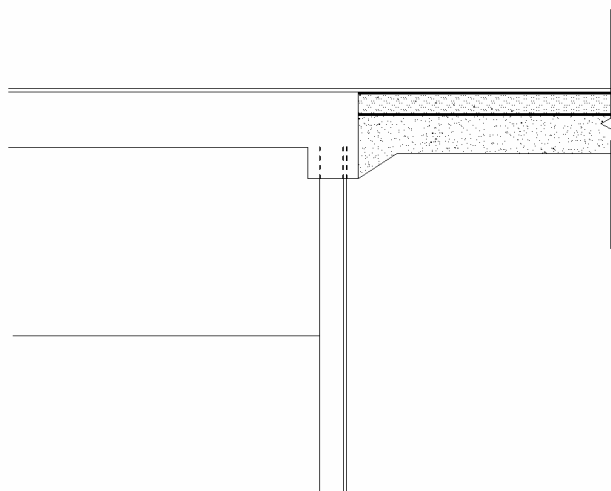


Fig 1.5: Embedded abutment

(5) End Screen Abutment

Wall structure cast monolithic with and supported off the end of bridge deck providing retaining wall for adjoining ground, but not acting as a support for vertical loads (*Fig. 1.6*).

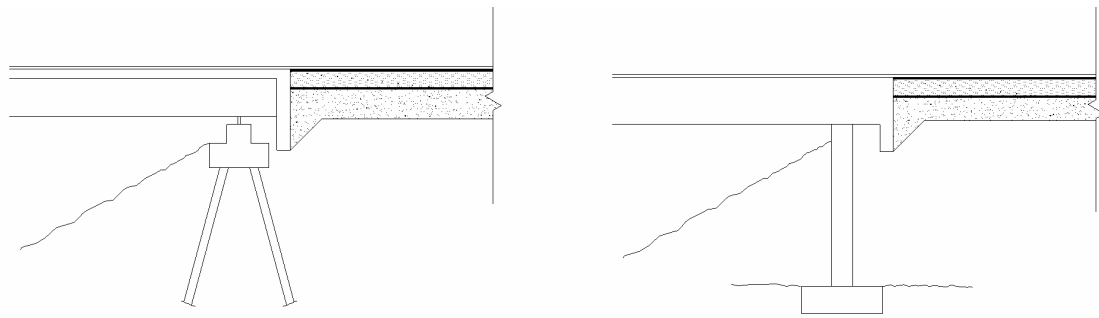


Fig. 1.6: End screen abutment

(6) Extended Deck/Deck Extension

A deck which is extended continuously forward approach with expansion joint at the end of the extended deck (*Fig. 1.7*).

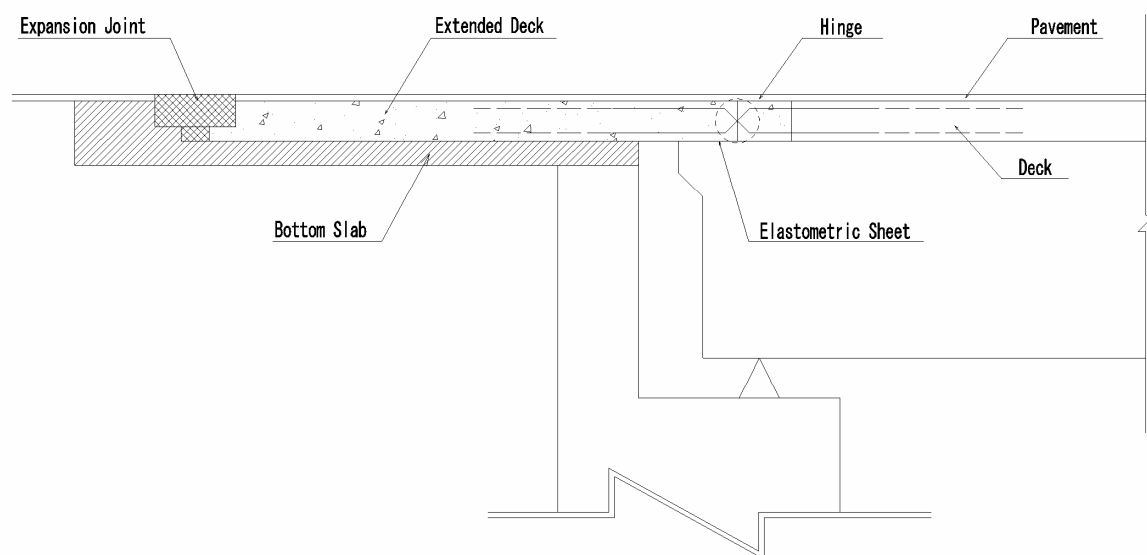


Fig. 1.7: Example of extended deck detail

(7) Frame Abutment

End support for bridge constructed integrally with the deck and acting as a retaining wall for adjoining pavement and ground below (*Fig. 1.8*).

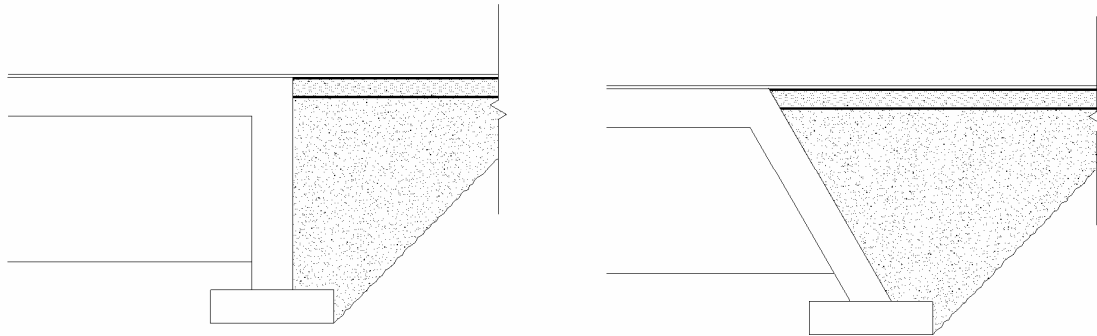


Fig. 1.8: Frame abutment

(8) Granular Backfill

Selected granular material placed adjacent to the abutment wall and forming the subgrade for the adjoining pavement construction.

(9) Integral Abutment

Bridge abutment which is connected to the bridge deck without any movement joint for expansion or contraction of the deck (*Figs. 1.9 and 1.10*).

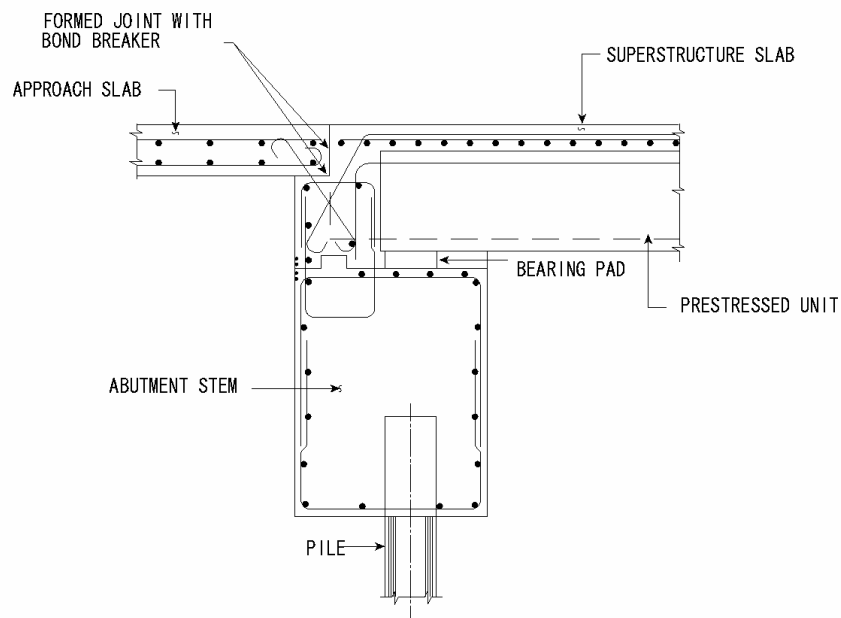


Fig. 1.9: Prestressed concrete superstructure integral abutment

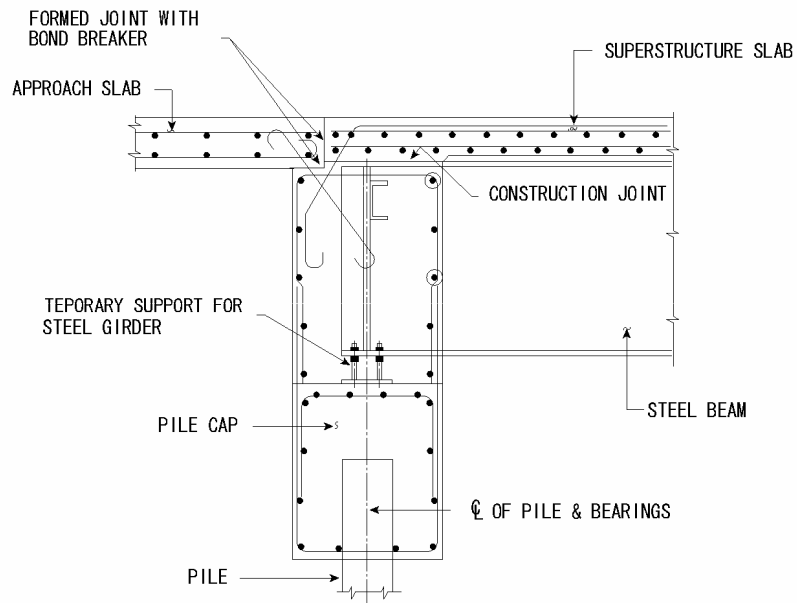


Fig. 1.10: Steel superstructure integral abutment

(10) Integral Bridge

A bridge with integral abutments (Fig. 1.11).

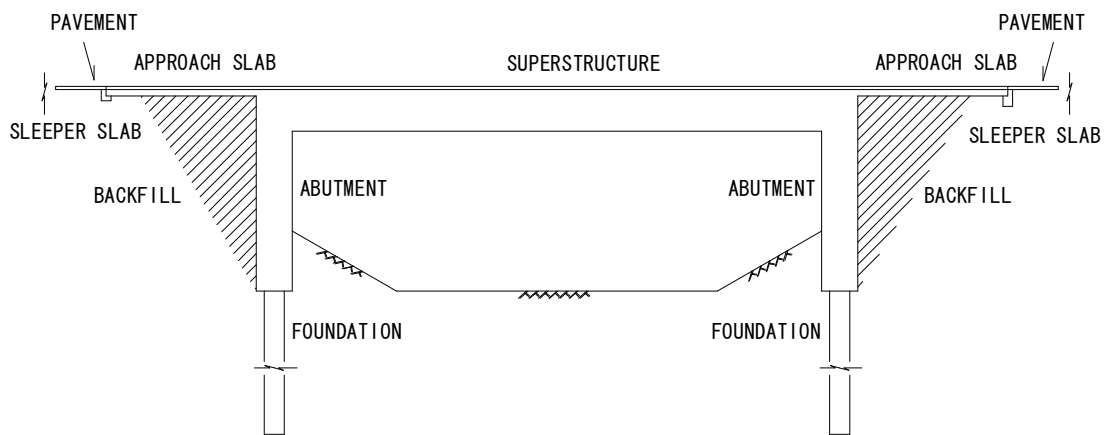


Fig. 1.11: Elevation of typical integral bridge

(11) Pavement/Abutment Interface

The interface between the pavement construction and back face of the abutment.

(12) Range

Change (of temperature, strain) between extreme minimum and extreme maximum.

(13) Semi-Integral Bridge

A bridge which has bearings beneath the short piers on the abutments without expansion joints (*Fig. 1.12*).

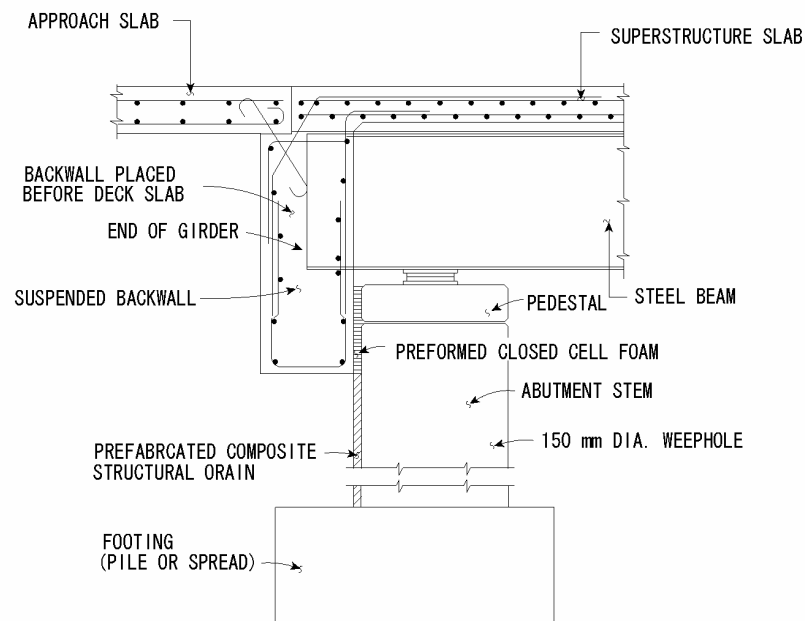


Fig. 1.12: Semi-integral abutment

(14) Stationary Point

The point on a bridge in plan which does not move when the bridge experiences expansion or contraction during changes in bridge temperature.

(15) Sub-surface Drainage

A system for draining water from water from within the surfacing.

(16) Surface

The carriageway or footway surface.

(17) Surfacing

Carriageway or footway wearing course and base course materials.

References

- [1-1] http://fr.wikipedia.org/wiki/Pont_du_Gard
- [1-2] BURKE M.P.Jr. *Integral Bridges - Attributes and limitations*, Transp. Res. Rec. 1993, pp.1-8, Transportation Research Board, 2003.
- [1-3] POTZL, M., SCHLAICH, J. *Robust Concrete Bridges without Bearings and Joints*, Structural Engineering International, Vol.6, No.4, International Association for Bridge and Structural Engineering, Zurich, pp.266-268, Dec. 1996.

Chapter 2 State of Art of Integral Bridge Construction

2.1 Introduction

Integral bridge construction is widely employed and developed in many countries. Especially, numerous integral bridges have been constructed and maintained for decades in U.S.A., the U.K., and Canada.

Since integral bridge construction is not popular in Japan compared with above countries, the research of state of art over recent years in foreign countries would be of good use to consider feature design and construction of integral bridges in Japan.

Hereinafter state of art of integral bridges in each country and region is described including present situation in Japan.

2.2 State of Art of Integral Bridges in Japan

2.2.1 Design Codes

Although integral bridges in Japan are not popular compared with the U.K. and North America, they are increasingly employed in expressway and highway bridges. The major reasons of the boost of the integral bridge application are cost efficiency and maintenance friendliness.

Specifications for Highway Bridges and *Design Standards of Railway Structures* neither specify nor refer to the integral bridges and integral abutments [2-1, 2-2].

However, NEXCO companies (East, Central and West Nippon Expressway Corporation) specify the single span integral bridge, so-called portal rigid frame bridge, in their *Design Guidelines Part II* [2-3]. It specifies the follows.

- Skews:
Skews shall be basically 0° , however they can be allowed up to 15° when skewed condition is inevitable.
- Earth pressure:
One side earth pressure shall be considered for each abutment; Coulomb earth pressure model shall be employed. Surcharge load by live load for earth pressure calculation shall be assumed as $0,01 \text{ N/mm}^2$.
- Structural modelling
- Allowable crack width(*Table 2.1*):

Table 2.1: Allowable crack width (mm)

Type of member	Allowable crack width	Remarks
Upper edge of abutment	0,0035C	C: cover
Other members	0,0050C	

- Redistribution of stress after cracking:
The stress of upper edge of tensile reinforcement shall be taken as 110 % of the calculated value by elastic analysis.
- Structural details
- Construction procedure and its attentions

On the other hand, Public Works Research Centre and Nippon Steel Corporation have proposed *Guidelines for Planning of Steel Integral Bridges (draft)* [2-4]. The Guidelines does not scope only single span integral bridges, but also multiple span bridges. It specifies the follows.

- Approximate applicable bridge length is up to ca. 50 m.
- Skew should be basically 0°.
- Single row pile foundation is recommended for its little constraint of displacement and stress.
- Modelling for structural design
- Earth pressure
- Structural details
- Construction procedure and its attentions

2.2.2 Examples of Actual Integral Bridges in Japan

(1) Kujira Bridge

Kujira bridge is 107 m long prestressed concrete single span integral bridge, constructed as a foot bridge in the east district of Tama New Town, located in the outskirts of Tokyo Metropolitan (*Photo 2.1*) [2-5, 2-6].

The span length, 100,5 m, is the longest among single span prestressed concrete bridges in Japan (*Figs. 2.1 and 2.2*). The bridge comprises roundly curved "ship bottom" shaped 4-cell multiple girder that was determined for the aesthetic reason.

The author engaged in structural design and construction; it completed in June 1997.

The author made field visual inspection for the bridge in May 2007, approximately 10 years later from the completion.

Although there pavement cracks has appeared at the both ends of the approach slabs (*Photo 2.2*), they do not obstacles any serviceability as a foot bridge. In addition, there is no prominent deterioration nor cracks appeared in the structural members as of the day of 10 years since the inauguration.

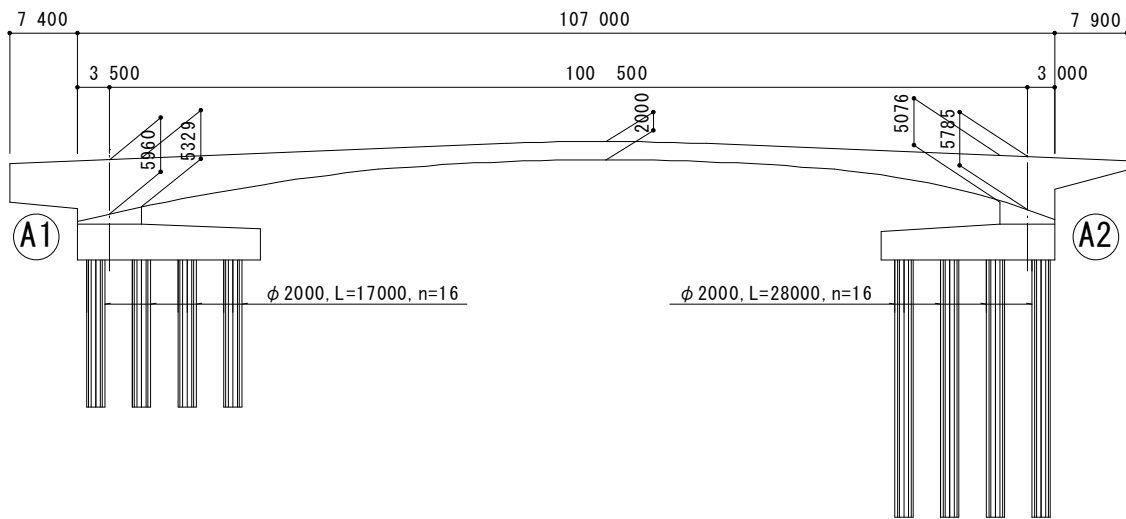


Fig. 2.1: Elevation of Kujira Bridge

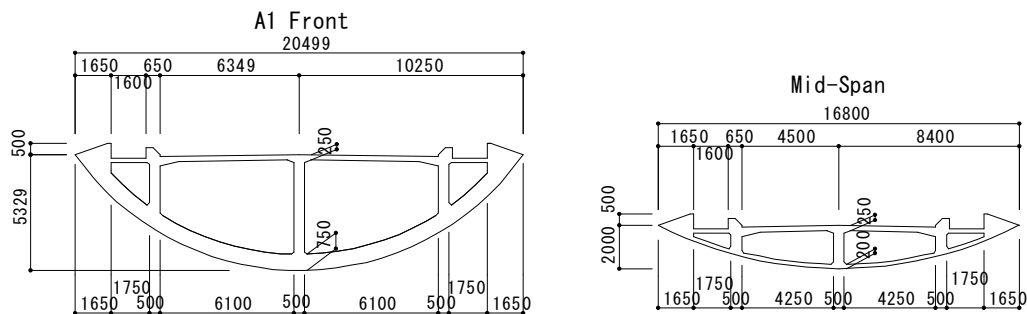


Fig. 2.2: Cross section of Kujira Bridge



Photo 2.1: General view of Kujira Bridge



Photo 2.2: Crack of pavement at the end of approach slab of Kujira Bridge

(2) Koitogawa Bridge, Tateyama Expressway

Multiple span integral bridges have also employed over recent years in expressway construction. For instance, Koitogawa Bridge, Tateyama Expressway is 120,8 m long 2 spans continuous integral bridge with rigid articulation at intermediate pier and both abutments (*Photo 2.3, Figs. 2.3 and 2.4*).

The superstructure is single cell box girder prestressed concrete structure. The foundations comprise cast-in-situ multiple rows piles to secure seismic resistance. Cement treated soil is employed for the backfill to enlighten the earth pressure on the abutment stems and to avoid the settlement of approach backfill.

The design and construction was performed based on *Design Guidelines Part II* of East Nippon Expressway Corporation.

Generally, seismic design for abutment and integral bridge is conducted by static method only for level 1 earthquake for the damping effect of backfill soil of the abutments. However, seismic design by ductility design method was conducted for level 2 earthquakes in this case, since cement treated soil was employed for the backfill of the abutments in this bridge construction.



Photo 2.3: Koitogawa Bridge, Tateyama Expressway (Chiba pref.)

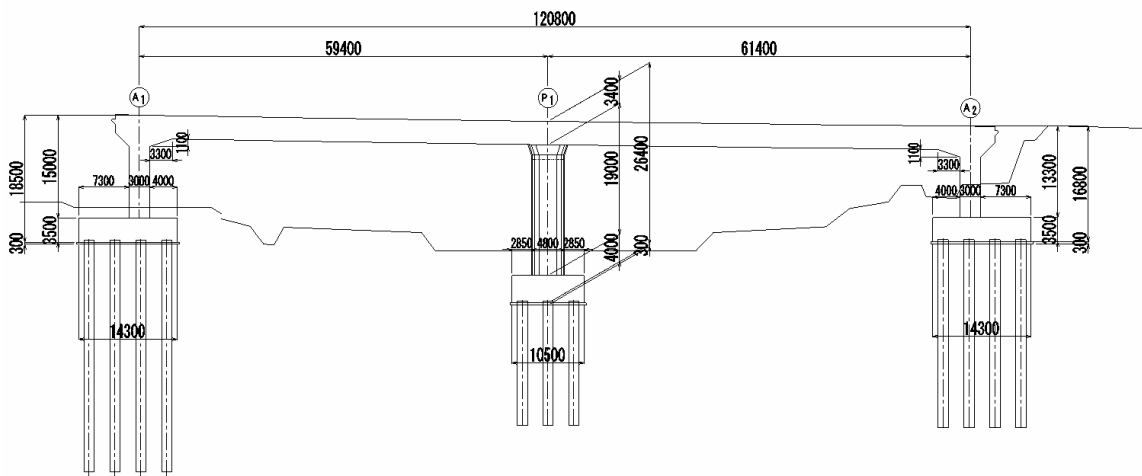


Fig. 2.3: Elevation of Koitogawa Bridge, Tateyama Expressway (Chiba pref.)

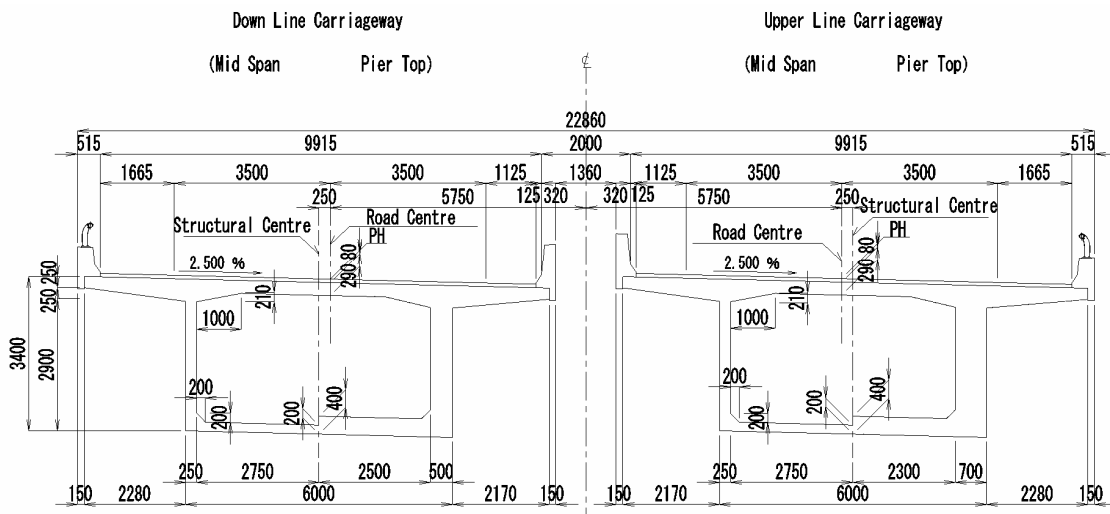


Fig. 2.4: Cross sections of Koitogawa Bridge, Tateyama Expressway (Chiba pref.)

(3) Recent Development of Composite Slab Integral Bridge with H Shaped Steel Beam

- Kuratsuki Flume Bridge, Kanazawa Port -

Integral bridge with H shaped steel beam composite slab is recently developed. The benefits of the composite slab bridge are rapid construction period, low construction cost, maintenance friendliness and easy constructionability. This type of bridge is increasingly employed for short span bridges.

Kuratsuki Flume Bridge, Kanazawa Port is an example of integral bridge construction using composite slab with H shaped steel beam (*Photo 2.4*). The bridge located in Kanazawa City was completed in Dec. 2006. The overall bridge length and span length are 9,2 m and 7,7 m with 10,0 m width. The foundation comprises single row steel piles, 4 piles in each row.

The elevation and cross section of the bridge is shown in *Figs. 2.5* and *2.6*.



*Photo 2.4: Kuratsuki Flume Bridge, Kanazawa Port (Ishikawa pref.)
(By favour of Mitsuhiro TOKUNO)*

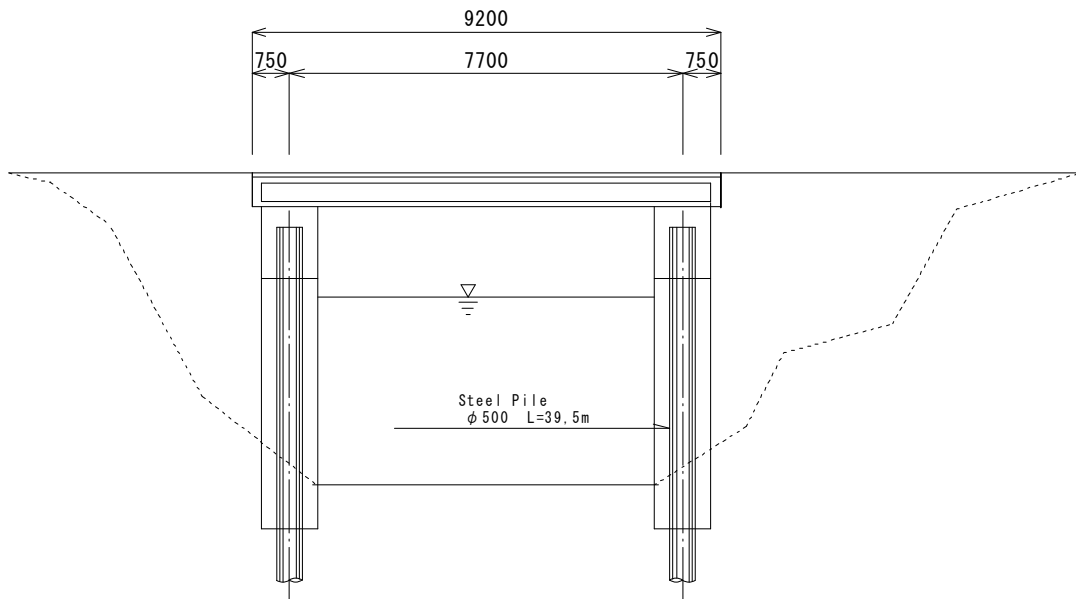


Fig. 2.5: Elevation of Kuratsuki Flume Bridge, Kanazawa Port

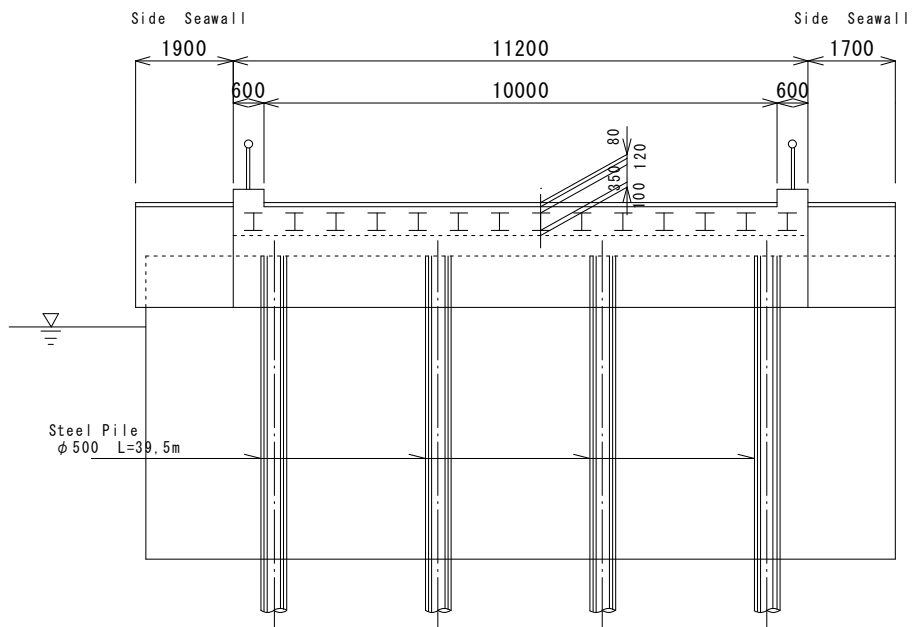


Fig. 2.6: Cross section of Kuratsuki Flume Bridge, Kanazawa Port

2.3 State of Art of Integral Bridges in the U.K.

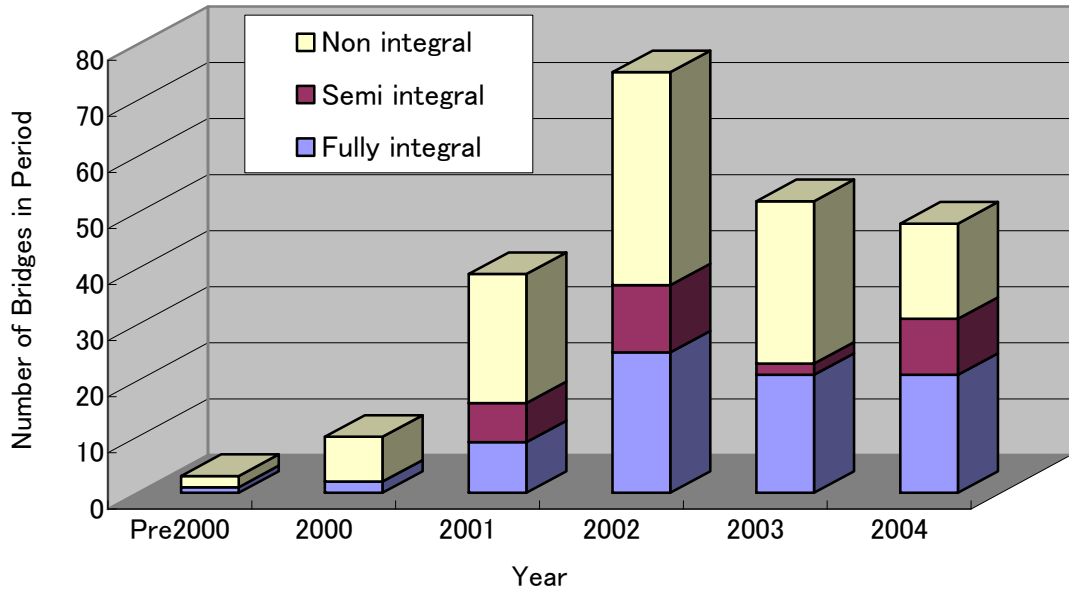
Integral bridges have become increasingly popular in the U.K. over recent years. Problems and costs associated with failed expansion joints in conventional bridges do not only make integral bridges a cost-effective option but also mean they have longer life spans than their counterparts. Expansion joints are supposed to be prone to leak and to allow ingress of de-icing salts into the bridge deck and substructure, thereby resulting in severe durability problems.

The Highways Agency of the U.K. requires to consider the feasibility of integral bridge as the first choice of the selection of the structural system of the bridge that does not exceed 60 m overall bridge length and 30° of skew angle.

The Highways Agency of the U.K. established DB57 *Design for Durability* in 1995 and DB42 *The Design Manual for Road and Bridges* (hereinafter called "*The Design Manual*") to respond to the direction in DB57 [2-7]. The Design Manual specifies as follows.

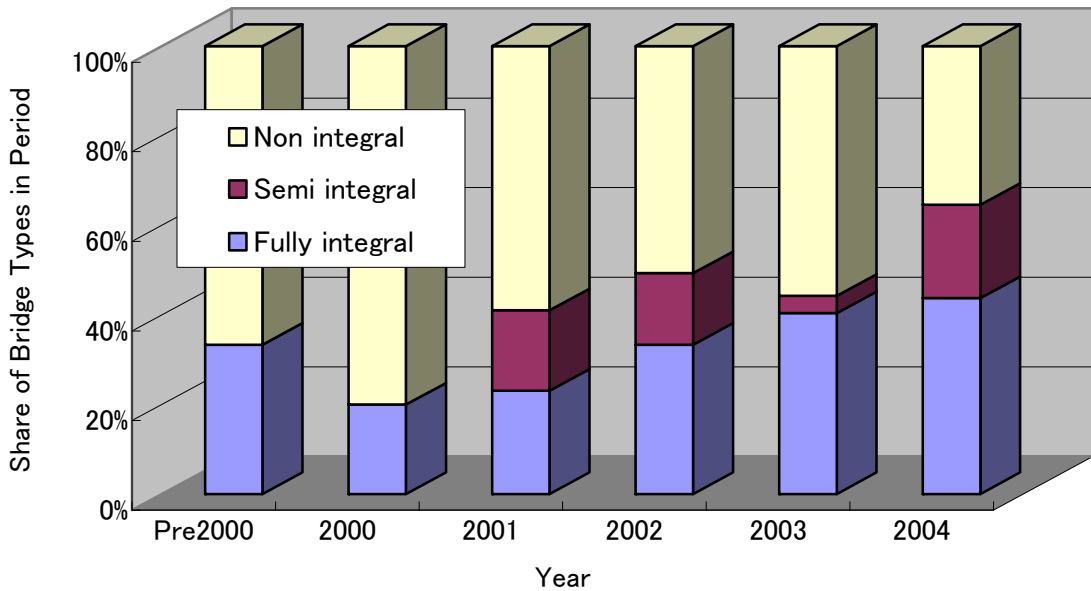
- Bridge Length: All new bridges of less than 60 m length should be of integral bridge wherever possible.
- Skew: not exceed 30°
- Thermally induced movement: not exceed ± 20 mm
- Full height frame abutments of overall length: not exceed 15 m

The survey of recent practice revealed that designers are designing fully integral bridges with skews up to or slightly above this value, but semi-integral bridges are rarely designed with skew above ca. 20°. The steelwork for the majority of highway bridges in the U.K. is fabricated by one particular fabricator. This fabricator agreed to provide SCI (Steel Construction Institute) with data about the sizes and types of bridge fabricated between 2000 and 2005, identifying in each case whether the bridge was integral or not. The data was analysed and an overall summary is presented in *Figs. 2.7* and *2.8*. The data shows the increasing trend of integral and semi-integral bridge construction.



Summary of Bridge Types by Date

Fig. 2.7: Summary of bridge types by date in number of bridges



Summary of Bridge Types by Date

Fig. 2.8: Summary of bridge types by date in share

2.4 State of Art of Integral Bridges in U.S.A.

Integral bridge construction is most energetic and prosperous in U.S.A. for the struggle and endeavour in many projects to develop and improve the integral bridge construction and maintenance. The accomplishments in U.S.A. for integral bridges are widely referred to foreign countries. The situations of integral bridges in U.S.A. are not simply discussed for their administrative reason, since the policies of the infrastructure plan, design, construction and maintenance are fundamentally based on each DOT's (Department of Transportation) decisions. In general, integral bridges are widely applied to highway bridge construction with positive evaluation.

The survey summary of *Integral Abutment and Jointless Bridge in 2004* by FHWA (IAJB 2004 Survey) reported the follows [2-8].

The purpose of the survey was to obtain a snapshot of current practices, policies and design criteria being employed nationally.

The survey included questions regarding the number of integral abutments designed, built and in service, the criteria used for design and construction, including span lengths, total bridge length, skew and curvature limitations imposed as well as any reported problems experienced with jointless bridge construction.

According to the 39 agencies who responded to the survey, there are approximately 13.000 jointless bridges on public highways; 9.000 equipped with fully integral abutments and 4.000 with semi-integral abutments (integral superstructure/backwall connections that move according to the thermal demands, but independent of the vertical load support system) (*q.v. Table 2.2*).

The aggregate number of jointless bridges is twice the number reported in a similar survey for a previous Integral Abutment Jointless Bridge Conference held in 1995.

Analysis of the survey found that there was a lack of uniformity in usage and ranges of applicability. For instance, 59 percent of responding agencies had over 50 jointless bridges in service, 31 percent had from 101 to 500 in service, 3 percent had from 501 to 1.000 and 15 percent had over 1.000 such bridges in service.

Permissible lengths for jointless prestressed concrete girder bridges ranged from 45,7 m to 358,2 m, allowable skews from 15 ° to 70 ° and

Table 2.3: Range of design criteria used for selection of integral abutments

		Steel Girder Bridge			Prestressed Concrete Bridge		
Maximum Span (m)	Full Integral	19,8	-	91,4	18,3	-	61,0
	Semi Integral	19,8	-	61,0	27,4	-	61,0
	Deck Extension	24,4	-	61,0	27,4	-	61,0
	Integral Piers	30,5	-	91,4	36,6	-	61,0
Total Length (m)	Full Integral	45,7	-	198,1	45,7	-	358,1
	Semi Integral	27,4	-	152,4	27,4	-	999,7
	Deck Extension	61,0	-	137,2	61,0	-	228,6
	Integral Piers	45,7	-	304,8	91,4	-	121,9

Some states specify the limit of horizontal abutment movement as shown in Table 2.4.

Table 2.4: Limit of horizontal abutment movement

	With approach slab	Without approach slab	Remarks
California	±25,4mm (±1,0 inch)	±12,7mm (±0,5 inch)	at top of abutment
Tennessee	±25,4mm (±1,0 inch)	-	at pile cap

FHWA (Federal Highway Agency) and NHI (National Highway Institute) established and published *LRFD Design Example for Steel Girder Superstructure Bridge* [2-9] and *Comprehensive Design Example for Prestressed Concrete Girder Superstructure Bridge with Commentary* [2-10]. They refer to the selection of the type of abutment including integral abutment and semi-integral abutment including worked examples. AISI (American Iron and Steel Institute) and NSBA (National Steel Bridge Alliance) also established *Integral Abutment for Steel Bridges in Highway Structures Design Handbook* in 1996 [2-11].

The report on the integral bridges in New York State by the officials of the DOT describes as follows [2-12].

- Bridges Length: less than 198,1 m (6590 ft) without limitation on individual span length
- Maximum Skew: maximum 45 °
- Abutment reveal*: less than 1,5 m (5 ft)
 - * Abutment reveal is the dimension from the bottom of the girder to the finished grade under the bridge at the abutment stem.
- Curvature: Curved integral bridge is not permitted.
- Maximum Bridge Grade: Maximum 5 %
- Steel H-piles or cast-in-place concrete piles are used; however cast-in-place concrete piles may only be used when the total bridge length is less than 48,8 m (160 ft).
- Steel H-piles are oriented with the strong axis parallel to the girders so that bending occurs about the weak axis of the pile to allow easy accommodation of the bridge movement.
- Piles must be driven a minimum of 6,1 m (20 ft) and are placed in pre-augured 3,0 m (10 ft) deep holes if the bridge length exceeds 30,5 m (100 ft).
- Wing walls are separated from abutment stems when their length exceeds 4,0 m (13 ft) to minimise the bending moment caused by passive earth pressures.
- Piles are still designed to carry vertical loads equally and there is no explicit requirement to consider bending moment in piles.

2.5 State of Art of Integral Bridges in Canada

Integral bridges are popular in Canada; many integral bridges have been constructed in last three and half decades. Summaries are as follows.

(1) Province of Alberta

Ministry of transportation (MOT) of Alberta established bridge design criteria including integral abutment design [2-13]. It specifies the four types of expansion joints at the ends of approach slabs with the applicable span ranges for expansion joints selection. It scopes the bridges longer than 100 m.

Guidelines of MOT of Alberta specifies as follows [2-14].

- For composite concrete girder bridges with a total length of less than 50 m, integral abutments should normally be used.
- For steel girder bridges with a total length of less than 40 m, integral abutments should normally be used.
- For longer bridge structures, integral abutments should be considered, however care must be taken to design proper details to accommodate cyclic thermal movements of the structure.
- Refer to Bridge Structure Design Criteria Appendix 'C' Integral Abutments for more detailed design considerations [2-13].

(2) Province of Ontario

The first integral bridges in province of Ontario were designed and constructed in 1960's. More than 100 bridges were constructed since the publication of the general guidelines of planning, design and construction in the province in 1993.

The ministry of transportation of Ontario reported performance of integral bridges from the monitoring of existing structures [2-15]. The observations of the report are as follows.

Observations:

The results of our observations are very encouraging. The structures are performing well and there is very little sign of deterioration or distress in any of the observed structures.

The followings are a few of the observations worth mentioning.

- Expansion joints (existing structures):

Well working expansion joints detail for bridges where the total length is less than 75 m for steel bridges and 100 m for concrete bridges is shown in *Fig. 2.10*.

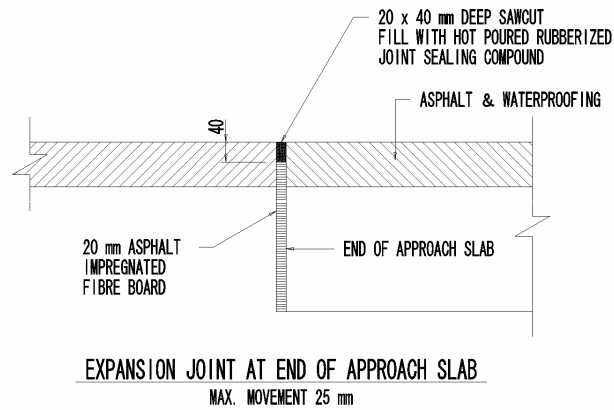


Fig. 2.10: Well working expansion joint detail

- Expansion joints (Developed by Ontario MOT):

MOT (Ministry of Transportation of Province of Ontario) developed a more elaborate expansion joint detail for bridges where the total length is more than 75 m for steel bridges and 100 m for concrete bridges is shown in *Fig. 2.11*.

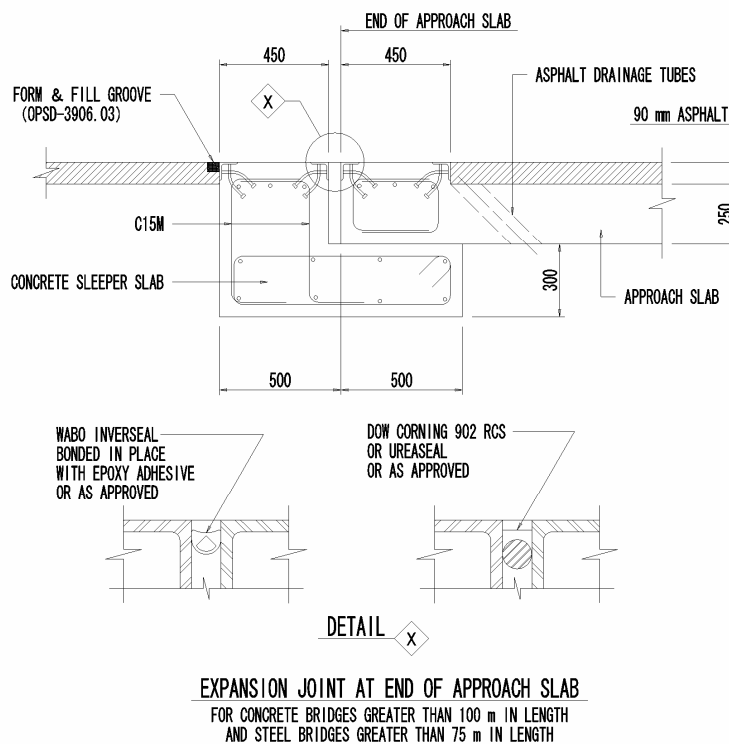


Fig. 2.11: Developed expansion joint detail by Ontario MOT

- Gaps between asphalt pavement and sealing compound:
The gap widens in winter and edges of asphalt pavement appear to separate from the sealing compound, however this gap closes again in summer and does not result in any loss of riding quality. It is anticipated that after a few years of repeated movements it may become necessary to replace the rubberised joint sealing compound and carry out minor repairs to the edges of asphalt pavement.

The report concluded and showed feature directions as follows.

Conclusion:

MOT of Ontario has obtained considerable experience in the design, construction and performance of integral bridges in the last few years. They say the follows that the experience to date has been very positive and it is expected that more such bridges will be designed and built in the feature. Bridges with less than 100 m in length have performed well and appear to be ideally suited for this design. Data on bridges in Ontario, with length more than 100 m, is limited, but with the suggested modifications to the control joint details, these bridges show the potential to also perform well in the long term.

Feature Directions:

It is intended the MOT of Ontario will continue to monitor the performance of these bridges and based on the results of this monitoring, it will revise its guidelines and policies to limit or extend their application. MOT intends to look into following:

- Extend the limit on total length of the structure
- Include post-tensioned deck type structures
- Explore the use of pipe and wood piles
- Use of semi-integral arrangements where integral design is not feasible
- Use of more rigid foundations for smaller spans

2.6 State of Art of Integral Bridges in Europe

Integral bridges are also employed with consideration of their conditions in European country. Elegant applications with utilisation of horizontal arch action to accommodate the displacement caused by thermal expansion and contraction, creep and shrinkage has also been successful in European country.

Sunniberg Bridge is 526 m long and ca. 60m high cable stayed bridge with a tight curvature of 503 m radius (*Photos 2.5 and 2.6*) [2-16],[2-17]. Due to the curvature in plan, the bridge deck is monolithically connected to the both abutments without expansion joints to allow the transformation of longitudinal displacement into horizontal sway.

The abutments essentially consist of earth-filled structures on a base slab. They are monolithically connected to the bridge deck and form the support points for the horizontal stabilisation of the structural system.

The massive pilecaps are situated in plan eccentrically toward the inside of the curvature, because the inner pier legs carry much more vertical load from the curved deck (*Fig. 2.12*).



Photo 2.5: Sunniberg Bridge (Klosters, Switzerland)



Photo 2.6: Sunniberg Bridge (Klosters, Switzerland)

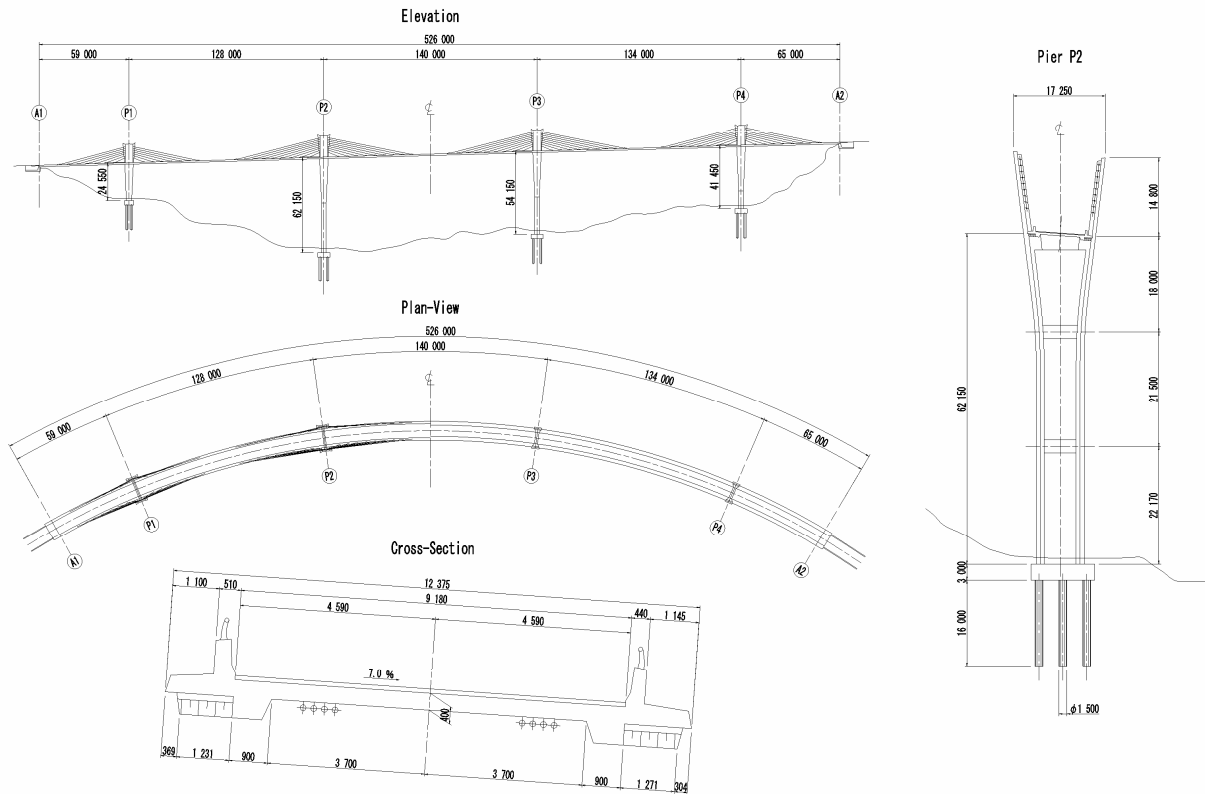


Fig. 2.12: Elevation, plan and cross section of Sunniberg Bridge

This kind of application is also applied to Yokomuki Bridge in Fukushima Pref., Japan.

By the way, integral bridges are also employed in central and east European countries. As shown in *Photos 2.7* and *2.8*, multiple spans integral bridges are also constructed in the region.

Foca Bridge across Dorina River that is one of the major tributaries of Danube River, as shown in *Photos 2.7* and *2.8*, is located in Foca city in Bosnia and Herzegovina. The bridge is 4 spans continuous prestressed concrete composite multiple I-Beam bridge with integral abutments. It has rubber expansion joints at the end of approach slabs. The articulations at the intermediate piers are formed with rubber sliding bearings for longitudinal direction, while the movement of transverse direction is fixed at each pier.

The author visited the bridge in 2005. From visual field research, there no deterioration or cracks were appeared; the rubber expansion joints at both ends of the approach slabs were also in good condition.



Photo 2.7: General view of Foca Bridge (Foca City, Bosnia and Herzegovina)



Photo 2.8: Side view of integral abutment of Foca Bridge

The integral bridge concept was also adopted for the project in Italy to retrofit the existing simply supported bridges that was completed in 2006 [2-18].

The conventional simple support articulation was changed into integral form of articulation. The 13 spans of 30,0m long simple supported single prestressed concrete bridges were refurbished into ca. 400 m long integral bridge with glued connections at the piers and abutments.

European countries have commenced INTAB Project (Economic and Durable Design of Composite Bridges with Integral Abutments) with the participation of the following partners in 2005: RWTH Aachen (Germany), University of Liege (Belgium), Profil ARBED (Luxembourg), Lulea University of Technology (Sweden), Ramboll (Sweden) and Schmitt Stumpf Fruehauf und Partner, Munich (Germany).

The main aim of the project is to allow for international comparison of different experiences in Europe, to promote theoretical studies, to carry out experimental tests and finally to draft a number of guidelines for the design of such kind of bridges.

European countries recently seem to have a general inclination for integral bridges [2-19].

2.7 Conclusion

The conclusion of state of the art of integral bridge is summarised as follows.

- (1) Integral bridges in the U.K. and North America are quite common and often the first choice for the selection of structural system of bridge, particularly in the U.K. and some states/provinces in U.S.A. and Canada.
- (2) The integral bridge is commonly allied to the bridges with overall bridge length up to ca. 50 m - 60 m in the U.K. and North America. The range coincides to the *Guidelines for Planning of Steel Integral Bridges (draft) proposed by Public Works Research Centre and Nippon Steel Corporation.*
- (3) The research on integral bridges is keenly conducted in North America, the U.K. and European countries.
- (4) The development of integral bridges has been largely owed to the development in U.S.A.; it has been reflected in the specifications and design details worldwide.
- (5) The survey of the research on integral bridges highly and positively evaluates the performance, cost effectiveness, durability and maintainability.
- (6) Applications of integral bridges are also increasingly employed in Japan mainly in expressway construction.
- (7) Design codes and guidelines for integral bridge have been established and revised in North America and the U.K.; even in Europe and Japan, they are keenly establishing, too.
- (8) Semi-integral bridges are increasingly employed to the bridges that are impossible to employ the fully integral bridge for alternative solution in recent years.
- (9) Integral bridge solution is also employed in retrofitting of existing bridges.

References

- [2-1] *Specifications for Highway Bridges*, Japan Highway Association, Tokyo, Mar. 2002.
- [2-2] *Design Standards of Railway Structures (SI version)*, Institute of General Technology for Railways, 2004.
- [2-3] *Design Guidelines Part II*, NEXCO Companies, Mar. 2006.
- [2-4] *Guidelines for Planning of Steel Integral Bridges (draft)*, Public Works Research Centre and Nippon Steel Corporation, Mar. 2004.
- [2-5] TANAKA, J., AKIYAMA, H. *Elegant Prestressed Concrete Foot Bridge with Roundly Curved Girder - Kujira Bridge (Whale Bridge) -*, National Report of fib 2002 Congress, pp.49-52, Japan Prestressed Concrete Engineering Association, Oct. 2002.
- [2-6] TANABE, T., YOSHIDA, Y., AKIYAMA, H., SHOJI, K., IMAMAKI, S. *Design and Construction of Kujira Bridge*, Journal of Japan Prestressed Concrete Engineering Association, Vol.40, No.1, pp.8-16, JPCEA, Jan. 1998.
- [2-7] *Design Manual for Roads and Bridges, Vol. 1 Highway Structures, Approval Procedures and General Design, Sect. 3 General Design, Part 12 BA 42/96 Amendment No.1, The Design of Integral Bridges*, The Highways Agency, U.K., Mar. 2003.
- [2-8] MARURI, R., PETRO, S. *Integral Abutments and Jointless Bridges (IAJB) 2004 Survey Summary, Proceedings of The 2005-FHWA Conference Integral Abutment and Jointless Bridges (IAJB2005)*, pp.12-29, Baltimore, Mar. 2005.
- [2-9] *LRFD Design Example for Steel Girder Superstructure Bridge*, FHWA (Federal Highway Administration) and NHI (National Highway Institute), Washington D.C., Dec. 2003.
- [2-10] *Comprehensive Design Example for Prestressed Concrete Girder Superstructure Bridge with Commentary*, FHWA (Federal Highway Administration) and NHI (National Highway Institute), Washington D.C., Nov. 2003.
- [2-11] *Highway Structures Design Handbook*, AISI and NSBA, 1996.
- [2-12] YANNOTTI, A.P., ALAMPALLI, S.A., White II, H.L. *New York State Department of Transportation's Experience with Integral Abutment Bridges*, Technical Report, International Workshop on the Bridges with Integral Abutment - Topics of Relevance for the INTAB Project,

- Lulea University of Technology, Sweden, Oct. 2006.
- [2-13] *Bridge Structures Design Criteria ver.4.1, Appendix C: Guidelines for Design of Integral Abutments*, Ministry of Transportation of Province of Alberta, Feb. 2002.
- [2-14] *Best Practice Guidelines -Use of Integral Abutments-*, Ministry of Transportation of Province of Alberta, Feb. 2003.
- [2-15] *Performance of Integral Abutment Bridges*, Ministry of Transportation of Province of Ontario, Mar. 1999.
- [2-16] FIGI, H., MENN, C., BANZIGER, D.J., BACCHETTA, A. *Sunniberg Bridge, Klosters, Switzerland*, Structural Engineering International, Vol.7, No.1, pp.6-8, IABSE, Zurich, Feb. 1997.
- [2-17] http://en.wikipedia.org/wiki/Christian_Menn
- [2-18] ZORAN, T., BRISEGHELLA, B. *Attainment of an Integral Abutment Bridge through the Refurbishment of a Simply Supported Structure*, Structural Engineering International, Vol.17, No.3, pp.228-234, IABSE, Zurich, Jul. 2007.
- [2-19] COLLIN, P., VELJKOVIC, M., PETRSSON, H. *Technical Report, International Workshop on the Bridges with Integral Abutment - Topics of Relevance for the INTAB Project*, Lulea University of Technology, Sweden, Oct. 2006.

Chapter 3 Static Characteristics of Integral Bridges

3.1 Introduction

The selection of structural system is one of the most important factors in bridge design, since the structural system governs the behaviour of the structure. Cost effectiveness of construction and maintenance, durability, seismic performance, vibrational serviceability are largely influenced by structural system. Thus, the loads act on the bridges are appropriately modelled and calculated in design.

In general, the primary loads that need to be considered in the structural design of any bridges are the following.

- Dead loads
- Live loads
- Thermal effects
- Creep effects
- Shrinkage effects
- Seismic load
- Wind loads and/or other specific loads

Whether the bridge has simply supported span, is of continuous construction, or is an integral bridge, the effects of these loading groups are very similar, though the distribution of forces and deformations differ. The design of bridges with these different forms of articulation differs mainly in the treatment of constraint forces caused, for instance, by such as temperature and creep effects.

This chapter describes the effects of the temperature, shrinkage, and creep upon the structure, earth pressure and the interaction between the abutment of the integral bridge and backfill soil in turn, and in each case the consequences for the design of integral bridges are discussed with case studies.

3.2 Temperature Effects

3.2.1 Temperature loading

Specifications for roadway bridges [3-1] defines the temperature effects in two categories; changes in the effective temperature for the bridge, and differences in temperature through the thickness of the deck and other members.

3.2.2 Temperature Differences

Temperature difference loading causes a pattern of internal stress to form within the deck. *Specifications for roadway bridges (part I)* specifies the temperature difference between reinforced and/or prestressed concrete deck and other members as 5°C for concrete bridges and 10°C for steel bridges (*Fig. 3.1*).

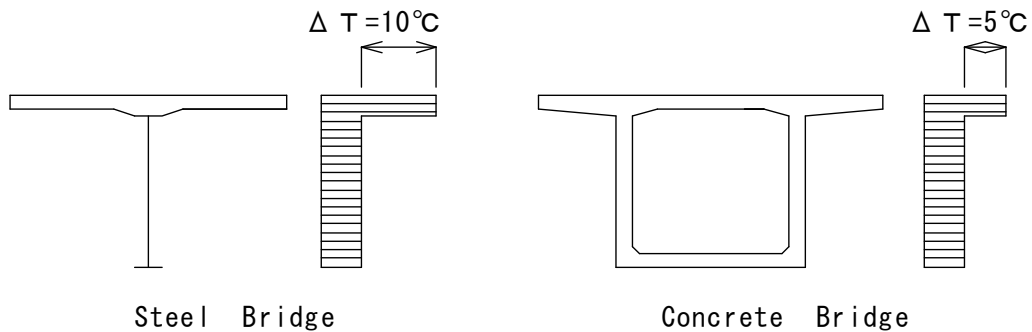


Fig. 3.1: Temperature difference

3.2.3 Effective Bridge Temperature

Changes in effective bridge temperature cause the deck expansion and contraction. As this is the most important effect governing the design of bridge joints, and also very significant in the design of bearings, it is worthwhile to summarise the way it affects bridges with different types of articulation:

(1) Simply supported bridges

A simply supported bridge span is allowed to expand and contract with little restraint. It therefore needs an expansion joint at one end, and sliding bearings to allow movement over that support. Temperature loading does not bring about longitudinal forces except due to bearing restraint or friction, though they are generally give only small influence upon the structure.



Fig. 3.2: Simply supported bridge

(2) Continuous bridges

Continuous bridge is defined as the bridge with continuous deck/girder without rigid articulation between deck/girder and substructures here. A continuous bridge is also allowed to expand and contract with little restraint.

Assuming it to be fixed at one abutment, it needs large expansion joints and sliding bearings at the other end, and sliding bearing over intermediate supports. Since elastometric bearings allocate the longitudinal movement to the both ends of expansion joints, the expansion joints can be downsized with equal sizes.

Temperature loading does not create large longitudinal forces;

- Effective temperature change makes little forces.
- Temperature difference creates sagging moment when continuous bridges are applied. It gives constraint tensile stress at the lower flange of superstructure.

The effective temperature change gives little influence upon the stress of bridge; on the other hand, temperature difference would often give critical state in serviceability limit state.

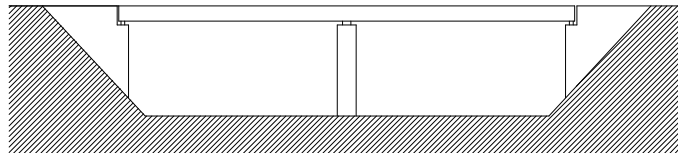


Fig. 3.3: Continuous bridge

(3) Integral bridges

In an integral bridge, expansion and contraction is partially restrained by the abutments, which move with the ends of the bridge. The size of the longitudinal force induced in the deck depends on the design of the abutments, and their interaction with the soil. No expansion joints or bearings are required. However, there is relative movement between the abutments and the approach load; accordingly a joint in the pavement is sometimes needed.



Fig. 3.4: Integral bridge

3.3 Shrinkage Effects

3.3.1 Shrinkage

Concrete shrinks slightly as it ages; this can affect stresses and deformations in bridges. In composite bridges, the separate components will generally shrink by different amounts, including a set of internal stresses and curvature of the deck, and also a small overall shortening. The internal stresses must be allowed in the design, and calculations take a similar form to those for temperature difference loadings. The overall shortening will be most significant in an all concrete bridge and composite bridge for longitudinal movement. A conservative value for long term shrinkage strain in concrete is ca. 200×10^{-6} , and about half of this occurs before the concrete has reached an age of 100 days. Even for an in-situ integral bridge, it is unlikely that integral behaviour of the abutments will start, or the pavement joint be made, before this age has been reached. Thus a realistic upper bound for overall shrinkage is usually ca. 100×10^{-6} , or 10 mm for 100 m bridge length. *Specifications of roadway bridges* allows using 150×10^{-6} for monolithic in-situ concrete structures; this would give conservative results for the structural design. The incremental analysis of shrinkage based on the actual construction procedure would give the reasonable shrinkage strain with smaller margin.

3.3.2 Effects of Shrinkage on Integral Bridge

When steel and/or prestressed concrete beam is used for the construction, the overall shortening of a bridge is much smaller than the range of thermal movement, and the gradual rate of movement will be swamped by the cyclical thermal movements. Shrinkage is not significant in the design of the abutments.

On the other hand, when reinforced or prestressed concrete bridge is monolithically constructed with in situ concrete, shrinkage is not negligible even the effects are reduced by creep. When monolithic in situ construction is employed, *Specifications for Roadway Bridges Part I* allows to assume the shrinkage strain as 150×10^{-6} to calculate the indeterminate force, if longitudinal reinforcement ratio is larger than 0,5 %; nor 200×10^{-6} shall be used.

3.4 Creep Effects

3.4.1 Creep

Like shrinkage, creep is a non-elastic deformation of concrete occurring over time. In the long term, creep increases the strain to ca. three times the elastic strain. Creep strain is described by a creep factor, given by symbol ϕ , and the creep strain is defined as ϕ times the elastic strain. The creep factor is time dependent, and normally has long term value of ca. two, but can only be calculated with a considerable degree of uncertainty.

Creep affects the deformations of all bridges where concrete is used, but its effects on the stresses depend on the type of construction. In a composite bridge, any stresses located in by differential shrinkage between girders and the deck will be relieved by creep. This can be dealt with in design simply by applying a reduction factor to the shrinkage strain.

Creep has a significant effect in prestressed concrete structures. In the case of post-tensioned construction and pre-tensioned beams, the effect is simply to reduce slightly tensioning force and the forces and stresses resulting from it. The reduction of the forces is generally ca. 10 %. This is taken into account in the design simply by including creep strain with other prestress losses, e.g. relaxation etc.

3.4.2 Design Using Prestressed Beams

This section relates to the design of both continuous and integral bridges, as creep affects these in the same way.

The difficulty of precast prestressed concrete beam construction arises because the prestress is not continuous over the supports. Shortening of the bottom flange of the beams due to creep causes the individual beams to hog, and opens up cracks at the bottom of the beams over the supports. The beams can be restrained so that these cracks do not occur, but this involves designing for a substantial sagging moment at the beam ends.

It is interesting to compare the bending moment diagrams when hogging of the beams is restrained (fully continuous construction) and when there is no restraint (simply supported).

Fig. 3.5 shows on the left bending moment diagrams for a simply-supported

span, made up from the combination of dead and live load. On the centre are the equivalent diagrams for a precast beam in a continuous structure (integral bridge). Dead loads are carried on the beam acting as simply-supported, continuity under live loads leads to hogging moments at the ends. Creep of the concrete leads to a uniform sagging moment, including over the supports. On the right are the equivalent diagrams for a cast-in-situ post tensioned prestressed concrete bridge in a continuous structure (integral bridge). It acts as continuous structure for any loads.

Comparing between precast beam structure and in situ structure, the difference is the behaviour for dead load before continualisation, *i.e.* self load of super structure. The precast beam structure is suitable for relatively short span structure, while in situ structure is suitable for larger span structure, because of the balances with other loads (*c.f.* total bending moment diagrams).

The absolute values of bending moment and deflections of continuous structure are lowered than simply supported structure.

The lower absolute values of bending moment give economical construction. Continuous structure (integral bridge) gives lower deflection for live load; it is inferred that this would lead to better bridge serviceability for traffic loads. The details are described and discussed in chapter 5.

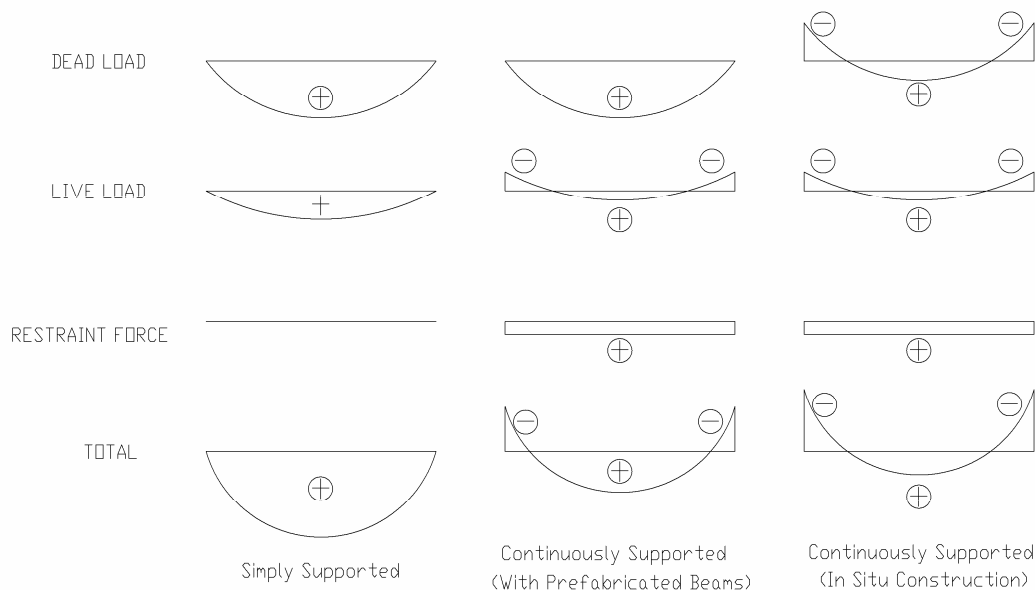


Fig. 3.5: Bending moment diagrams of single span bridges

3.5 Earth Pressure

3.5.1 Summary

The earth pressure is almost common with conventional supported bridges. However, some kinds of characteristic behaviour of integral bridge shall be considered in the design. They include the follows.

- Influence of surcharge by live load
- Earth pressure in earthquake
- Rotation in plan of skewed integral bridge

3.5.2 Influence of Surcharge by Live Load

Design Guidelines Part II of NEXCO Companies specifies the earth pressure for single span integral bridges, so-called portal frame bridges, as follows.

The earth pressure should include the influence of surcharge by live load. The one-side and both-side loading shall be considered to secure the safety for all the members.

$$P_l = K_h \times q \quad (3.1)$$

with,

P_l : Earth pressure intensity on integral abutment stems caused by surcharge load (N/mm²)

K_h : Horizontal earth pressure coefficient

q : Surcharge load intensity by live load
(Generally, $q=0,01$ N/mm²)

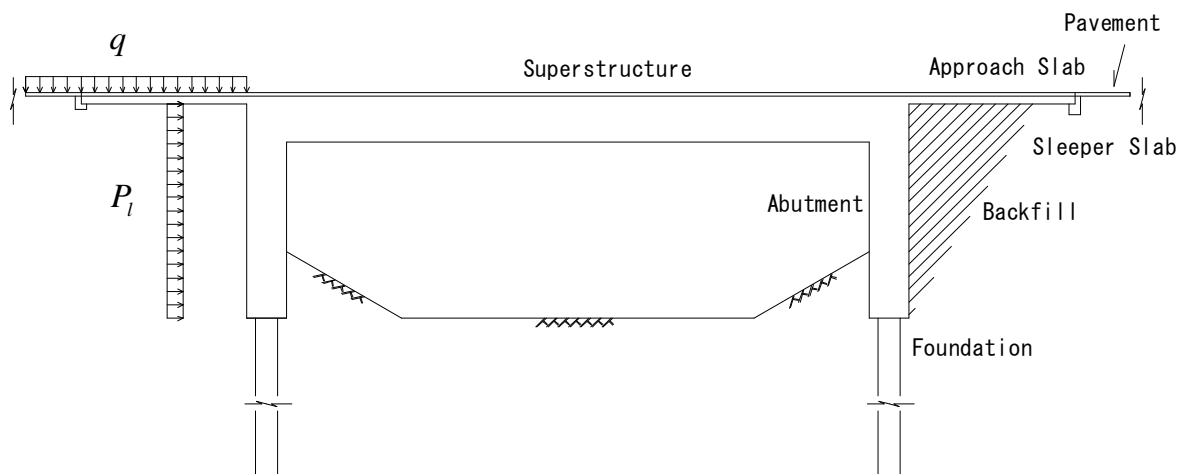


Fig. 3.6: Earth pressure by live load

3.5.3 Earth Pressure in Earthquake

The earth pressure in earthquake shall be generally considered by Coulomb earth pressure model as one-side loading for general backfill soil. On the other hand, when cement treated soil is employed for backfill, 10 % of earth pressure coefficient shall be considered to calculate the earth pressure in level 2 earthquake, while earth pressure is omitted in non-earthquake loaded state.

3.5.4 Rotation in Plan for Skewed Integral Abutments

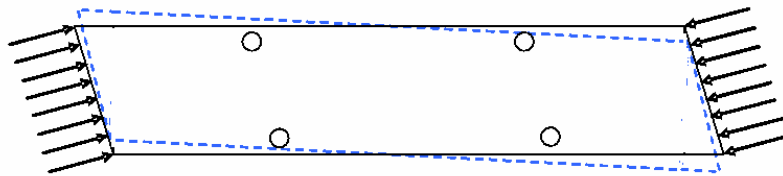


Fig. 3.7: Rotation in plan of bridge deck caused by earth pressure

Earth pressures cause bridge rotation in plan when skewed integral abutments are employed (*Fig. 3.7*). Thus the skew should be limited to restrict the rotation in plan, or detailed analysis and design shall be conducted for the interaction of earth pressure and whole structural system.

Design Guidelines Part II of NEXCO Companies specifies the maximum skew as 15° .

The survey of recent practice in the U.K. reported that designers are designing fully integral bridges with skews up to or slightly above 30° but semi-integral bridges are rarely designed with skew above ca. 20° . By way of parenthesis, *BD57 Design for durability* specifies the skew should not exceed 30° .

3.6 Soil-Structure Interaction of Integral Abutment

The soil-structure interaction of integral abutment under cyclic temperature loading is one of the most complex issues related to integral bridges. The settlement of backfill, stress escalation of earth pressure on abutment wall and wing wall are characteristic and important factors in design of integral bridges.

Vigorous research on this issue was conducted by England, G. L. *et al.* as a joint research project of Imperial College and The Highways Agency in the U.K. [3-3]. The experimental and analytical study has proved the following.

- (1) Cyclic loading of Leighton Buzzard sand has confirmed the existence of strain ratcheting behaviour during cyclic stress loading, and the stress changes with cyclic strain loading leading to a shakedown state.
- (2) Parametric studies from both the numerical simulations and the model retaining wall tests have identified the significant roles played by each of the diurnal and seasonal temperature fluctuations of the bridge deck.
 - Long-term soil stresses on the abutment wall are little affected by the initial density of the backfill material or by the season (summer, winter, etc.) during which the structure enters service. However, the early performance is influenced by both parameters. The initial rate of stress escalation is higher for bridges completed in winter.
 - The significance of daily wall movements (approximately one-quarter to one-tenth of the seasonal movements) is to induce more soil densification and deformation. In comparison with values for seasonal movements alone, the inclusion of daily wall movements increased the settlement adjacent to the wall by 100 % and the heave away from the wall by 150 %.
 - Daily wall movements encourage the soil stresses to remain closer to hydrostatic values initially and later to become similar to those for seasonal cycles alone, after additional soil densification has occurred.
- (3) Settlement of abutments, for bridges up to 60 m long and with strip

footings, is not considered to be significant.

- (4) If run-on slabs (approach slab) are used to span the settlement region adjacent to the abutment, a highly compacted backfill should be avoided in order to reduce the heave which could cause buckling of the pavement slab.
- (5) In its present form the information contained in BA 42 provides a conservative design loading for integral bridge abutments for bridges up to 60 m long. However, it does not provide any information for the determination of soil deformation (in particular, heaving), or the consequent changes to the lateral earth pressures on the wing walls. Unsafe wing wall design could thus result.
- (6) Due to the existence of significant granular flow in the backfill material, wing walls of reinforced soil construction are not recommended.
- (7) The current limit of a 60 m maximum bridge length for integral bridge is considered reasonable and should be maintained until a better understanding of the consequences resulting from the formation of active slip planes in longer span bridges can be developed.
- (8) Because seasonal and daily temperature cycles each play an important role in defining the interaction problem both should be considered in calculations.

3.7 Case study on Static Behaviour of Single Span Integral Bridge

- A Study on the Long Span Integral Bridge for Longitudinal Movement, Constraint Stress and Prestressing Efficiency -

3.7.1 Summary

Since integral bridges are highly indeterminate and rigid structure, constraint stresses are larger than those of non-integral bridges. The constraint stresses of integral bridges by temperature effects and indeterminate stress caused by prestressing force are different from those of non-integral bridges.

Especially, indeterminate stress of prestressing force sometimes governs the structural design, because it inevitably influences the efficiency of the prestressing force, *i.e.* the low prestressing efficiency means unfeasibility of prestressed concrete structure; the indeterminate force is intimately dependent on the structure's capacity of the deformation. In addition, the longitudinal movement of the abutments is important to evaluate the feasibility of the integral bridge as specified by some design guidelines, *e.g.* DB42 *The Design Manual for Road and Bridges* of the U.K [3.4].

The structural system of the bridge, especially the stiffness of the foundation, greatly influences the behaviour of the structure. As a case study, the longitudinal movement of the abutments and prestressing efficiency are discussed below with parametric studies using the structural model of Kujira Bridge (*Photo 3.1, Figs. 3.8, 3.9 and 3.10*).



Photo 3.1: Kujira Bridge

3.7.2 Parameters for the Studies

As the support condition of the structure is crucial and governs the structural characteristics, parametric studies on the longitudinal movement and prestressing efficiency are conducted. The parameters of the support condition are shown in *Table 3.1*.

Table 3.1: Parameter of support condition

	Support condition of foundations	
CASE-1	Pile foundation (actual value of Kujira Bridge)	
	A1 Abutment	$K_x = 4,6584 \times 10^6$ (kN/m) $K_z = 4,5262 \times 10^6$ (kN/m) $K_\theta = 3,4832 \times 10^8$ (kN·m/rad)
	A2 Abutment	$K_x = 2,1672 \times 10^6$ (kN/m) $K_z = 4,3398 \times 10^6$ (kN/m) $K_\theta = 2,9867 \times 10^8$ (kN·m/rad)
CASE-2	Pile foundation (the spring values are twice of actual value of Kujira Bridge)	
CASE-3	Pile foundation (the spring values are half of actual value of Kujira Bridge)	
CASE-4	Spread footing (Completely fixed condition)	
CASE-5	Pile foundation with hinge between column and footing (pile condition is same as CASE-1)	

3.7.3 Longitudinal Movement of the Abutments

The results of longitudinal movement of the abutments are shown in *Table 3.2*. The items of "Creep and Shrinkage" are the values of the longitudinal movement caused by creep and shrinkage from the commencement of the service through the terminal state of creep and shrinkage. The results are summarised and discussed as follows.

- 1) The results of CASE-1, 2 and 3 (fully integral bridge models with pile foundations) says that the influence of the spring values of the pile foundation is not greatly sensitive for the longitudinal movement of the abutments.
- 2) The movement of A1 abutment in CASE-5 (semi-integral bridge model) is considerably large for the rotation of the piers and asymmetric structural characteristics of the superstructure by the influence of the hinges to release the rotational fixity of the foundations.
- 3) The movement of 44 mm of A1 abutment in CASE-5 is supposed to be

difficult to accommodate without expansion joints. There is possibility to be cracked due to temperature change and movement by creep and shrinkage when creep and shrinkage is proceeding.

- 4) The longitudinal movement for the temperature change in CASE-5 is not increased than other cases compared with the creep and shrinkage. The increase of hogging or deflection due to the arch effects with the hinges prevents the increase of the longitudinal movement, for the bridge develops a sort of arch rise in elevation.
- 5) The influence of the condition of the foundation is quite slight for the movement by temperature change in all the cases.

Table 3.2: Longitudinal displacement of abutments

Unit: mm

		A1	A2
CASE-1	Creep & Shrinkage	9, 18	14, 42
	Temperature (-20°C)	5, 81	8, 75
	Total	15, 0	23, 2
CASE-2	Creep & Shrinkage	6, 07	9, 61
	Temperature (-20°C)	5, 18	7, 81
	Total	11, 2	17, 4
CASE-3	Creep & Shrinkage	12, 07	18, 49
	Temperature (-20°C)	6, 20	9, 31
	Total	18, 3	27, 8
CASE-4	Creep & Shrinkage	0, 54	0, 96
	Temperature (-20°C)	0, 13	0, 18
	Total	0, 7	1, 1
CASE-5	Creep & Shrinkage	37, 44	4, 73
	Temperature (-20°C)	6, 54	7, 85
	Total	44, 0	12, 6

3.7.4 Prestressing Efficiency

The prestressing efficiency, with the symbol ζ is defined as the ratio of residual prestressing force vs. the applied prestressing force considering indeterminate force for prestressing force.

The prestressing efficiency ζ is defined as follows.

$$\zeta = \frac{\sigma_1 + \sigma_2}{\sigma_1} \quad (3.2)$$

with

σ_1 : prestressing stress applied to the section

σ_2 : indeterminate prestressing stress of the section

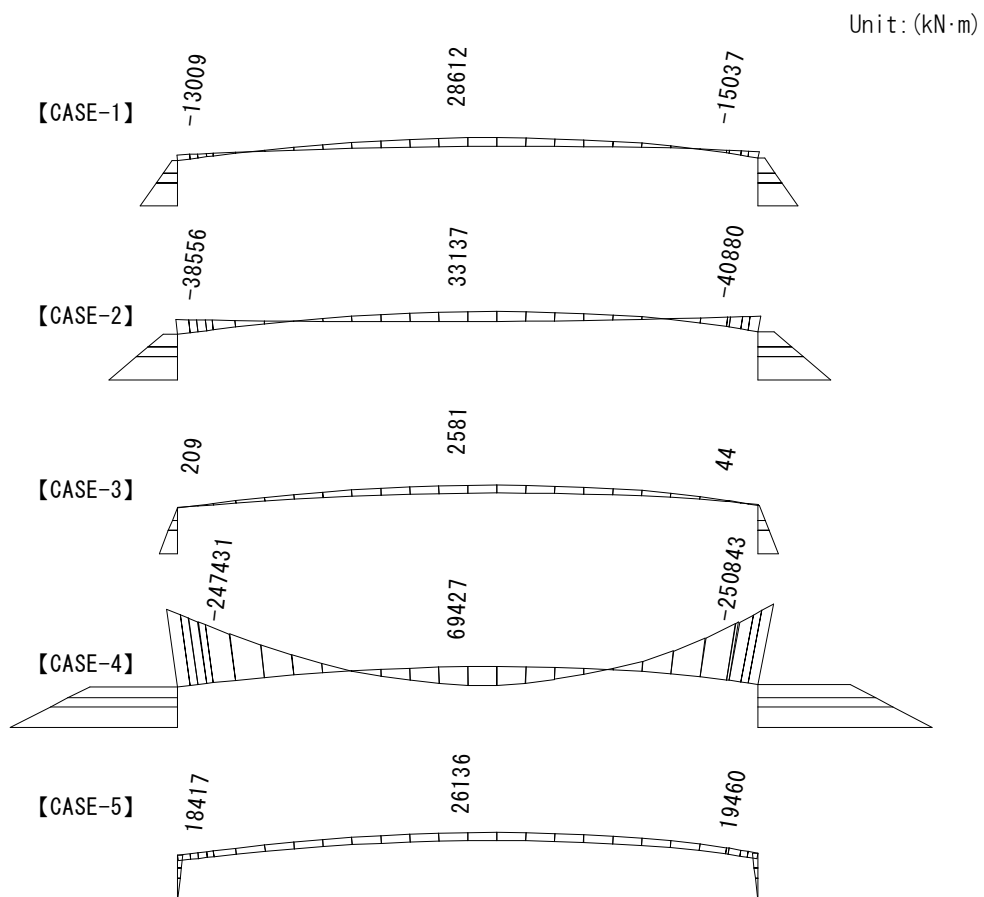


Fig. 3. 11: Indeterminate bending moment of prestressing force

Table 3.3: Results of prestressing efficiency (ζ)

	prestressing efficiency (ζ) at the tensile edge		
	Sect-3	Sect-14	Sect-25
CASE-1	93, 2%	66, 5%	92, 8%
CASE-2	84, 7%	58, 7%	84, 1%
CASE-3	98, 3%	71, 2%	98, 0%
CASE-4	15, 2%	3, 7%	13, 3%
CASE-5	103, 6%	72, 7%	104, 0%

The results are shown in *Fig. 3.11* and *Table 3.3*. The prestressing efficiency ζ is calculated at the tensile edge of each section in *Table 3.3*. The figures in *Fig. 3.11* are the values of bending moment at the sections of No.3, 14 and 25 (q.v. *Fig. 3.10*).

The results are summarised and discussed as follows.

- 1) The results of CASE-1, 2, and 3 (fully integral bridge models) show that the variance of prestressing efficiency ζ is around 5 % to 9 % , even the spring value of the foundation is twice or half of the actually designed value (CASE-1).

This means that some variance and/or difference of the assumed design parameters of foundations from actual values, would not give large influence for the prestressing efficiency.

- 2) The results of CASE-4 (spread footing foundation model) mean the high-fixity foundation is not feasible for prestressed concrete structures for their large indeterminate force. For reference, DOT of state of Maine, U.S.A recommends the range of integral bridge length with spread footings; 24,4 m (80 ft) for steel structure, 41,2 m (135 ft) for concrete structure.

- 3) The results of CASE-5 (semi-integral bridge model) mean the performance of flexibility by the hinges. This kind of structural system can be applicable for rigid foundations. But, the foundation of integral bridge should be basically flexible for the excellent durability and structural redundancy of the higher indeterminate system by the application of hingeless and monolithic structural system.

3.8 Case Study on Static Behaviour of Multiple Spanned Integral Bridge with Curvature in Plan

3.8.1 Summary

The integral bridge with curvature in plan has unique characteristics. If appropriately designed, the curved integral bridge has eminent merits; the deck moves alike an arch in plan against temperature change. Prosperous examples of the curved integral bridges are for instance Yokomuki Bridge (*Photo 3.2*) and Sunniberg Bridge (*Photos 2.5* and *2.6*).



*Photo 3.2: Yokomuki Bridge (Fukushima pref.)
(By favour of Takashi OOURA)*

The constraint stresses due to temperature change, etc. are released by the escaping horizontal movement in plan (*Fig. 3.12*), though transverse bending moment would be generated in the deck/girder. The "arch effect" makes the constraint stresses of the deck lower and enables longer integral bridge construction than straight ones.

In addition, the integral bridge solution can also increase seismic resistance for following reasons.

- High redundancy for its high indeterminate structural system
- Cancelling out of earth pressure and seismic inertial force by the retaining action of the pair of integral abutments
- Damping effect by the abutment backfill

The solution also avoids the collapse and fall down of the superstructure for its monolithic form of structure, even extreme and unexpected scale seismic force acts on the bridge for monolithic form of structural system.

On the other hand, integral bridges are influenced by constraint stresses due to temperature change, shrinkage, settlement, etc. because of their rigid and highly indeterminate structural characteristics.

The temperature change gives largest influence upon the constraint stress in the deck, because time dependent influences such as shrinkage and settlement are mitigated by creep.

Thus, the influence of the temperature change should be clarified for the application of integral bridge system with curvature in plan.

The influence of temperature change for the conventional supported bridges, integral bridges and semi-integral bridges are discussed with parametric studies and discussed below [3-7, 3-8, 3-9].

3.8.2 Parameters of Analysis for the Temperature Induced Constraint Stress

The constraint stresses depend on the deformation capability of the structure. They reach their maximum when deformations are eliminated. A bridge system's capacity to lower constraint stresses is mainly determined by its support and geometric conditions.

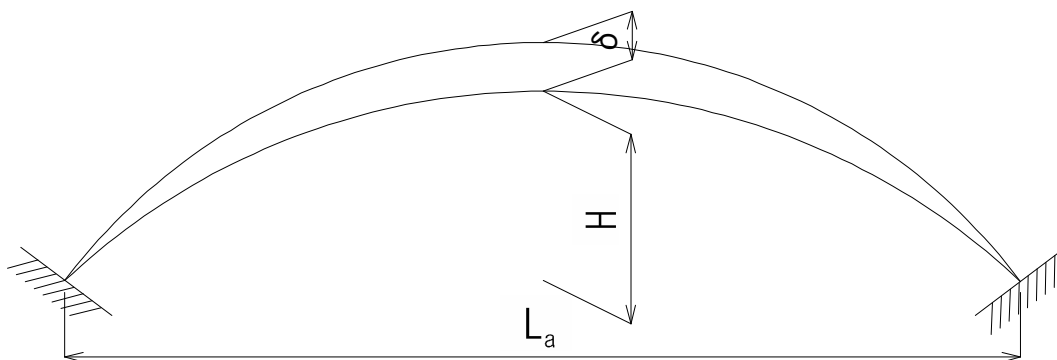
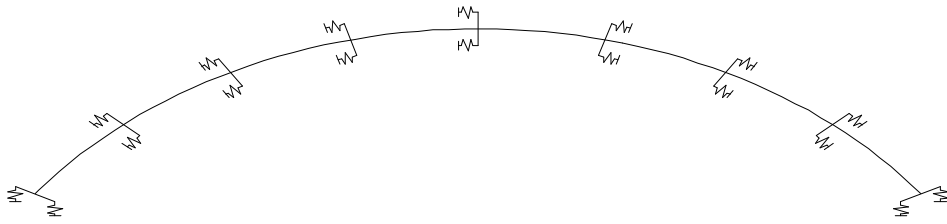


Fig. 3.12: Horizontal deformation due to temperature rise

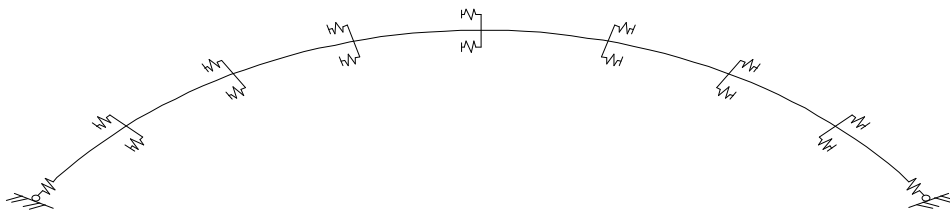
The temperature induced constraint stress in the deck is influenced by some conditions - curvature in plan, distance between abutments, structural system (support condition), deck stiffness, stiffness of bearings, etc. Among these factors, the curvature in plan, distance of abutments and support condition are dominant to govern the structural behaviour, *i.e.* the deformation and constraint stress in the deck. The distance of the abutments, the curvature in plan with singular radius (*i.e.* it also means the proportion of arch in plan - H/L_a) and structural systems - integral model, semi-integral model and conventional model - are taken as the parameters to calculate the temperature change induced deformation and stress of the deck (*Table 3.4*).

As the structural models for the parametric study, 6 span and 8 span continuous box girder concrete bridges are considered for $L_a=300$ m models and $L_a=400$ m models respectively (*Figs. 3.13* and *3.14*). The side span length are arranged to be 65 % of that of main spans. The both ends of the integral model and semi-integral model are assumed rigid abutment for the analysis.

1) conventional model



2) semi-integral model



3) integral model

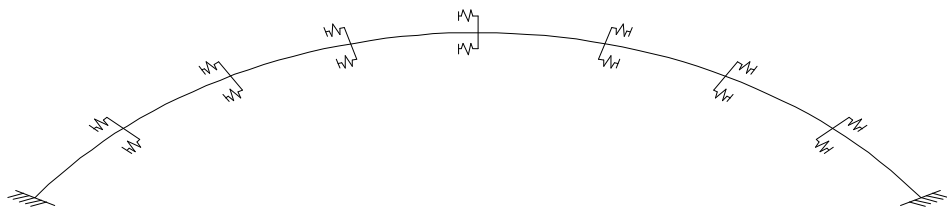


Fig. 3.13: Plan of structural model ($L_a=400m$)

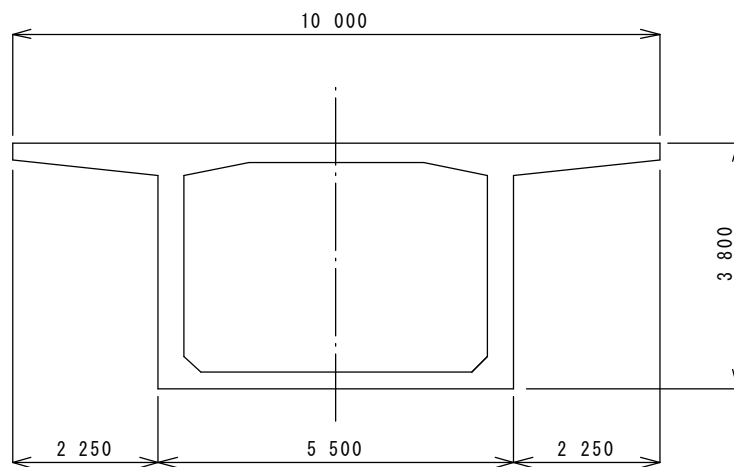


Fig. 3.14: Cross section

Table 3.4: Parameters of analysis

L_a	R	H/ L_a	Support condition
m	m	—	—
300	∞	—	1) Conventional rubber bearing supported model
	400	1/10, 3	$K_h=1,0 \times 10^4$ kN/m
	350	1/8, 9	
	300	1/7, 5	$K_v=5,0 \times 10^6$ kN/m
	250	1/6, 0	
	200	1/4, 4	2) Semi integral model
	175	1/3, 5	$K_h=1,0 \times 10^4$ kN/m
	150	1/2, 0	
400	∞	—	$K_{EI}=2,5 \times 10^5$ kN/m
	600	1/11, 7	$K_{Et}=2,0 \times 10^4$ kN/m
	500	1/9, 6	$K_{Ev}=4,0 \times 10^6$ kN/m
	400	1/7, 5	
	350	1/6, 4	3) Integral model
	300	1/5, 2	$K_h=1,0 \times 10^4$ kN/m
	250	1/4, 0	
	200	1/2, 0	$K_v=5,0 \times 10^6$ kN/m

The bearing stiffness is defined as follows.

L_a : distance between both abutments

R: radius of curvature in plan

H: rise of arch in plan

K_h : horizontal stiffness of a pair of bearings on each support

K_v : vertical stiffness of a pair of bearings on each support

K_{EI} : longitudinal stiffness of bearing at the abutment in semi integral model

K_{Et} : transverse stiffness of bearing at the abutment in semi integral model

K_{Ev} : vertical stiffness of bearing at the abutment in semi integral model

3.8.3 Displacement Due to Temperature Change

The sway at the crown δ (q.v. Fig. 3.12), which is the displacement in plan at the mid-structure for 15 ° C temperature change of each case is shown in Figs. 3.15 and 3.16. The results are summarised and discussed below.

- 1) The sway of integral model is larger than semi-integral model and conventional model for the higher axis force, especially for low rise arch in plan (q.v. "H" in Fig. 3.12).
- 2) The sway of semi-integral model is almost constant for each model.
- 3) The sway of the conventional model is slightly influenced by the structural rise, but the sway is quite small due to the release of constraint stress.

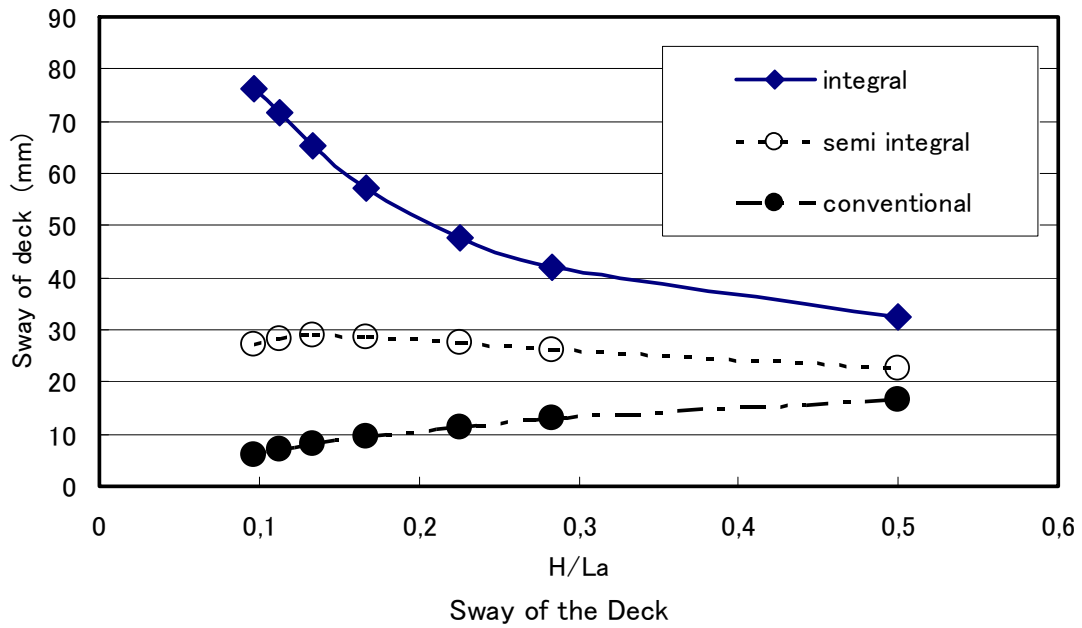


Fig. 3.15: Sway at the crown ($L_a=300m$)

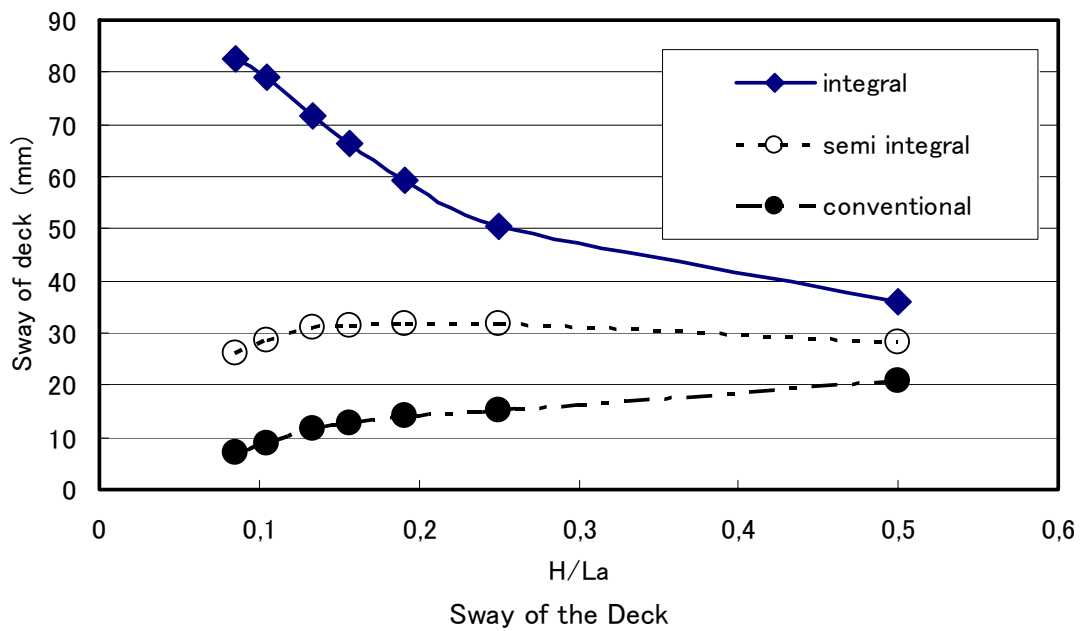


Fig. 3.16: Sway at the crown ($L_a=400m$)

3.8.4 Constraint Stress for Temperature Change

The diagrams of 15°C temperature change induced constraint transverse bending moment for integral, semi-integral and conventional models are shown in Figs. 3.17, 3.18, 3.19 and 3.20.

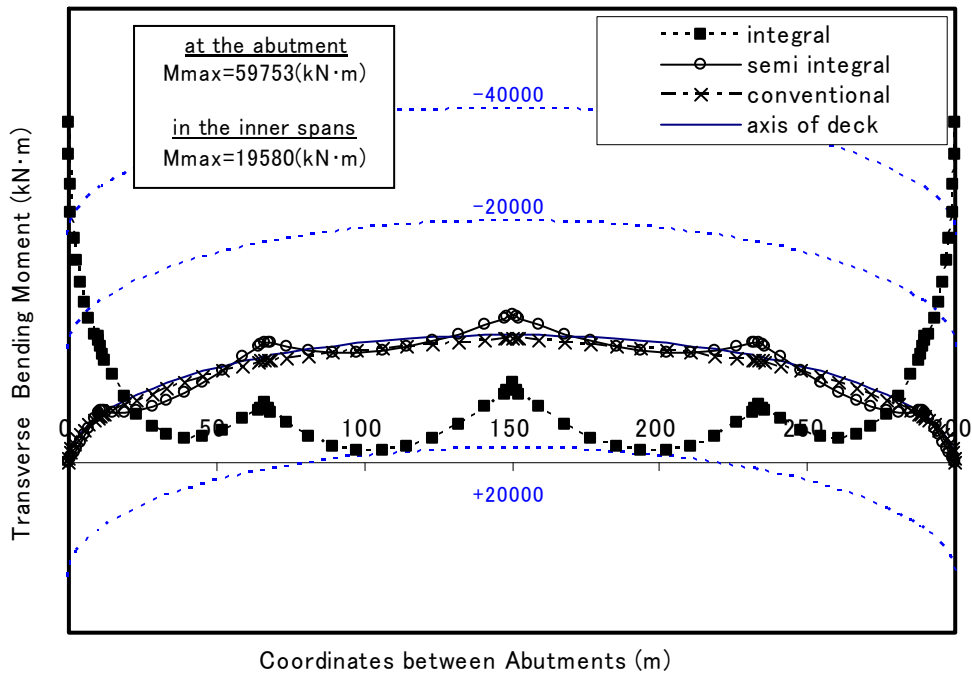


Fig. 3.17: Transverse bending moment ($L_a=300m$, $R=400m$, $H/L_a=1/10, 3$)

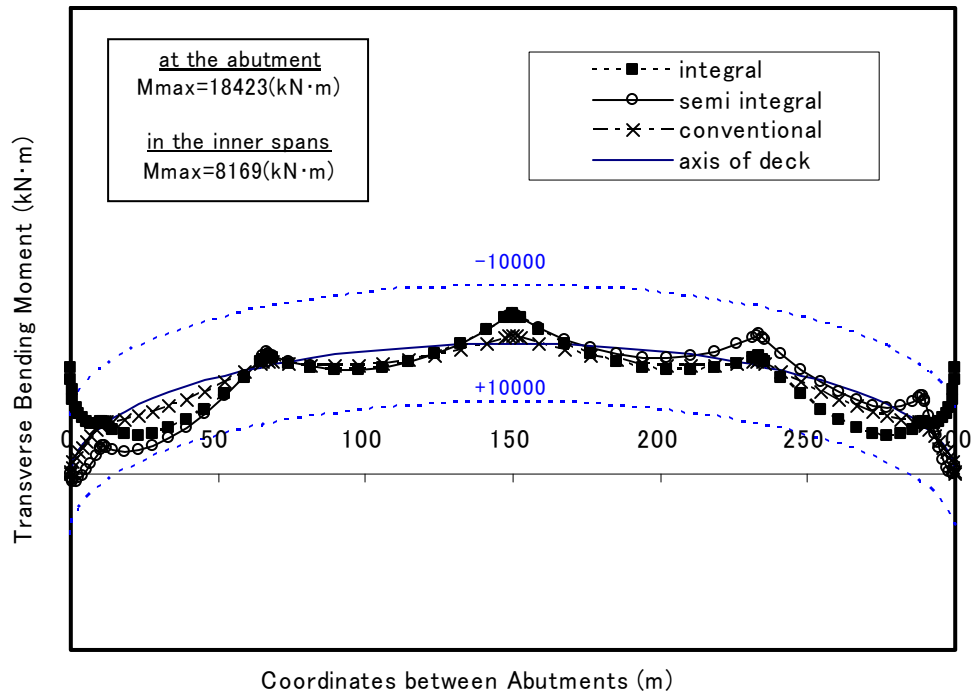


Fig. 3.18: Transverse bending moment ($L_a=300m$, $R=150m$, $H/L_a=1/2, 0$)

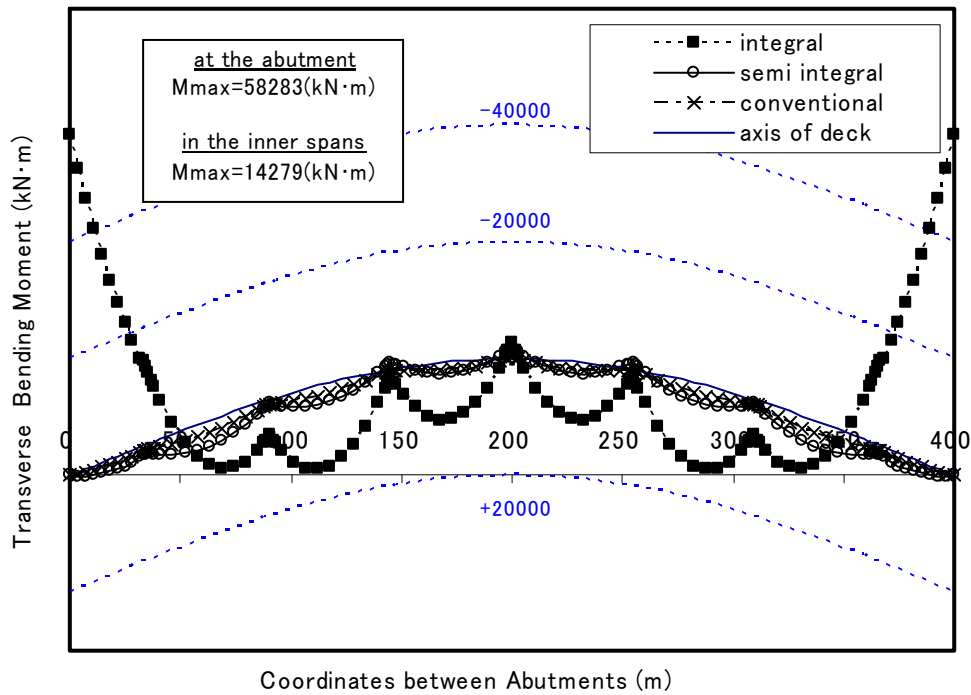


Fig. 3.19: Transverse bending moment ($L_a=400m$, $R=600m$, $H/L_a=1/10, 3$)

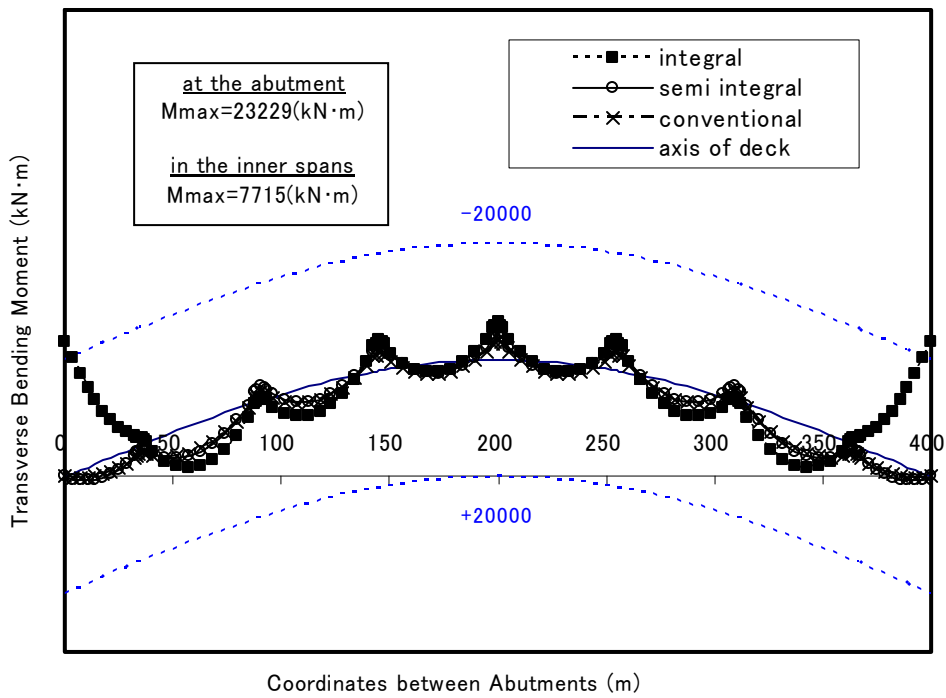
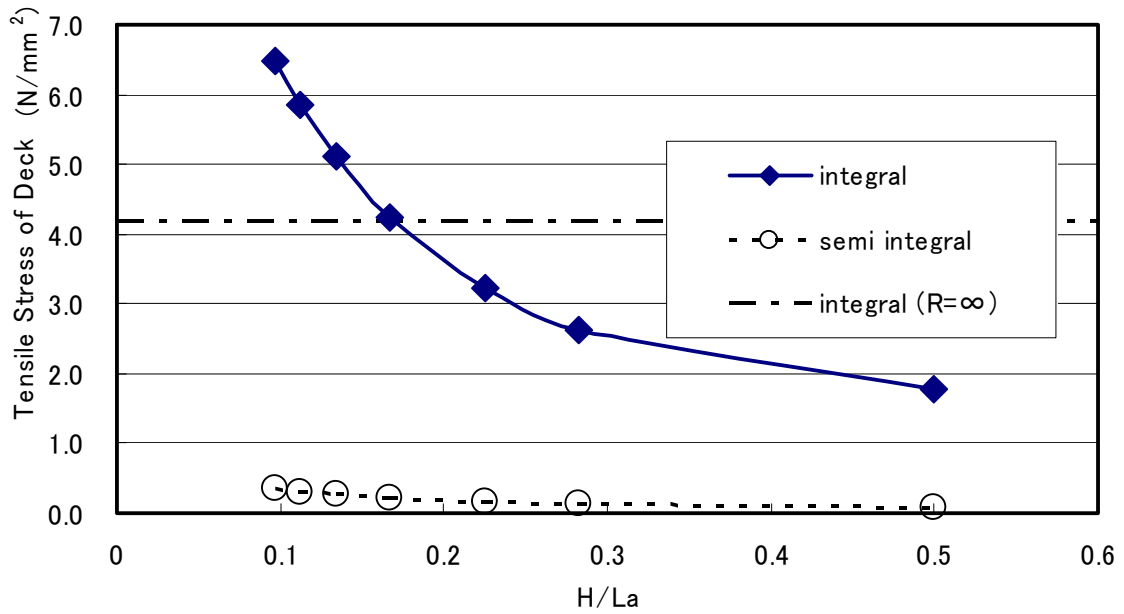


Fig. 3.20: Transverse bending moment ($L_a=400m$, $R=200m$, $H/L_a=1/2, 0$)

The diagrams of maximum transverse tensile stress of the deck caused by 15°C temperature change constraint stress with relationship to H/L_a and L_a are shown in *Figs. 3.21, 3.22, 3.23* and *3.24*.

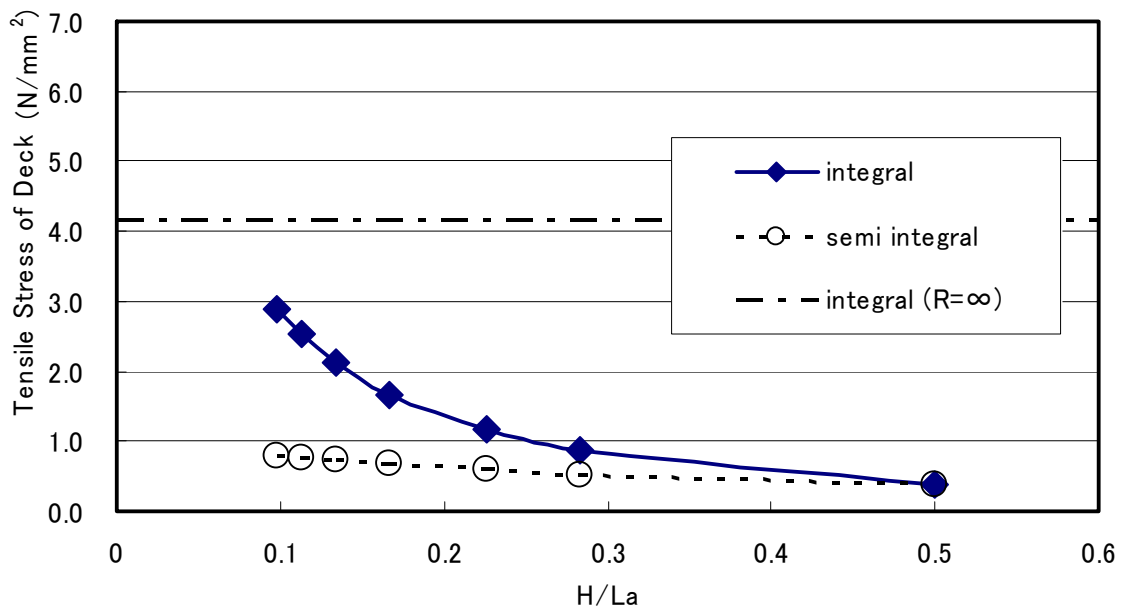
The stress of conventional model is omitted in these diagrams, since it is obvious to be quite little. The results are summarised and discussed as follows.

- 1) The curvature in plan gives around 3,2 times and 2,5 times difference of the transverse bending moment at the abutments for $L_a=300$ m model and $L_a=400$ m model respectively.
- 2) The curvature in plan gives around 2,4 times and 1,85 times difference of the maximum values of transverse bending moment in the inner spans for $L_a=300$ m model and $L_a=400$ m model respectively.
- 3) The high rise integral models ($H/L_a=2,0$) lower the transverse bending moment throughout the structures.
- 4) The transverse tensile stress of deck at the abutment of integral model decreases to half of the value of straight integral model when H/L_a is around $1/2,5$ for $L_a=300$ m model and $1/5$ for $L_a=400$ m model.
- 5) The maximum transverse tensile stress of deck in the inner spans is around half of the value at the abutment.
- 6) Semi-integral model gives quite little constraint stress throughout the structure almost regardless of H/L_a .
- 7) The longer distance between abutments (L_a) gives lower constraint stress at the abutment because of its lower flexural stiffness as the superstructure is considered as arch ring of the arch in plan (*q.v. Figs. 3.21* and *3.23*).



Thermal Stress of the Deck (15°C) at the abutments

Fig. 3.21: Transverse tensile stress of deck at the abutment ($L_a=300m$)



Thermal Stress of the Deck (15°C) at the Crown

Fig. 3.22: Maximum transverse tensile stress of deck in the inner spans ($L_a=300m$)

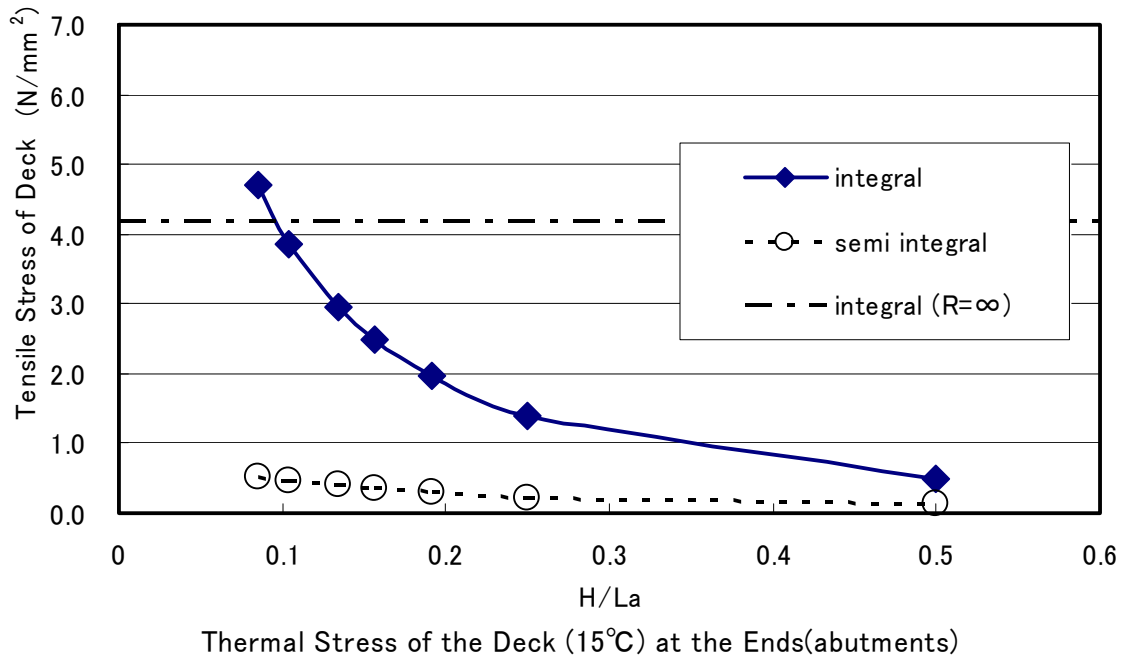


Fig. 3.23: Transverse tensile stress of deck at the abutment ($L_a=400m$)

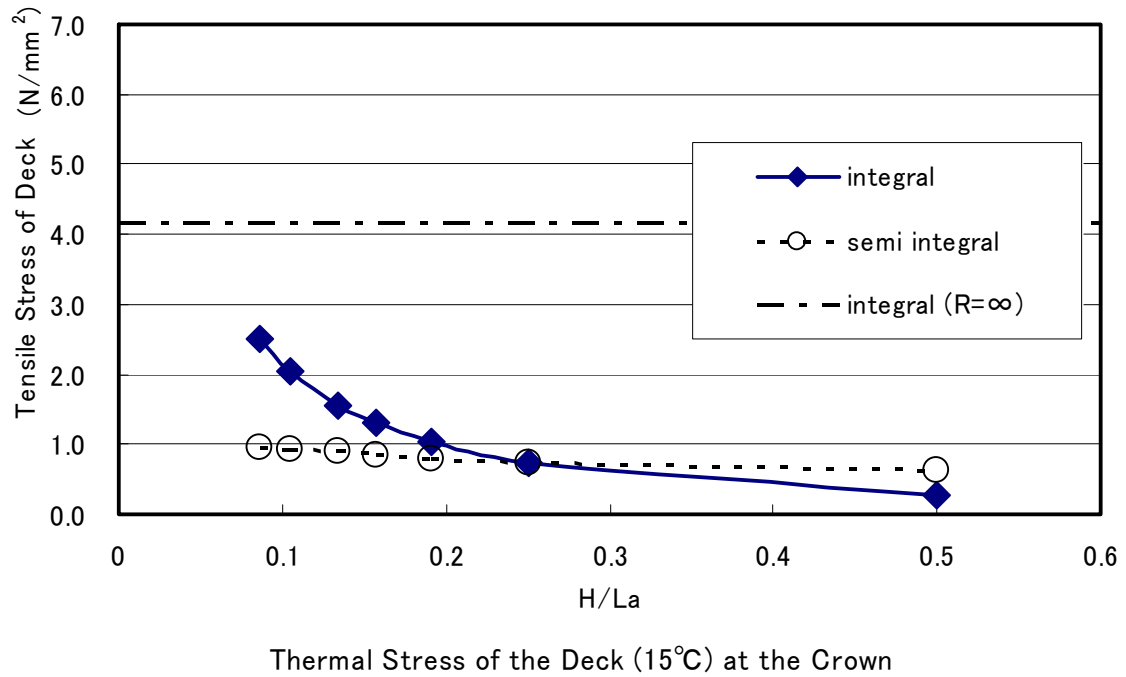


Fig. 3.24: Maximum transverse tensile stress of deck in the inner spans ($L_a=400m$)

The cracking of the deck eases the transverse bending moment by 37,3 % at the abutment and 11,5 % for the maximum of the inner spans. This also suggests that partially prestressed concrete structure is suitable for integral bridge system for its lower constraint stress than fully prestressed concrete structure.

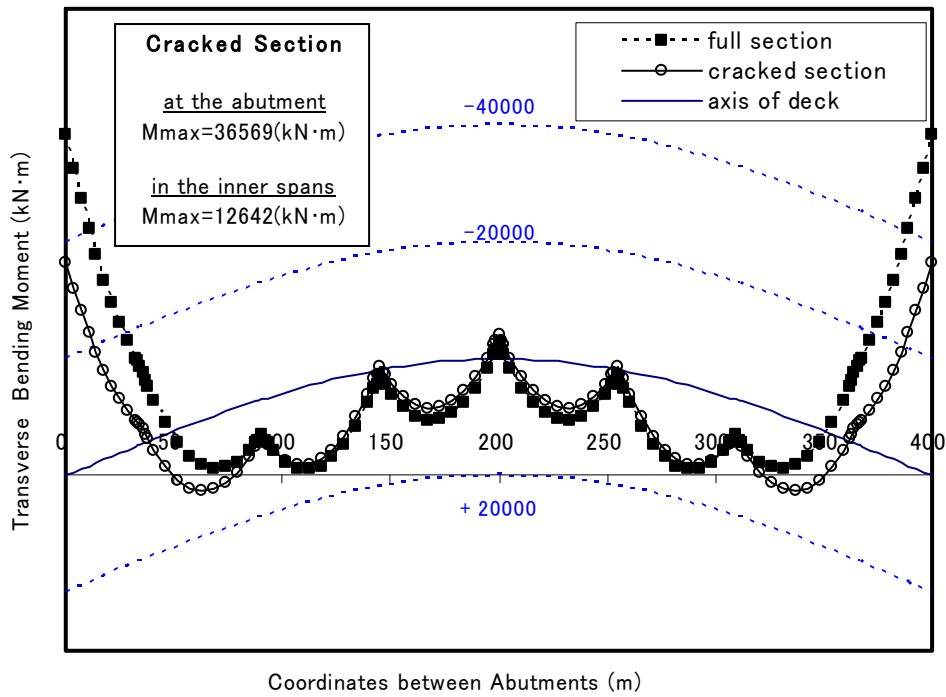


Fig. 3.26: Transverse bending moment of integral models ($L_a=400m$, $R=600m$, $L_a=1/11, 7$)

Table 3.5: Comparison of transverse bending moment

		kN·m	
		Abutment	Maximum of inner spans
(1)	Full section	58 282	14 279
(2)	Cracked section	36 569	12 642
(2) / (1)		62,7 %	88,5 %

3.9 Conclusion

The study on the static behaviour of integral bridge is concluded as follows.

- (1) Hinge connection for column (pier) - foundation is highly applicable for the bridge with rigid foundation.
- (2) The prestressing efficiency ζ is greatly influenced by the types of foundations, but not largely sensitive for the variance of the spring value of pile foundation. This means the feasibility of post-tensioned prestressed concrete integral bridge with pile foundation.
- (3) The extremely low prestressing efficiency of the model with spread footing means unfeasibility of post-tensioned prestressed concrete integral bridge. Thus, pile foundation should be applied to post-tensioned prestressed concrete integral bridge.
- (4) The curvature in plan of integral model lowers the constraint stress for its arch effects in plan to release the influences of temperature change, shrinkage, etc. by the sway deformation.
- (5) The lower H/L_a gives lower constraint stress for its higher arch effects.
- (6) The longer distance between abutments (L_a) gives lower constraint stress for its lower flexural stiffness of the arch in plan. This would suggest the good feasibility for long multi span curved integral bridge.
- (7) The cracking of the section releases constraint stress compared with uncracked section (*i.e.* full section) for its higher flexibility.
- (8) Partially prestressed concrete structure has better suitability than fully prestressed concrete structure, because it can lower the constraint stress by cracks with less prestressing, while full prestressing structure leads to higher constraint stress and requires more quantity of prestressing tendon.

References

- [3-1] *Specifications for Roadway Bridges*, Japan Road Association, Tokyo, Mar. 2002.
- [3-2] *Design Manual for Roads and Bridges*, Vol. 1 Highway Structures: Approval Procedures and General Design, Sect. 3 General Design, Part 7 BD 57/01 Design for Durability, The Highways Agency, U.K., Mar. 2003.
- [3-3] ENGLAND, G.L., TSANG, N.C.M., BUSH, D.I. *Integral Bridges - A Fundamental Approach to The Time-Temperature Loading Problem -*, Imperial College & The Highway Agency, U.K., Thomas Telford, 2000.
- [3-4] *Design Manual for Roads and Bridges*, Vol. 1 Highway Structures: Approval Procedures and General Design, Sect. 3 General Design, Part 12 BA 42/96 Amendment No.1, The Design of Integral Bridges, The Highways Agency, U.K., Mar. 2003.
- [3-5] TANAKA, J. and AKIYAMA, H. *Elegantly Curved Bridge -Kujira Bridge-*, National Report of fib Congress Osaka 2002, Japan Prestressed Concrete Engineering Association, Tokyo, 2002.
- [3-6] AKIYAMA, H., YOSHIDA, Y., HATADA, S., IMAMAKI, S. *Design and Construction of Inagi Central Park Cross Bridge*, Proceedings of the 7th Symposium on Developments in Prestressed Concrete, Japan Prestressed Concrete Engineering Association, Tokyo, pp.461-464, Oct., 1997.
- [3-7] KUTSUZAWA, K., SEKINE, Y., TANI, M., SASAKI, Y. *Construction of Yokomuki 1st Bridge By Incremental Launching Method*, Bridge & Foundation Engineering, Kensetsu Tosho, Tokyo, Vol.24, No.6, pp. 2-8, June, 1990.
- [3-8] MAEDA, H., KOMIYA, M., SAKAI, H. *A Study on the Analytical Method of PC Continuous and Curved Box Girders and Effect of Prestressing*, Japan Prestressed Concrete Engineering Association, Tokyo, Vol.45 No.3, pp. 87-96, May, 2003.
- [3-9] MAEDA, H., SAKAI, H., SO, S., MITSUI, Y. *Creep Analysis Study of PC Curved Box Girder Bridge*, Japan Prestressed Concrete Engineering Association, Tokyo, Vol.46 No.4, pp. 73-82, Jul., 2004.
- [3-10] *Standard Specifications for Concrete Structure-2002, Structural Performance Verification*, Japan Society of Civil Engineers, Tokyo, 2002.

Chapter 4 Seismic Design of Integral Bridges

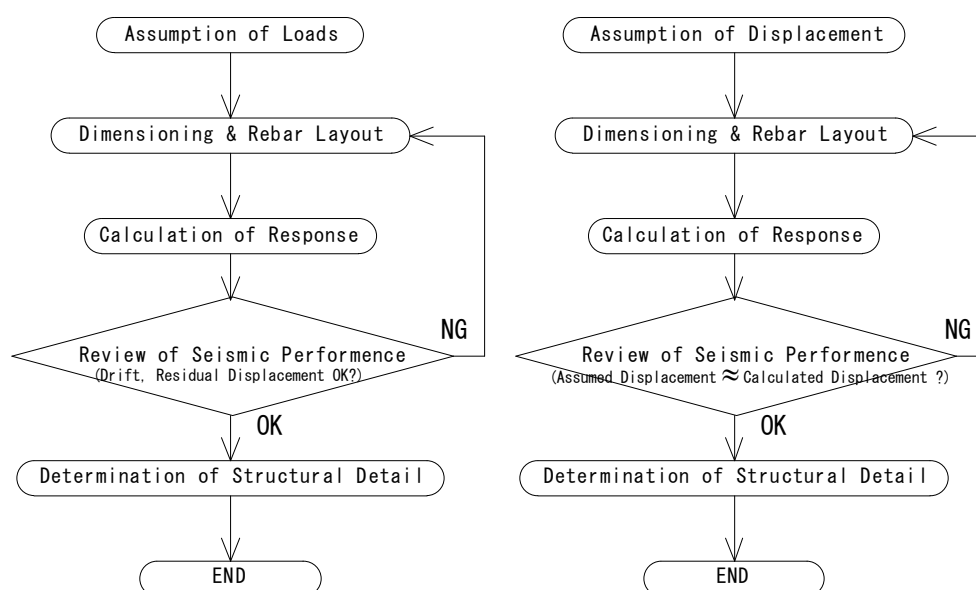
4.1 Introduction

Structural system of bridge is often determined by the requirement for seismic design in high seismic zone, since structural system is dominant factor for seismic characteristics of the structure.

Among alternatives, integral bridge solution does not only give eminent benefits for breaking loads resistance, but also for seismic performance. The benefits of integral bridges for seismic performance compared with conventional simply supported bridges are as following.

- Higher redundancy for high indeterminate structural system
- Higher damping effect by both abutment backfill
- Smaller displacement
- Avoidance of fall-down of superstructure for its monolithic form of structural system without failsafe devices (fall-down prevention devices)

By the way, force based design method has been widely used for bridge design for decades in Japan. Force based design is simple and easy to calculate the loads and responses for designers, however the limit state is not easy to imagine, understand and evaluate the serviceability of the structure damaged by earthquake.



Flow of Force Based Design

Flow of Displacement Based Design

Fig. 4.1: Flows of force based design and displacement based design

As an alternative solution for seismic design, displacement based design, that is employed by Caltrans (California Department of Transportation), is unique and reasonable design method. The procedure of displacement design is as following.

AT first, the limit displacement is specified. Second, trials of dimensioning and reinforcement layout are made to obtain enough deformation capacity for the specific earthquakes (*Fig. 4.1*). Finally, structural details are determined in accordance with appropriate specifications.

Displacement based design is rational design method, because it gives the results by displacements that is clear and easy to understand the limit state. In addition, it enables to make the deformation capacity in earthquake close to the assumed deformation capacity; it also leads to economical design.

By the way, not a few cases were appeared that happened gaps between abutments and approach parts among past damaged cases caused by earthquakes (*Photo 4.1*). When happened with jammed traffic, the gaps would possibly outbreak serious secondary diseases.



*Photo 4.1: Gap at the abutment caused by Noto Peninsula Earthquake, 2007
(By favour of Hiroshi MASUYA)*

The employment of integral bridges and cement treated soil for backfill would be predominant candidate for the countermeasure to mitigate the gaps in earthquake. Cement treated soil has good stability even in case of large scale earthquake, however damping effect is not clearly quantified and evaluated, while normal soil.

Thus, backfill is empirically evaluated to have high damping effect for earthquake. Thus, conventional static design can not be applied for the abutments with cement treated soil; ductility design is essential for designing the abutments with cement treated soil.

Besides, the setting of limit displacement after earthquake is also effective policy to secure the serviceability for highway drivers. Displacement based design is supposed to be suitable for such cases, *i.e.* in case of setting the limit displacement at the initial step of the design, because it explicitly gives the results of the design by displacement.

So as to apply the displacement based design in Japan, however code calibration is essential to prevent large differences between the results of different design methods. Especially, the evaluation of ductility is crucial for the seismic design.

Thus, calculation of confining reinforcement is the focus of the assignment on displacement based design and its code calibration.

The outline of the displacement based design is described with the response displacement convert diagrams from response acceleration spectrum diagrams of *Specifications for Roadway Bridges Part V (Seismic Design)* for each type of earthquake and soil class.

A case study on the confining reinforcement is discussed for with single span integral bridge model comparison between *Specifications for Roadway Bridges* and *Caltrans Seismic Criteria*, JIS Standard and ASTM Standard.

4.2 Displacement Based Design Concept

4.2.1 Procedure of Displacement Based Design

The procedure of displacement based design with equivalent linear method proposed by M.J.N.Priestley *et al.* is shown in *Table 4.1* [4.3].

There are two alternative ways to set the limit displacement; one is to set the limit as the design displacement Δ_d at the position of inertial centroid, the other is to set the plastic drift θ_p at the plastic hinges. Here, the latter is employed in the case study described in following clauses to specify the damage limit state at the plastic hinges for convenience as $\theta_p=0,03$.

Table 4.1: Procedure of displacement based design

	Contents	Description
1	Assumption of initial value of yield displacement Δ_y	Empirically " $\Delta_y=0,05H$ " is assumed (H : Distance between lower hinge of substructure and centroid of inertial force of superstructure)
2	Setting of plastic drift θ_p	Generally set as $\theta_p=0,03$
3	Calculate the design displacement Δ_d when the drift of plastic hinge achieves to the limit state	Calculate the yield displacement by pushover analysis. Calculate the design displacement Δ_d that is the displacement when the drift of plastic hinge achieves the limit state. $\Delta_d = \Delta_y + \theta_p \cdot H \quad (4.1)$
4	Estimation of equivalent damping ratio ξ	Estimate appropriate relation of Responed plastic ratio - Damping Ratio. (Degrading Takeda Model is employed in this study.)
5	Calculate equivalent natural period T_d correspondent with the design displacement Δ_d	Detailed below (<i>q. v.</i> equations (4.4), (4.5))
6	Calculation of design horizontal force	Detailed below (<i>q. v.</i> equations (4.6), (4.7), <i>Fig. 4.9</i>)
7	Calculation of elastic stiffness and yield displacement	Calculate the yield displacement by elastic theory with elastic stiffness
8	Judgement of convergence	Trial until convergence of the results. Calculate ultimate displacement, responed plastic ratio, equivalent damping ratio with trials of dimensioning and rebar layout.
9	Calculation of confining rebar, structural details	Calculate required confining rebar

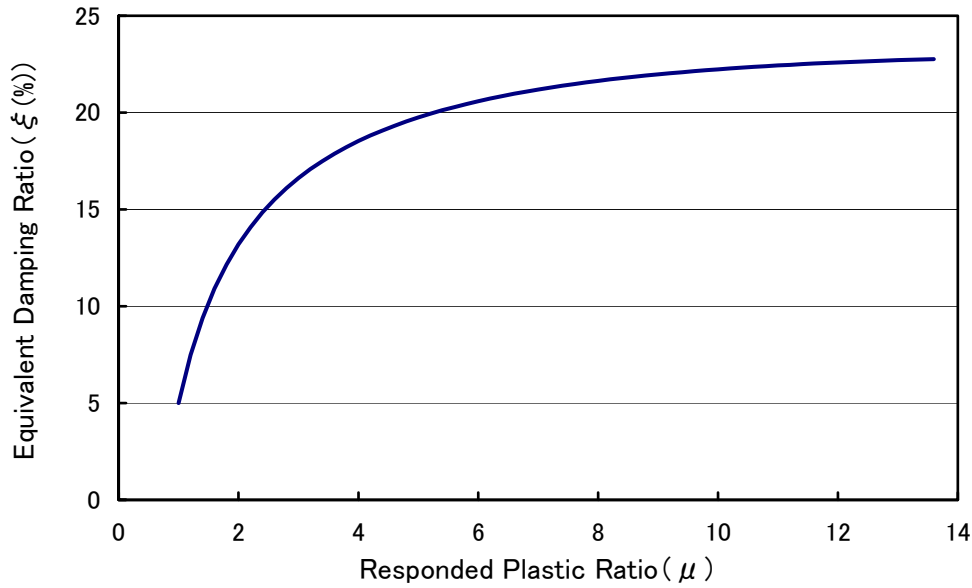


Fig. 4.2: Equivalent damping ratio-responded plastic ratio relationship

$$\xi = 0,05 + \frac{(1 - \frac{1-\gamma}{\sqrt{\mu}} - \gamma\sqrt{\mu})}{\pi} \quad (4.2)$$

where,

γ : secondary stiffness ratio in bi-linear model

(generally, $r=0,05$ for reinforced concrete members)

μ : responded plastic ratio(= Δ_d / Δ_y)

Displacement response spectrums are converted from the acceleration response spectrums which are shown in *Specifications for Roadway Bridges Part V (Seismic Design)*.

The conversion is conducted by following equation (4.3).

$$S_d = \frac{S_a}{\omega^2} \quad (4.3)$$

where,

S_d : displacement response spectrum

S_a : acceleration response spectrum

ω : natural circular frequency (Hz)

The displacement-acceleration response spectrum diagrams of *Specifications for Roadway Bridges* are shown in *Figs. 4.1 - 4.6*.

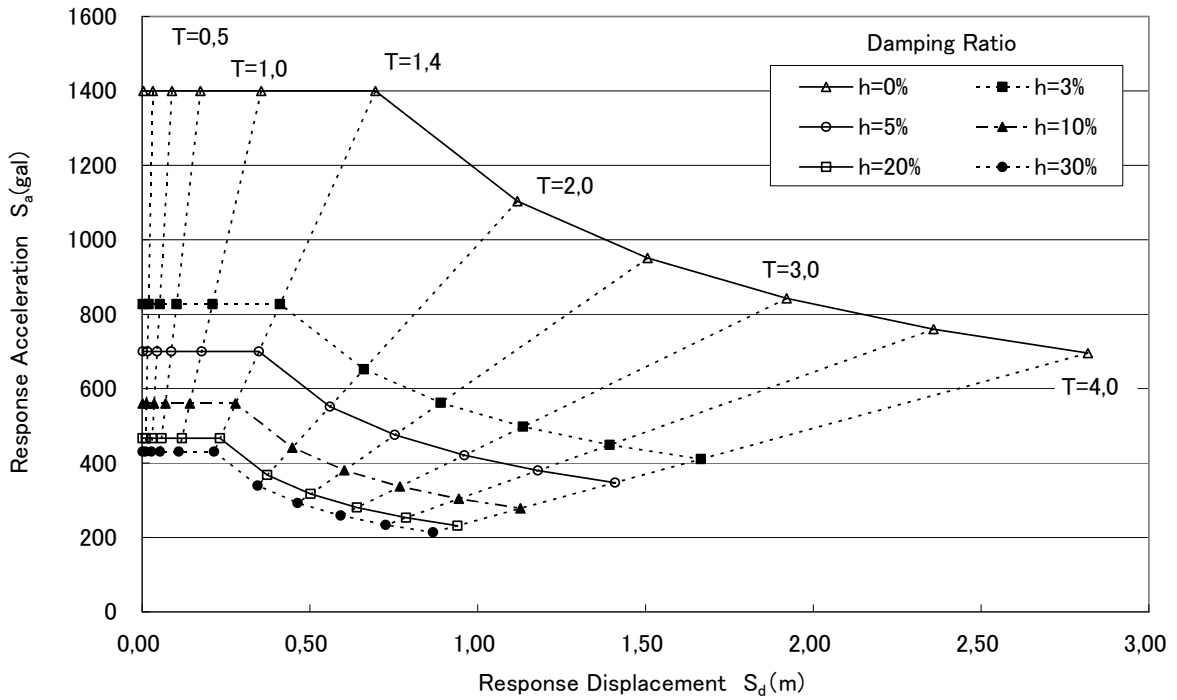


Fig. 4.3: Displacement-acceleration response spectrum diagram
(Type I earthquake, Soil class I)

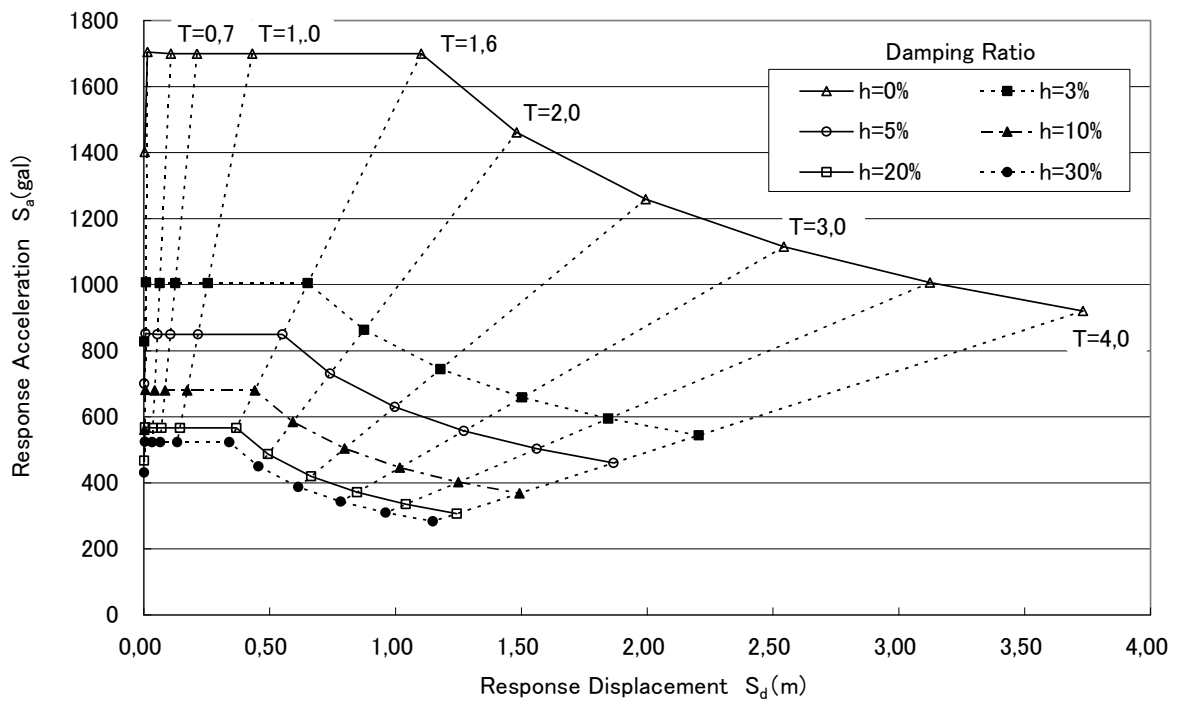


Fig. 4.4: Displacement-acceleration response spectrum diagram
(Type I earthquake, Soil class II)

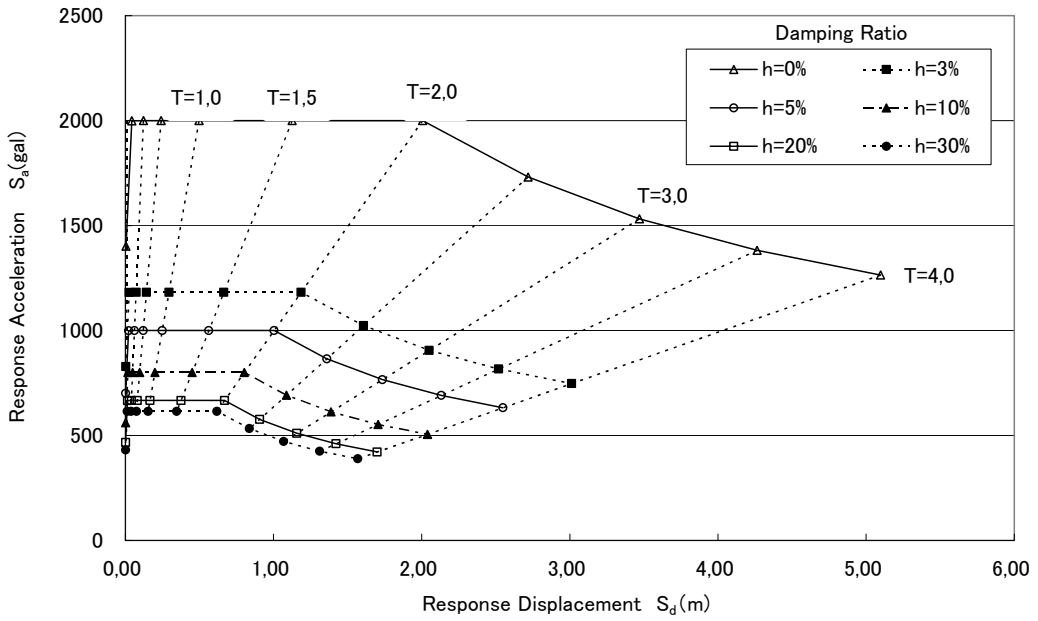


Fig. 4.5: Displacement-acceleration response spectrum diagram
(Type I earthquake, Soil class III)

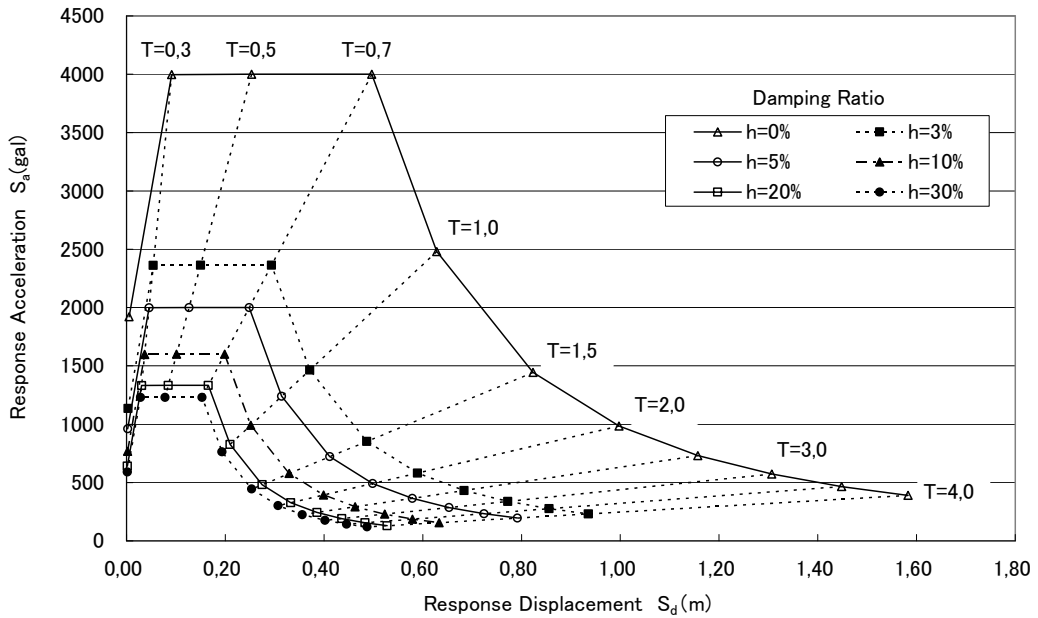


Fig. 4.6: Displacement-acceleration response spectrum diagram
(Type II earthquake, Soil class I)

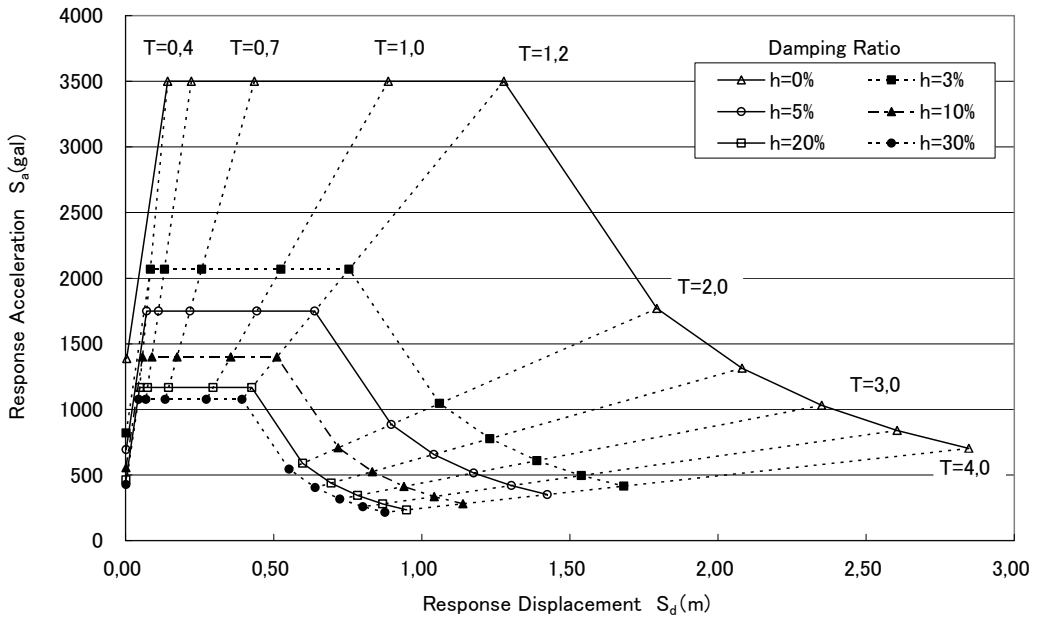


Fig. 4.7: Displacement-acceleration response spectrum diagram
(Type II earthquake, Soil class II)

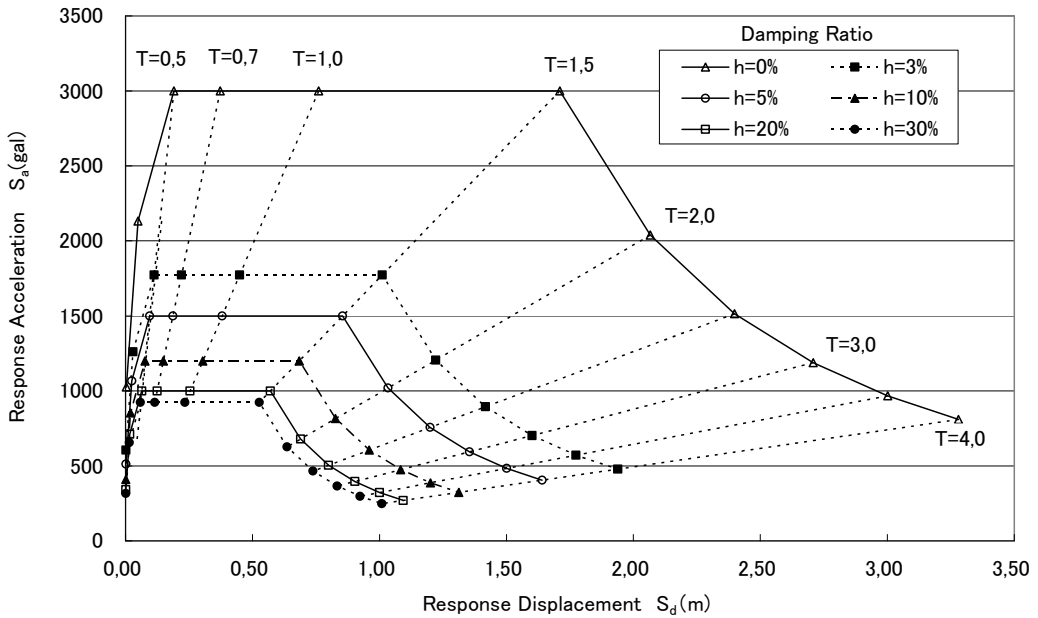


Fig. 4.8: Displacement-acceleration response spectrum diagram
(Type II earthquake, Soil class III)

The equivalent natural period at maximum response (T_d) and its equivalent stiffness (K_e) are described by following equations.

$$T_d = 2\pi \sqrt{\frac{M}{K_e}} \quad (4.4)$$

$$K_e = \frac{4\pi^2}{T_d^2} M \quad (4.5)$$

where, M is equivalent mass.

The required resistance at maximum response (F_u) is calculated by following equation.

$$F_u = K_e \Delta_d \quad (4.6)$$

The design required resistance (F_n) in equivalent bi-linear response model is calculated as following equation.

$$F_n = \frac{F_u}{\gamma\mu - \gamma + 1} \quad (4.7)$$

Calculate the yield displacement (Δ_y) and design displacement (Δ_d) with elastic stiffness (K_i) that is calculated by elastic theory with the dimensions and reinforcement layout assumed in the preliminary design (Fig. 4.9).

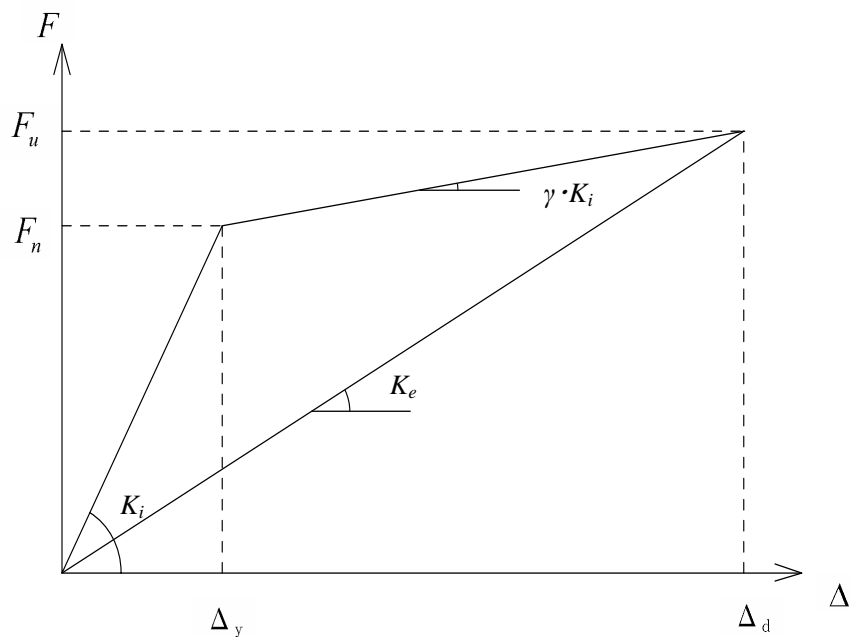


Fig. 4.9: Displacement - resistance diagram

The calculation of displacement, optimisation of dimension and reinforcement layout would be conducted repeating the trials of total displacement, responded plastic ratio and equivalent damping ratio through the process of 5-8 in *Table 4.1* to obtain the converged results. The criterion of the convergence of the calculation is assumed as $\pm 5\%$ in this case study.

The damage limit state is defined as the state when overtook, it becomes impossible to retrofit for economical and technical aspects [4.3]; the plastic drift of plastic hinge is proposed to be $3,0\%$ ($\theta_p=0,03$) as of the appropriate damage limit state. The plastic drift, $3,0\%$, is also employed as the damage limit state in this study.

There are two methods to calculate the required confinement. One is to calculate it in accordance with *Specifications for Roadway Bridges* to obtain enough deformation performance to implement to deform to Δ_d , the other is to calculate it by the design equations between ultimate strain of confined concrete (ϵ_{cu}) and confinement ratio (ρ_s) in accordance with *Caltrans Seismic Criteria* described by eq. (4.8).

$$\rho_s = (\epsilon_{cu} - 0,004) \times \frac{f'_{cc}}{1,4 \times f_{sy} \times \epsilon_{su}} \quad (4.8)$$

where,

ϵ_{cu} : ultimate strain of confined concrete

f'_{cc} : maximum stress of confined concrete

f_{sy} : yield stress of confining rebar

ϵ_{su} : confining rebar strain at the tensile strength

Caltrans Seismic Criteria specifies the confining rebar strain at the tensile strength as 12% that is larger than the requirement of ASTM A 615M for the reflection of actual property of generally available products.

In general, Grade 60 of ASTM A 615M [4.5] ($60 \text{ ksi} = 420 \text{ N/mm}^2$) rebar is widely used in U.S.A., while SD345 of JIS G 3112 [4.6] rebar is widely used in Japan.

JIS G 3112 specifies yield strength, tensile strength and elongation; however it does not specify the strain at tensile strength.

Thus, tests are conducted to research the strain at tensile strength

using rebar of SD345 (D25) as the preliminary research. The results are shown in *Table 4.2* with the specified values of ASTM and JIS.

Table 4.2: Specifications of rebar and test results

Standard	Grade	Yield strength	Tensile strength	Elongation
		N/mm ²	N/mm ²	%
ASTM A 615M	Grade60	420	620	9
JIS G 3112	SD345	345	490	20
JIS G 3112* (Test Results (D25))	SD345	406, 5	605, 8	51, 8

※The strain at Tensile Strength was 27, 4%.

The result of tensile strain at tensile strength was 27,4 % that was 1,37 times of the requirement of rebar elongation of JIS G 3112. As the test results are always larger than the requirement of the specifications, the characteristic values should be determined by actual values of generally available material. However the actual value of the tensile strain at tensile strength of SD345 was not clarified for scant data in this study.

The characteristic values of the strain at tensile strength (ϵ_{su}) when calculated in accordance with *Caltrans Seismic Criteria* with SD345 rebar is employed for the confinement were assumed as 12 % and 20 %. The former is Caltrans' requirement; the latter is the required elongation of JIS G 3112 in the following case study to obtain conservative results.

4.3 Case Study on Single Span Integral Bridge

4.3.1 Structural Model

The model in this study is partially prestressed concrete single span rigid frame bridge which has 35,0 m span and cement treated soil for abutment backfill as shown in *Figs. 4.10* and *4.11*.

Conventional static design method is usually applied to the abutment design only for level 1 earthquake for the damping effects of the backfill soil, however ductility design for level 2 earthquake is necessary when cement treated soil is employed without considering damping effects of the backfill soil.

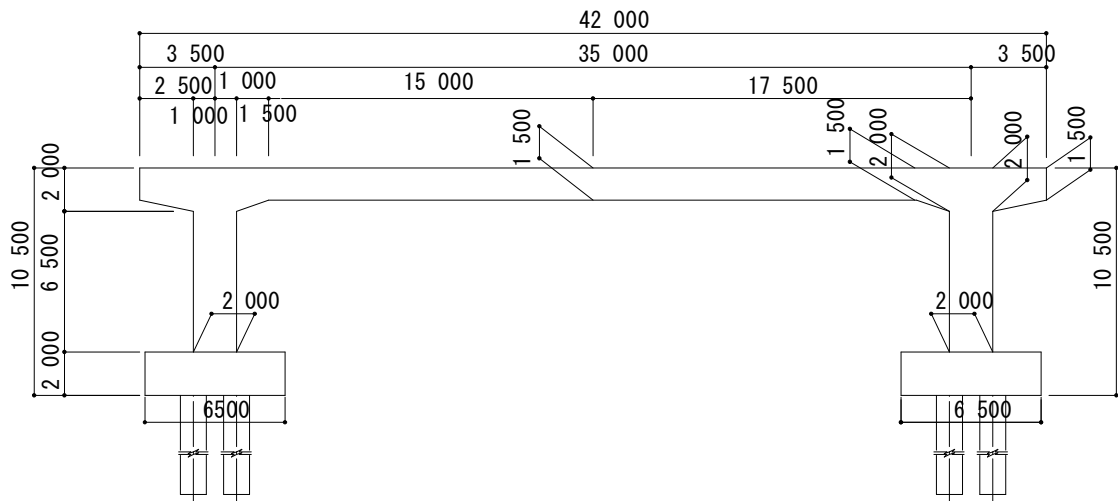


Fig. 4.10: Elevation of model bridge

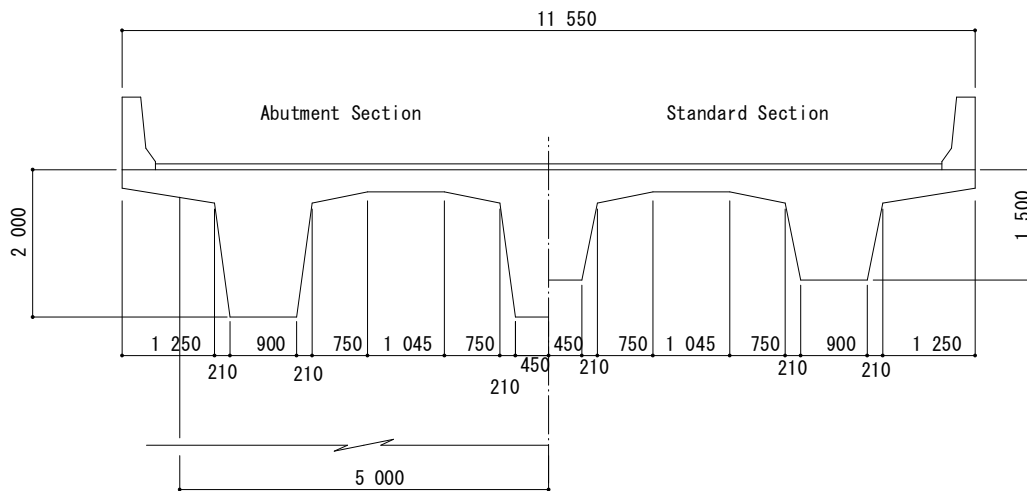


Fig. 4.11: Cross section of model bridge

The structural model is shown in Fig. 4.11. Each member is modelled as shown in Table 4.3.

Table 4.3: Element modelling

Member classification		Element classification
Superstructure	All members	Linear frame elements
Substructure	Plastic hinges	Non-linear rotation spring elements (Bi-linear model)
	Members except plastic hinges	Linear frame elements
Foundation	Pile foundations	Linear rotation spring elements

The plastic hinges were modelled by non-linear rotational spring elements in accordance with *Specifications for Roadway Bridges* as complete elasto-plastic model (bi-linear model). The yield displacement was defined as the displacement at the centroid of inertial force of superstructure when the first plastic hinge came to initial yield state. Foundations were modelled by linear spring elements, since foundations were designed within pre-yield state in general roadway bridge design. The material specifications are shown in Table 4.4.

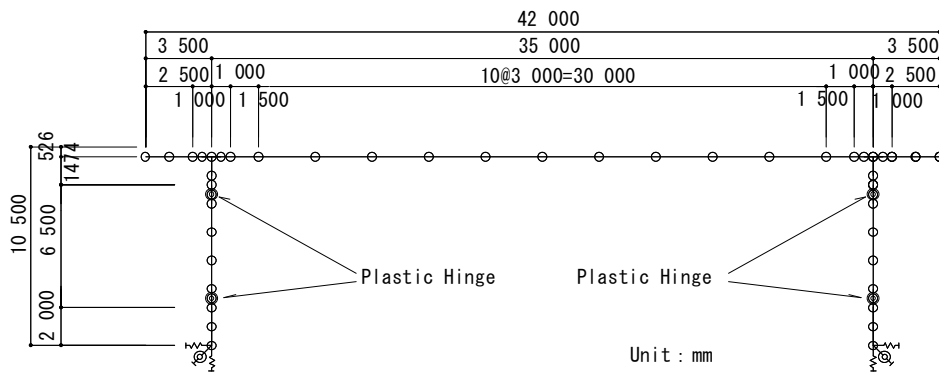


Fig. 4.12: Skelton of structural model

Table 4.4: Element modelling

Material classification	Grade	Remarks
Superstructure concrete	40N/mm ²	
Substructure concrete	30N/mm ²	
Reinforcement	SD345	
Prestressing steel	SWPR19L 1S28.6	

4.3.2 Results

Eigen value analysis was conducted; the vibration mode diagram of first longitudinal mode is shown in *Fig. 4.13*.

The natural period of first longitudinal mode and effective mass ratio are 0,54 sec and 92,0 % respectively. These results suggest the suitability of application of equivalent linear method to this structural model.

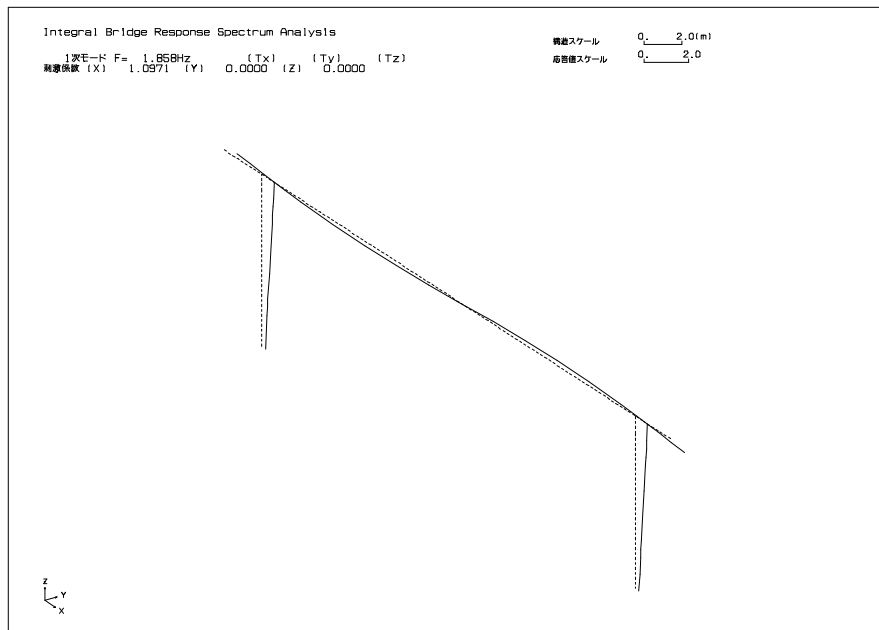


Fig. 4.13: Vibration mode diagram of first longitudinal mode

The staple values of the results are shown in *Table 4.5*. The modified yield displacement (Δ_y) and modified ultimate displacement (Δ_u) in *Table 4.5* mean the results by trial calculations for dimensioning and rebar layout from initial assumptions.

The results of the displacement based design with equivalent linear method for partially prestressed concrete single span rigid frame bridge in this case study are summarised as following.

- (1) The confining rebar strain at tensile strength largely influences upon the plastic hinge length and required confining reinforcement ratio. Thus, appropriate strain should be specified.
- (2) *Caltrans Seismic Criteria* estimates larger value of the maximum compressive strength of confined concrete (f'_{cc}) than *Specifications for Roadway Bridges Part V (Seismic Design)*.

(3) The calculated amount of required confining reinforcement in accordance with *Caltrans Seismic Criteria* is relatively small as to be determined by minimum reinforcement ratio.

For reference, force based design in accordance with *AASHTO LRFD Design Specifications* contains resistance reduction factor in the process of performance review, while displacement based design in accordance with *Caltrans Seismic Criteria* does not contain deformation reduction factor. Thus, the comparisons with *Specifications for Roadway Bridges Part V* are not necessarily the same [4.7].

Table 4.5: Results of displacement based design

	Unit	Case 1	Case 2	Case3	Case 4
Design Code	-	Caltrans Seismic Criteria	Caltrans Seismic Criteria	Caltrans Seismic Criteria	Specifications for Roadway Bridges
Specification of Confinement	-	ASTM GR60	JIS SD345	JIS SD345	JIS SD345
Strain of Confinment at Maximum Stress ϵ_{su}	-	0,12	0,12	0,20	-
Plastic Drift of Plastic Hinge θ_p	rad	0,030	0,030	0,030	0,030
Distance between Lower Plastic Hinge and Inertial Centroid H	m	7,551	7,551	7,551	7,599
Plastic Hinge Length	m	0,847	0,847	0,847	0,750
Horizontal Ultimate Displacement Δ_u	m	0,246	0,246	0,246	0,247
Initial Value of Yield Displacement Δ_y	m	0,019	0,019	0,019	0,019
Responded Plastic Ratio μ	-	12,922	12,922	12,922	12,998
Equivalent Damping Ratio ξ	-	0,227	0,227	0,227	0,227
Equivalent Natural Period T_e	sec	1,320	1,320	1,320	1,320
Equivalent Mass M	t	1179,2	1179,2	1179,2	1179,2
Equivalent Stiffness K_e	kN/m	26718	26718	26718	26718
Elastic Stiffness K_i	kN/m	212436	212436	212436	207404
Ultimate Horizontal Force F_u	kN	6560	6560	6560	6599
Design Horizontal Force F_d	kN	4110	4110	4110	4124
Dimension of Cross Section	-	1,5 × 10,0m	1,5 × 10,0m	1,5 × 10,0m	1,5 × 10,0m
Longitudinal Reinforcement	-	D32 × ctc150 1,5 rows			
Modified Yield Displacement Δ_y	m	0,019	0,019	0,019	0,020
Modified Ultimate Displacement Δ_u	m	0,250	0,250	0,250	0,258
(Midified Δ_u /Initial Δ_u)	-	1,018	1,018	1,018	1,047
Judgement (Criterion: ±5%)		OK !	OK !	OK !	OK !
Confined Compressive Concrete Strength f'_{cc}	N/mm ²	45,90	44,73	44,73	42,90
Ultimate Strain of Confined Concrete ϵ'_{cu}	-	0,0064	0,0064	0,0064	0,0069
Calculated Required Confinement Volum Ratio ρ_{s1}	-	0,00141	0,00167	0,00100	0,01351
Minimum Confinment Ratio ρ_{s2}	-	0,00687	0,00687	0,00687	0,00169
Required Confinement Ratio ρ_s	-	0,00687	0,00687	0,00687	0,01351
Area of Required Confinement A_w	cm ²	2,577	2,577	2,577	5,067
Confinement Layout	-	D19ctc150	D19ctc150	D19ctc150	D25ctc150

4.4 Conclusion

The conclusion and further assignments are as following.

- (1) The influence of the strain at tensile strength of confining rebar largely influences upon the confining reinforcement ratio when calculated by equation (4.8).
- (2) The design equation is highly expected to enables the reflection of tensile strength and strain of confinement upon the stress-strain curve of confined concrete and required confinement ratio in order to cover the use of various materials such as high strength rebars.
- (3) As not a little difference appeared in the results between design codes, the design specifications should also reflect the local conditions such as material properties, earthquake characteristics, performance requirements, design philosophies etc.
- (4) The establishment of design equation based on *Specifications for Roadway Bridges* is highly expected to reflect past achievement of research and Japanese local conditions such as the earthquake classifications (Type I and II), locally available and popular material properties including over strength etc.
- (5) Besides above described matters, the establishment of the specifications on the serviceability limit displacement of superstructure damaged by large scale earthquake is also crucial issue for the better bridge performance.

Displacement is more important index than force or resistance to evaluate damage intensity and serviceability after earthquake. In this sense, displacement based design is useful design solution, especially when integral bridge such as portal rigid frame bridges are applied. In addition, when necessary to restrict the gap between abutment and approach, displacement based design is reasonable and suitable design method for its clear and explicit evaluation.

Besides resolutions of above assignments, code calibration of partial safety factors is essential for the establishment of rational limit state design based on displacement based design method with partial safety factors.

References

- [4.1] *Seismic Design Criteria Version 1.3*, Caltrans, 2004.
- [4.2] *Specifications for Roadway Bridges Part V (Seismic Design)*, Japan Road Association, Mar., 2002.
- [4.3] PRIESTLEY, M.J.N., SEIBLE, F. CALVI, G.M. *Seismic Design and Retrofit of Bridges* (Japanese Version:KAWASHIMA, K. (trans.)), Gihodo Shuppan, Tokyo, 1998,.
- [4.4] Kowalsky, M.J., PRIESTLEY, M.J.N., MACRAE, G.A. *Displacement-Based Design: "A Methodology for Seismic Design Applied to single Degree of Freedom Reinforced Concrete Structures"*, Department of Applied Mechanics and Engineering Science, University of California, San Diego, Structural Systems Research Project SSRP 94/16, Oct. 1994.
- [4.5] American Society for Testing and Materials *ASTM A 615/A 615M Standard Specification for Deformed and Plain Carbon-Steel Bars for Concrete Reinforcement*, Mar. 2007.
- [4.6] *JIS Handbook, 12 Civil Engineering II*, Japan Standard Association, 2003.
- [4.7] HOSHIKUMA, J., UNJOH, S. *Comparison of Seismic Design of Reinforced Concrete Bridge Column between U.S. and Japan*, Proceedings of the Japan Concrete Institute, Vol.25, No.2, pp.1435-1440, 2003.
- [4.8] AKIYAMA, H., MIZUTORI, K., YAMAHANA, Y., KAJIKAWA, Y. *A Study on The Application of Displacement Based Design to Portal Rigid Frame Bridge*, Proceedings of Symposium on Development Prestressed Concrete, Vol.15, Japan Prestressed Concrete Engineering Association, pp.153-156, Oct., 2006.
- [4.9] AKIYAMA, H., FUKADA, S., MIZUTORI, K., KAJIKAWA, Y. *A Study on The Calculation of Confining Reinforcement of Displacement Based Design*, Proceedings of Symposium on Development Prestressed Concrete, Vol.16, Japan Prestressed Concrete Engineering Association, pp.25-30, Oct., 2007.

Chapter 5 Vibrational Serviceability of Integral Bridges

5.1 Introduction

The vibration under traffic load is often the major focus of bridge serviceability and environmental problems, especially when a flexible structure is constructed in urban areas where the ground is soft [5-1], because the traffic load sometimes brings about undesirable vibration phenomena, e.g. uncomfortable vibration for pedestrians, infrasound and ground vibration. These vibration phenomena are caused mainly by low frequency vibration, which in turn is caused by the interaction between vehicles and structures.

By the way, the characteristics of bridge vibration is dependent upon the bridge system, stiffness of the bridge and foundation, live load, roughness of the road surface, etc.; among many factors for bridge vibration, appropriate selection of structural system for the bridge is essential to control the bridge vibration caused by live load.

This chapter presents the studies on four bridge systems as shown in *Fig. 5.1*.

The first, the most popular structural system, is the conventional simple girder bridge that sometimes has problems related to traffic vibration as described above. The extended deck solution is sometimes employed in Japan to control the infrasound and ground vibration [5-2, 5-3]. On the other hand, integral bridges are recently being more often applied to single span bridges to ease the vibrational problems because of the cost and maintenance aspects, while semi-integral bridges can be applied to short abutments to eliminate expansion joints at the ends of the girders.

The definitions of the structures are as follows (*Fig. 5.1*).

Conventional bridge is the most simple and popular bridge system, with bearings and expansion joints at both ends of the girders (*Fig. 5.1(A)*).

Extended deck bridge has bearings and the extended seamless and continuous deck forward approach with expansion joints at the ends of the extended decks. This kind of structural system is sometimes applied to new bridge construction projects and retrofitting projects on location, with sensitive environmental requirements for infrasound and ground vibration, in Japan (*Fig. 5.1(B)*).

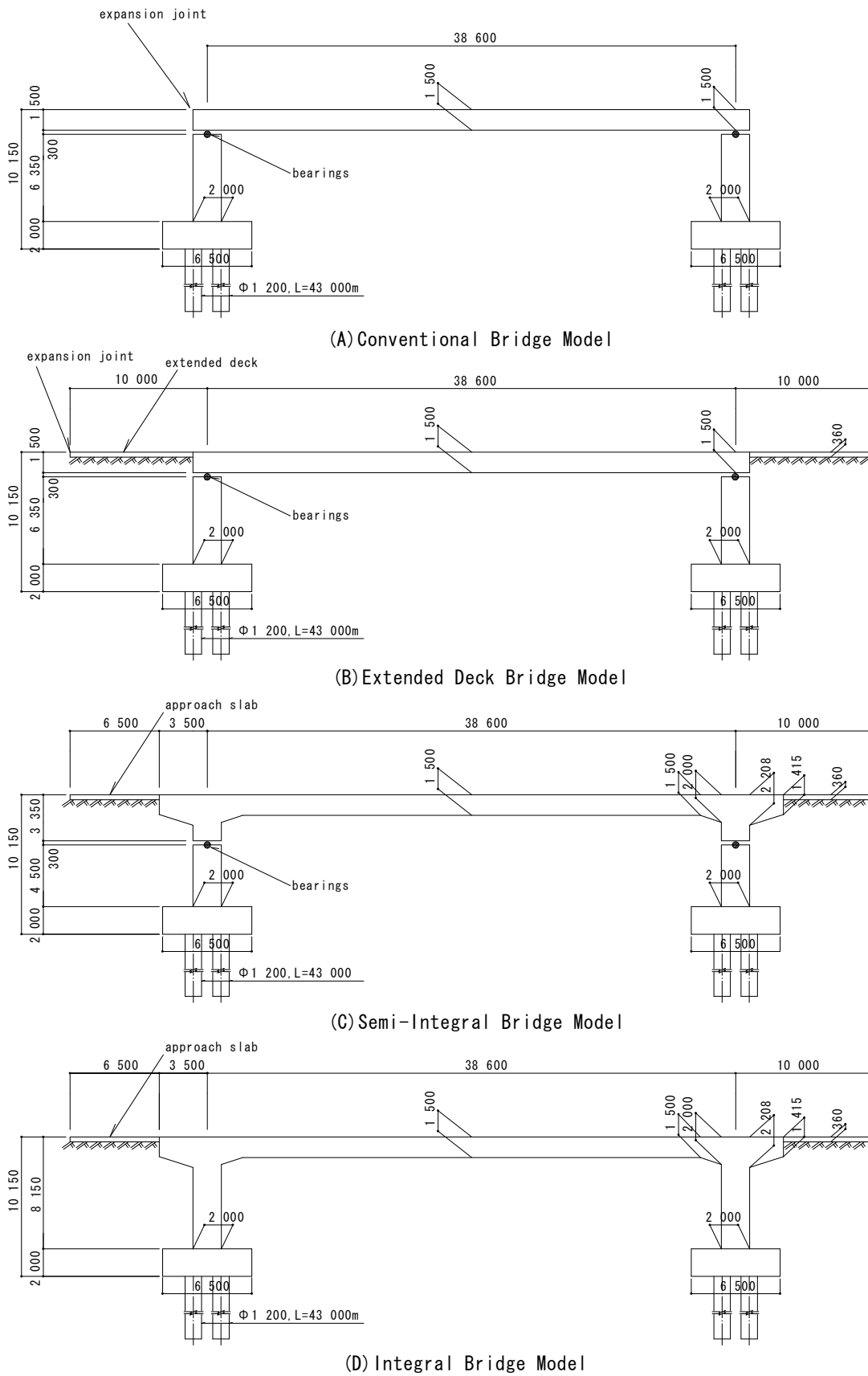


Fig. 5.1: Structural models

Semi-integral bridge [5-4] has bearings beneath the short piers on the abutments without expansion joints, but the horizontal force is not released by the bearings to minimise the movement (*Fig. 5.1(C)*). Integral bridge [5-5, 5-6] has neither bearings nor expansion joints (*Fig. 5.1(D)*).

The author studied the vibrational impact of these structural systems upon the vibrational serviceability and environmental impacts, *i.e.* infrasound and ground vibration. The analyses were conducted for flexible single span bridge models on soft ground to study the vibrational problems described above, with the knowledge obtained from past studies, including field monitoring of existing bridges.

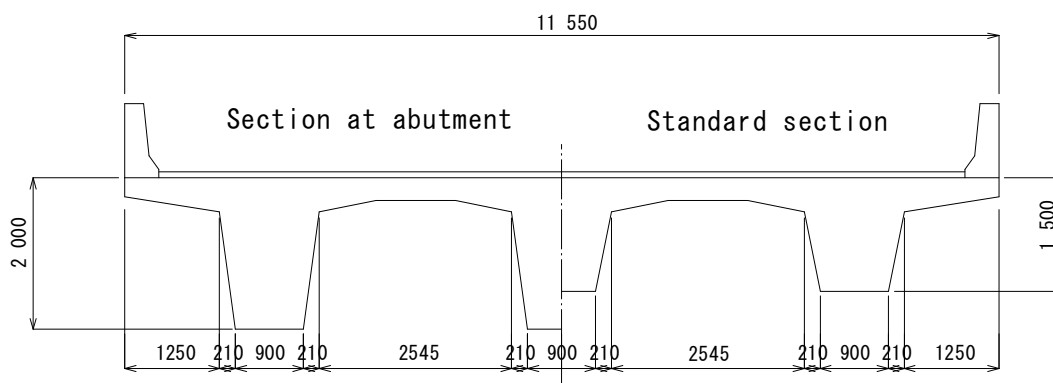


Fig. 5.2: Cross section of super structure

5.2 General Description of the Numerical Study

5.2.1 Parameters of the Analyses

The analyses were conducted with the finite element method that includes structural models of the superstructure, substructure, bearings, approach slab, extended deck and moving truck model whose wheels comprise two-degree-of-freedom systems of suspension springs and tire springs (*Fig. 5.5*) [5-7]. The parameters for the numerical study are as follows (*Table 5.1*).

- Approach Length
- Stiffness of the approach slab bed/extended deck bed (ground beneath the approach slab/extended deck)
- Stiffness of bearings
- Stiffness of the foundations (completely rigid foundations or pile foundations on the soft ground)
- Tracking lane (lateral location of the moving truck)
- Speed of the moving truck

Table 5.1: Analytical cases

		Conventional	Extended Deck	Semi-Integral Bridge	Integral Bridge
		C	E	S	I
Approach Length	0m	00	—	—	—
	3m	—	03	—	—
	6m	—	06	—	—
	10m	—	10	10	10
Stiffness of Approach Slabs Bed	Nominal	—	G	G	G
	Fix	—	F	F	F
Stiffness of Bearings	Nominal	B	B	B	—
	20 times	H	H	H	—
Stiffness of Foundations	Nominal	P	P	P	P
	Rigid	R	R	R	R
Tracking Lane	Central	C	C	C	C
	Side	S	S	S	S
Speed	40km/hour	40	40	40	40
	80km/hour	80	80	80	80

example : The case name "110FPC80" means the following.
Integral model, 10m approach, Fixed approach slab bed, nominal Pile foundation stiffness, Central tracking, 80km/hour

5.2.2 Structural Modelling

The vibrational characteristics under heavy vehicle were numerically studied with three-dimensional (3D) finite element models for four different structural models (Figs 5.1 and 5.2). The finite element mesh of the integral bridge model is shown in Fig. 5.3. The deck, extended decks, approach slabs, webs of the girder and cross beams were modelled with shell elements. Abutments were modelled with frame elements. The foundations, bearings and soil under the extended deck and approach slab were modelled with spring elements (Fig. 5.4). The webs and deck were rigidly connected. Barriers were only considered as masses without any stiffness for the structure. As the initial stiffness of the non-linear stress-strain curve of the elastometric bearing largely influences the displacement of the bearings under small amplitude vibration, two kinds

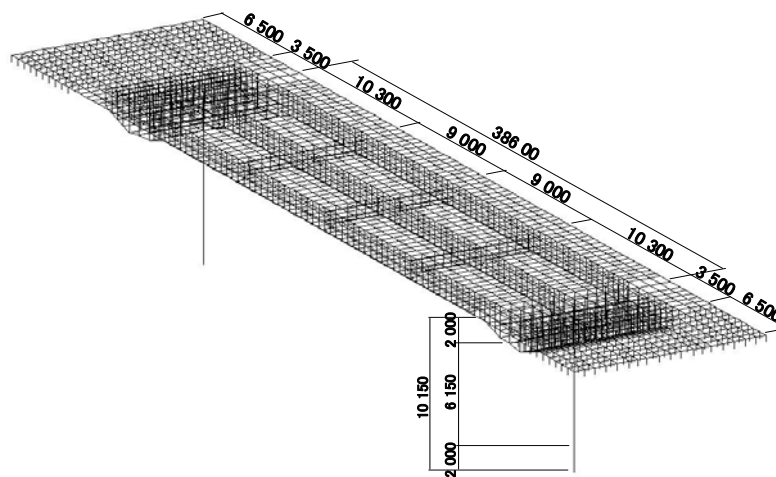


Fig. 5.3: Finite element model of integral bridge

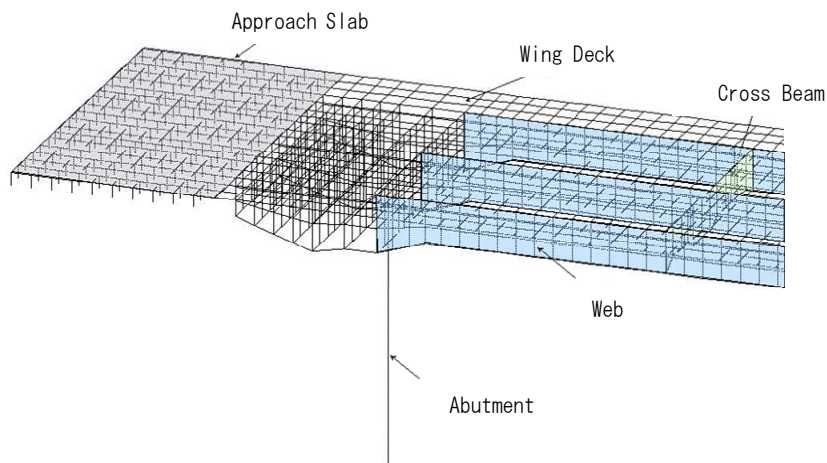


Fig. 5.4: Finite element model of integral bridge

of bearing stiffness were set to study the influence, nominal equivalent linear stiffness and 20 times the nominal value. From our past studies of existing bridges, the modified elastic modulus for the small amplitude vibration analysis is empirically known to give a good fitting [5-7, 5-8].

This chapter presents the static characteristics, vibrational characteristics (natural frequencies, vibration modes and strain energy share for damping) by eigen value analysis with sub-space method and dynamic response characteristics under vehicular live load with interaction between the structure and heavy vehicle (truck) by dynamic analysis for four types of different structures. The dynamic response analysis was conducted with Newmark- β method ($t = 0,005$ sec, $\beta = 1/4$) [5-9, 5-10]. The damping was based on the Rayleigh damping model, with the frequencies of first bending mode and 20 Hz with 4,0 % damping constant, which were determined to fit the results of the strain energy proportional damping model so as not to overestimate the damping in high frequency modes [5-11].

5.2.3 Truck Modelling

A truck with leaf suspensions and 196 kN total weight was used as the heavy vehicle for the analysis, since it is a popular type of truck in Japan. The truck model for the analysis and parameters of half side wheels are shown in *Fig. 5.5* and *Table 5.2*. Each wheel was modelled as a

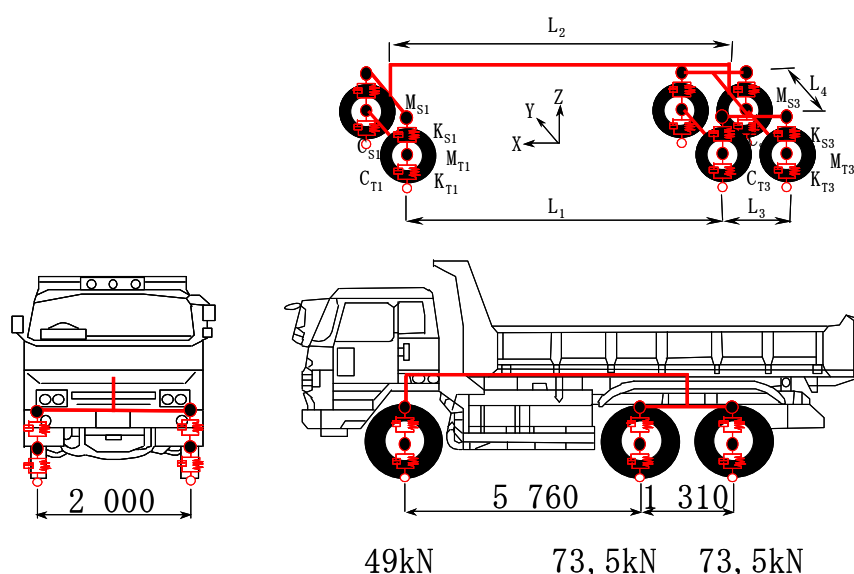


Fig. 5.5: Truck model

two-degree-of-freedom system of suspension spring and tire spring. The stiffness of each spring was determined so that the dominant frequency would conform to that of the regular trucks. The damping coefficients were determined according to the results of the complex eigen value analysis of the two-degree-of-freedom system model. Two cases of the driving speed of the truck, 40 km/hour and 80 km/hour, were considered for the analysis, which are the general speed limits for heavy vehicles on highways and expressways in Japan. Only one truck in each structural model was considered in the analysis. Two cases of the tracking lanes were also considered to study the influence of the eccentric loading, *i.e.* central tracking and side tracking. The analytical cases are shown in *Table 5.1*.

Table 5.2: Parameters of truck model

	Parameter	Symbol	Unit	Value
Total	Total weight	W	kN	196,0
	Wheel space	L_1	m	5,76
	Wheel space	L_2	m	6,41
	Wheel space	L_3	m	1,31
	Wheel space	L_4	m	2,00
Front wheels	Body mass	M_{S1}	kN/(m/sec ²)	1,90
	Suspension spring stiffness	K_{S1}	kN/m	735,0
	Suspension damping coefficient	C_{S1}	kN/(m/sec)	9,80
	Frequency of suspension spring	-	Hz	2,54
	Suspension damping constant	-	-	0,03
	Axle mass	M_{T1}	kN/(m/sec ²)	0,60
	Tire spring stiffness	K_{T1}	kN/m	1568,0
	Tire damping coefficient	C_{T1}	kN/(m/sec)	0,98
	Frequency of tire spring	-	Hz	10,03
Tire damping constant	-	-	0,16	
Rear wheels	Body mass	M_{S2}, M_{S3}	kN/(m/sec ²)	2,55
	Suspension spring stiffness	K_{S2}, K_{S3}	kN/m	1470,0
	Suspension damping coefficient	C_{S2}, C_{S3}	kN/(m/sec)	14,70
	Frequency of suspension spring	-	Hz	3,05
	Suspension damping constant	-	-	0,03
	Axle mass	M_{T2}, M_{T3}	kN/(m/sec ²)	1,20
	Tire spring stiffness	K_{T2}, K_{T3}	kN/m	3038,0
	Tire damping coefficient	C_{T2}, C_{T3}	kN/(m/sec)	0,98
	Frequency of tire spring	-	Hz	10,03
Tire damping constant	-	-	0,10	

5.2.4 Roughness

The dynamic behaviour of the structures is influenced by the interaction between the roughness of the expansion joints and the road surface, structures and vehicles. The roughness at the expansion joints was

modelled as 20 mm gaps after field research on existing bridges [5-12]. The gaps are located at the ends of the deck for the conventional model, at the ends of the extended decks for the extended deck model and at the ends of the approach slabs for the semi-integral and integral models. The roughness of the road surface is generally modelled by the direct or spectral methods. The former defines the measured road surface roughness on the road surface in the analysis. The latter is an indirect method with power spectral density of the road surface roughness that is employed when a stochastic study is conducted. The roughness of the road surface exerts a characteristic influence upon each analytical model. But the same roughness cannot be applied to these models, as the bridge lengths, including approach slabs or extended decks, are not the same. Hence the roughness of the road surface was not considered in this study in eliminating the influence of the characteristic interaction of the roughness of road surface, vehicle and structure, as the purpose of this numerical study was to clarify only the influence of the different structural systems, including approach parts. Therefore, the roughness at the expansion joints was only considered in the analyses.

5.3 Static Analysis

The static loaded deflections of the mid-span of the central girder in central tracking cases are plotted with relation to the position of the front axle of the truck in *Fig. 5.6*, which shows the flexibility of each structural model. The origin of the position of the front axle, 0 m in *Fig. 5.6*, is the left end of the approach slab, *i.e.* 10 m backward from the centroid of the abutment.

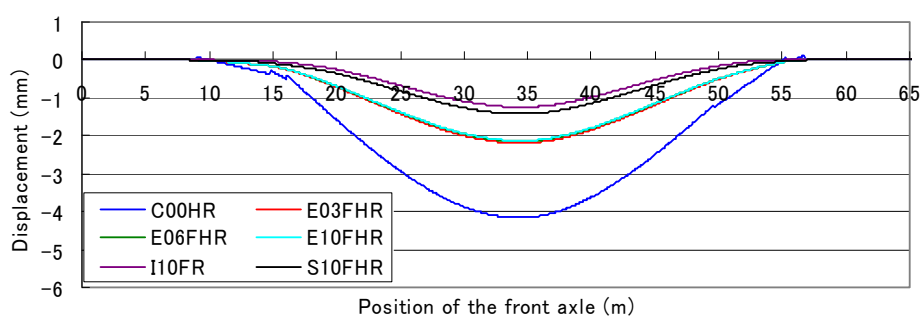


Fig. 5.6: Static deflection of mid-span

The following is a summary of main results of static analysis.

- The maximum deflection of the integral model is 30 % of the conventional model.
- The maximum deflection of the semi-integral model is 34 % of the conventional model due to the rigidity of the short piers and superstructure.
- The maximum deflection of the extended deck model is 51 % of the conventional model.
- The influence of the extended deck length is almost negligible for static deflection.

5.4 Eigen-value Analysis

The frequencies of each structural model are shown in *Figs. 5.7* and *5.8*. The major vibration modes of the integral model are shown in *Fig. 5.9*. The strain energy share of members for damping of each model is shown in *Fig. 5.10*. The results are summarised as follows:

- The influence of the extended deck length on the vibration modes is negligible.
- The influence of the stiffness of the approach slab bed and bearings on the vibration modes is slight.
- The frequencies of semi-integral models give intermediate results between extended deck models and integral models.
- Integral models give the most rigid vibrational behaviour among these four types of structural models, while conventional models give the most flexible behaviour.
- The influence of the flexibility of the foundation on the vibration modes is not prominent.
- Webs and deck play a great part in the strain energy share for damping.
- The foundations contribute to the damping of the bending modes of the extended deck model, semi-integral model and integral model; the more the structure gains rigidity, the more the energy share of the foundations for the damping increases (*Fig. 5.10*).
- The approach members (*i.e.* extended deck, extended deck bed, approach slab and approach slab bed) contribute to the damping of the bending modes, particularly in the case of extended deck and semi-integral models.
- The end cross beam contributes to the damping of torsional modes.

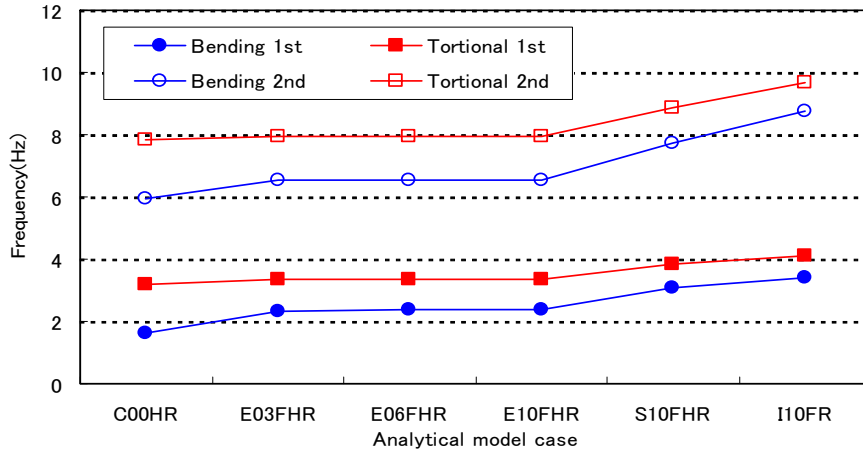


Fig. 5.7: Frequencies of rigid foundation models

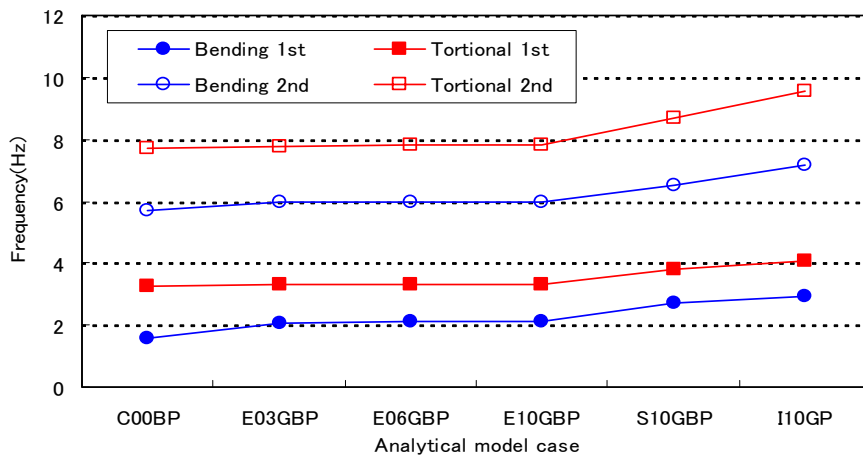


Fig. 5.8: Frequencies of pile foundation models

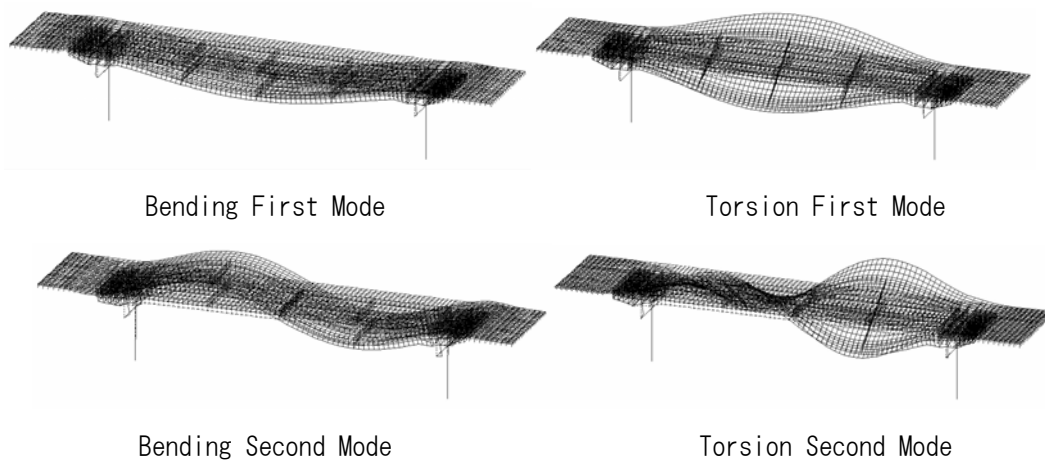


Fig. 5.9: Vibration modes of integral bridge model

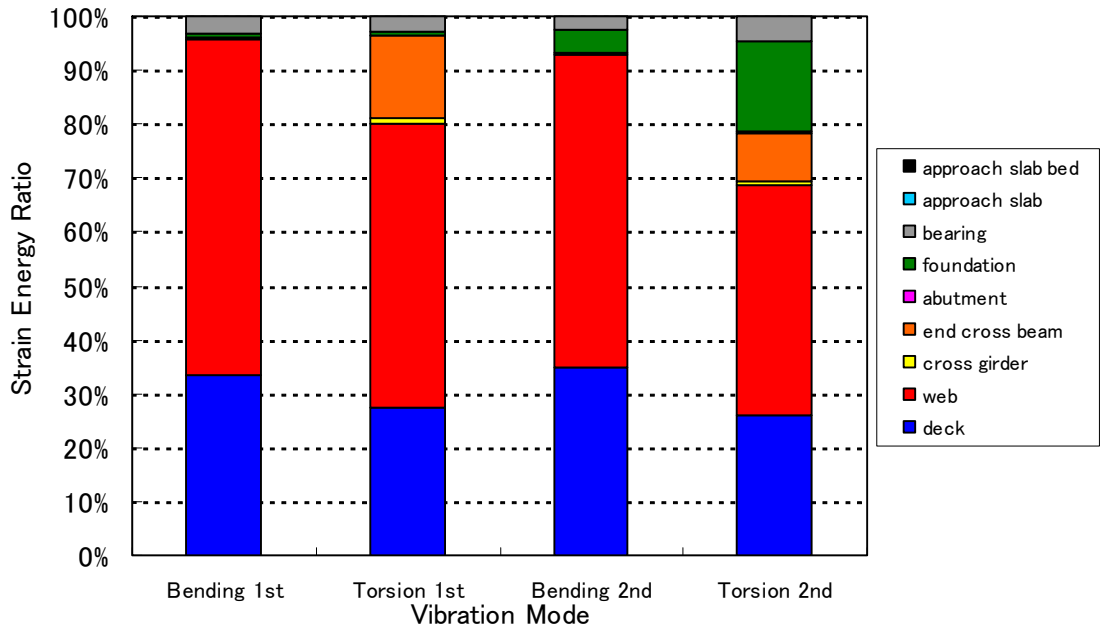


Fig. 5.10(a): Conventional model (C00BP)

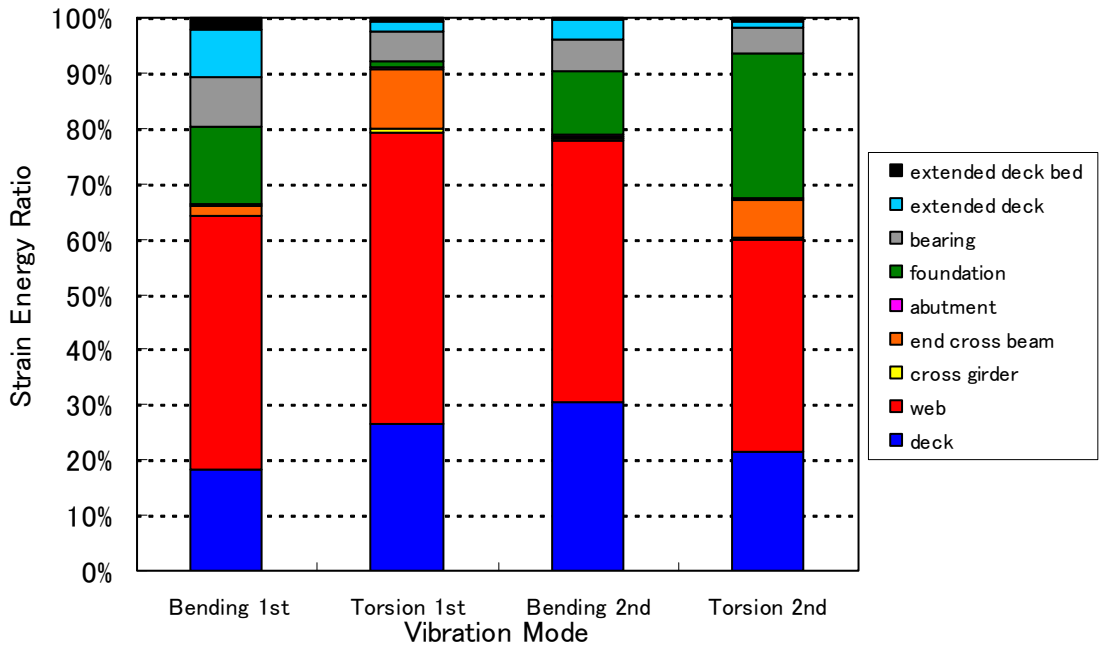


Fig. 5.10(b): Extended deck model (E10GBP)

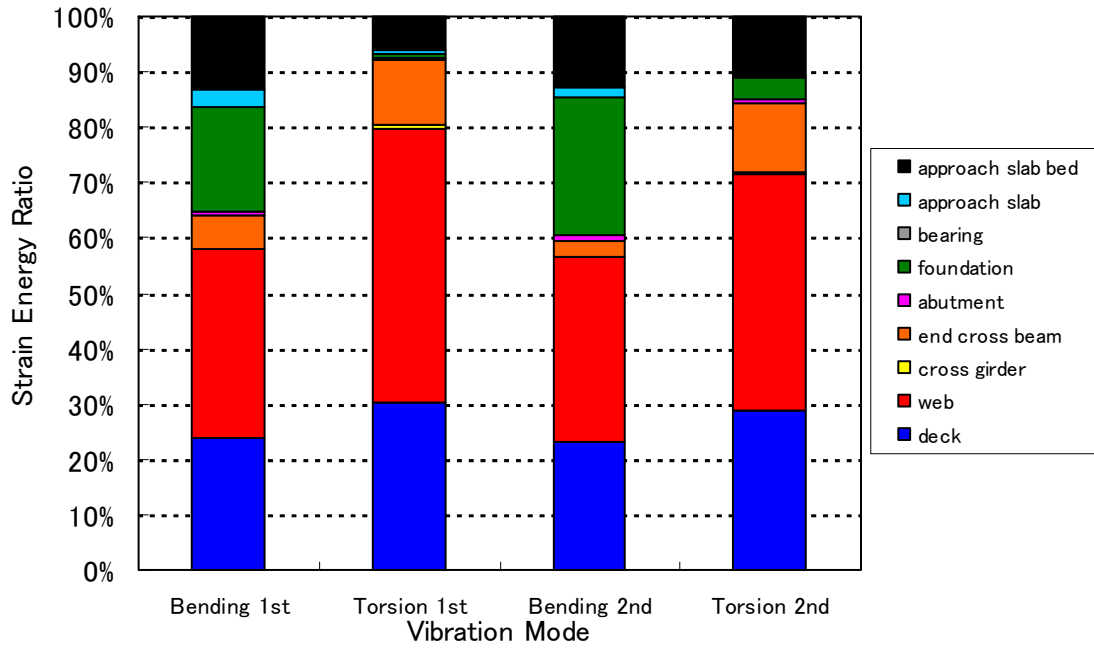


Fig. 5.10(c): Semi-integral model (S10GBP)

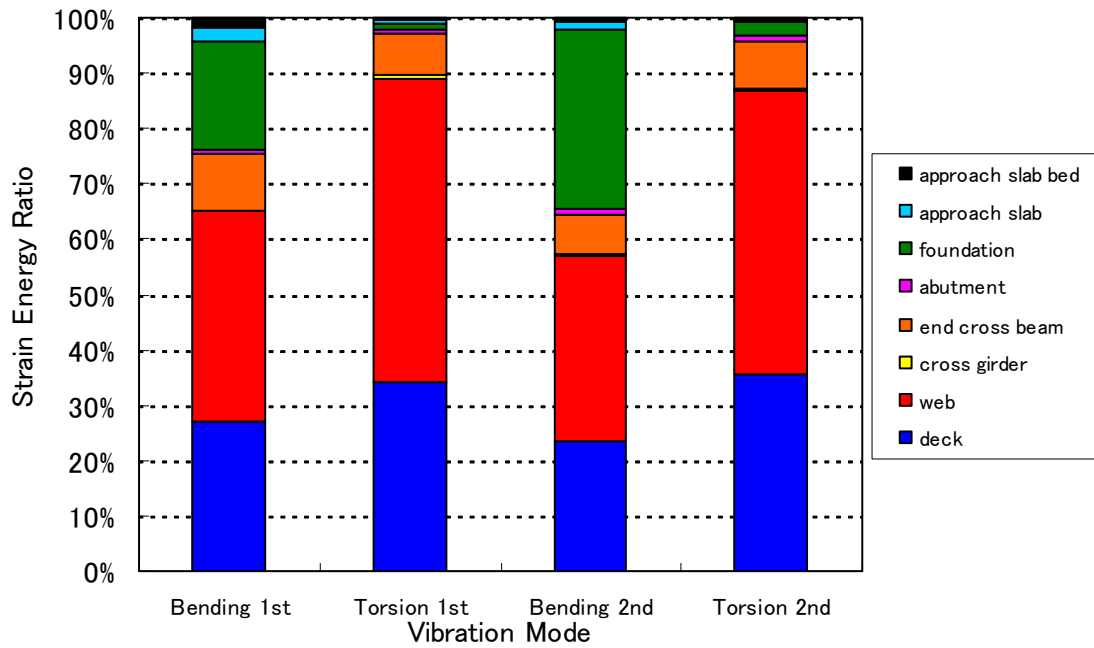


Fig. 5.10(d): Integral model (I10GBP)

Fig. 5.10: Strain energy share of members for damping

5.5 Dynamic Response Analysis - Serviceability for Pedestrians -

The ergonomic serviceability of bridge with respect to the vibration for pedestrians is well-evaluated with the effective value of response velocity, viz. the maximum of root mean square (RMS) of the response velocity, from past studies [5-13, 5-14]. In Japan, the evaluation of response velocity by RMS is widely applied to the evaluation of vibrational bridge serviceability for pedestrians. The relation between the degree of comfort and RMS of the response velocity from field walking tests is shown in *Table 5.3*. The RMS of the response velocity is recommended to control less than 1,70 cm/sec to prevent discomfort for pedestrians from the studies by KAJIKAWA, Y. *et al.* [5-13, 5-14]. The acceptable values of vibration magnitude for comfort are dependent on many factors that vary with each application; a limit for the comfort of pedestrians is not defined in ISO 2631. It gives only approximate indications of likely reactions to various magnitudes of overall vibration values for passengers sitting in public transport, as shown in *Table 5.4* [5-15].

Table 5.3: Relation between R. M. S. of response velocity and degree of comfort for pedestrians

Category No.	R. M. S. of response velocity (cm/sec)	Content of Category
0	0 - 0,42	Not perceptible
1	0,42 - 0,85	Lightly perceptible
2	0,85 - 1,70	Definitely perceptible
3	1,70 - 2,70	Lightly hard to walk
4	Greater than 2,70	Extremely hard to walk

Table 5.4: Approximate indications of the relation between acceleration level and degree of comfort in ISO2631-1

Acceleration (m/sec ²)	Degree of comfort
Less than 0,315	Not uncomfortable
0,315 - 0,63	A little uncomfortable
0,5 - 1,0	Fairly uncomfortable
0,8 - 1,6	Uncomfortable
1,25 - 2,5	Very uncomfortable
Greater than 2	Extremely uncomfortable

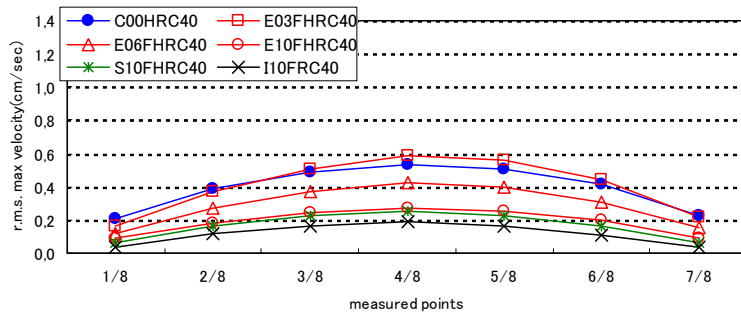


Fig. 5.11: Maximum R.M.S. of velocity of side girder of rigid foundation models in 40km/hour driving of central tracking lane

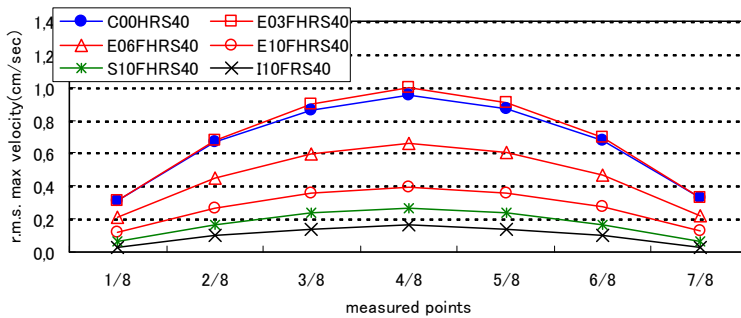


Fig. 5.12: Maximum R.M.S. of velocity of side girder of rigid foundation models in 40km/hour driving of side tracking lane

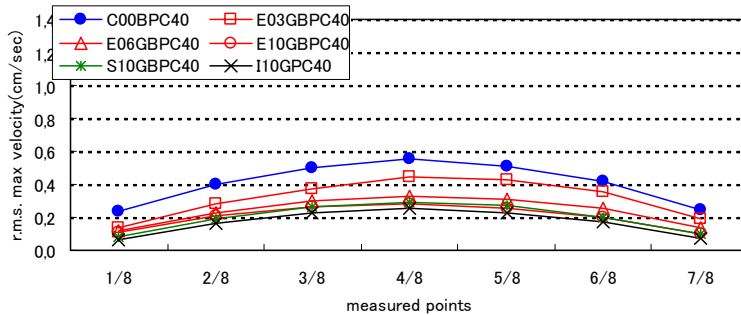


Fig. 5.13: Maximum R.M.S. of velocity of side girder of soft foundation models in 40km/hour driving of central tracking lane

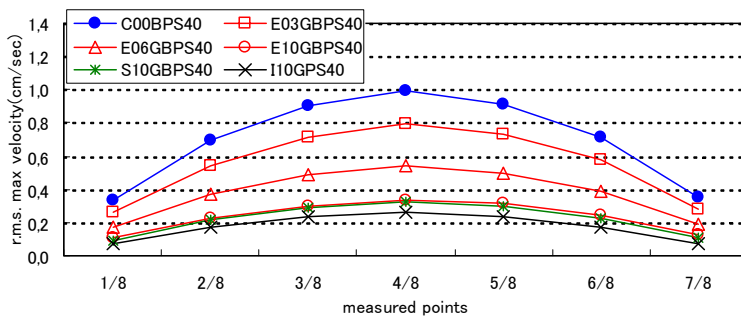


Fig. 5.14: Maximum R.M.S. of velocity of side girder of soft foundation models in 40km/hour driving of side tracking lane

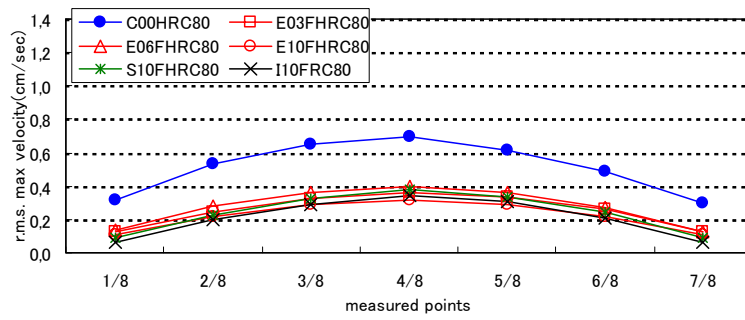


Fig. 5.15: Maximum R.M.S. of velocity of side girder of rigid foundation models in 80km/hour driving of central tracking lane

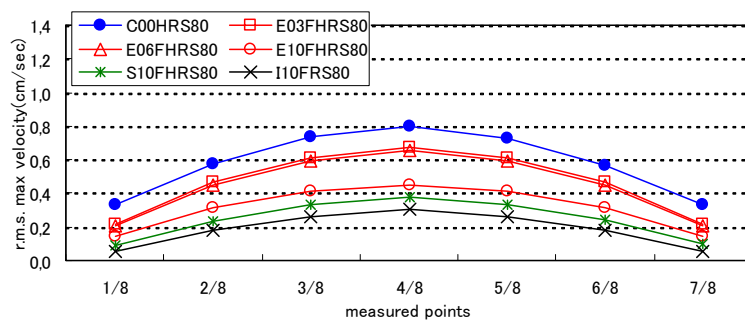


Fig. 5.16: Maximum R.M.S. of velocity of side girder of rigid foundation models in 80km/hour driving of side tracking lane

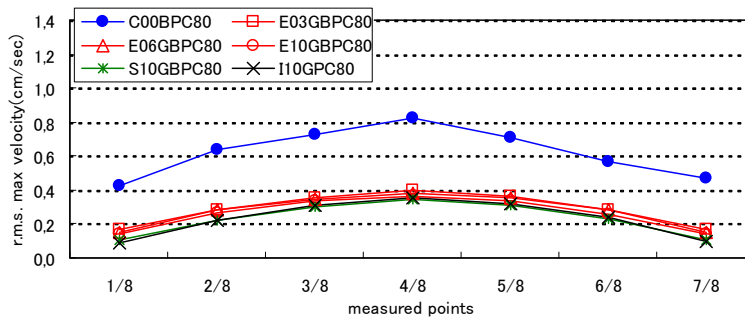


Fig. 5.17: Maximum R.M.S. of velocity of side girder of soft foundation models in 80km/hour driving of central tracking lane

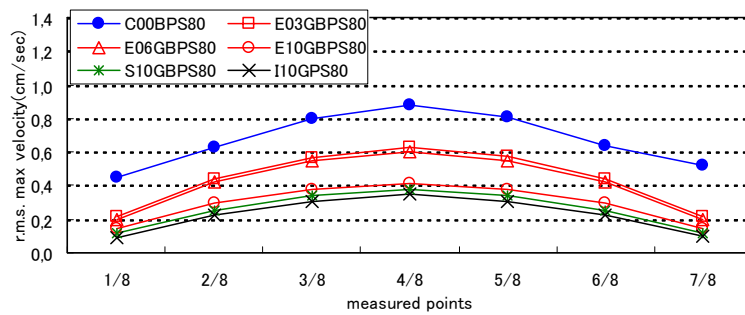


Fig. 5.18: Maximum R.M.S. of velocity of side girder of soft foundation models in 80km/hour driving of side tracking lane

Thus the serviceability for the pedestrian is evaluated in this paper with the maximum of RMS of response velocity of the deck. The tracking lanes have a large influence upon the response. Because the natural frequencies of the vehicle and torsional first mode of the structures are both around 3 Hz, the side girders gain larger responses than the central girder from the influence of torsional modes. The results of the maximum RMS of the velocity on the side girder at 40 km/hour and 80 km/hour are shown in *Figs. 5. 11-5. 14* and *Figs. 5. 15-5. 18* respectively. The results are summarised as follows:

- The tracking lanes greatly influence the response of torsional vibration modes.
- Conventional models give the largest response and stand out among all the structural models.
- The responses of the extended deck models become lower as their lengths become longer; the responses come close to those of semi-integral models and integral models, when the lengths of extended decks are 10 m. To ensure stable serviceability of the extended deck solution, 10 m of extended deck is recommended.
- Integral models gained the lowest responses in all the cases. However, semi-integral models came close in response to the integral models.
- Higher driving speed does not necessarily give a larger response velocity for the interaction between vehicle and structures (*cf. Figs. 5. 12 and 5. 16*). This suggests the existence of a driving speed with the maximum response for each structure.

5.6 Dynamic Response Analysis - Infrasound -

The infrasound radiation power of the slab with a large area compared to the wavelength of the sound is theoretically defined in Equation (5.1) when all the points of the slab are in piston movement with same phase and amplitude [5-16].

$$w = \rho c S v^2 \quad (5.1)$$

where

w : sound radiation power

ρ : density of air

c : sound velocity

S : area of slab

v : effective value of slab velocity

As described above, the sound radiation power of the infrasound caused by the interaction between the structures and vehicle was estimated by Eq. (5.1). The results of the maximum sound radiation power are shown in *Figs. 5.19* and *5.20* and summarised as follows.

- The tracking lanes have only a small influence on the sound radiation power of the infrasound.
- The longer extended deck length would not essentially give smaller responses for the interaction between the vehicle and the structures. The vibration modes, driving speed and tracking lane interact with each other for the response of sound radiation power.
- When the length of the extended deck is 10 m, the extended deck model has good control of sound radiation power.
- Semi-integral models and integral models also have good control of sound radiation power.
- The influence of the structural system on the sound radiation power of the infrasound is prominent, especially between the conventional model and the others.

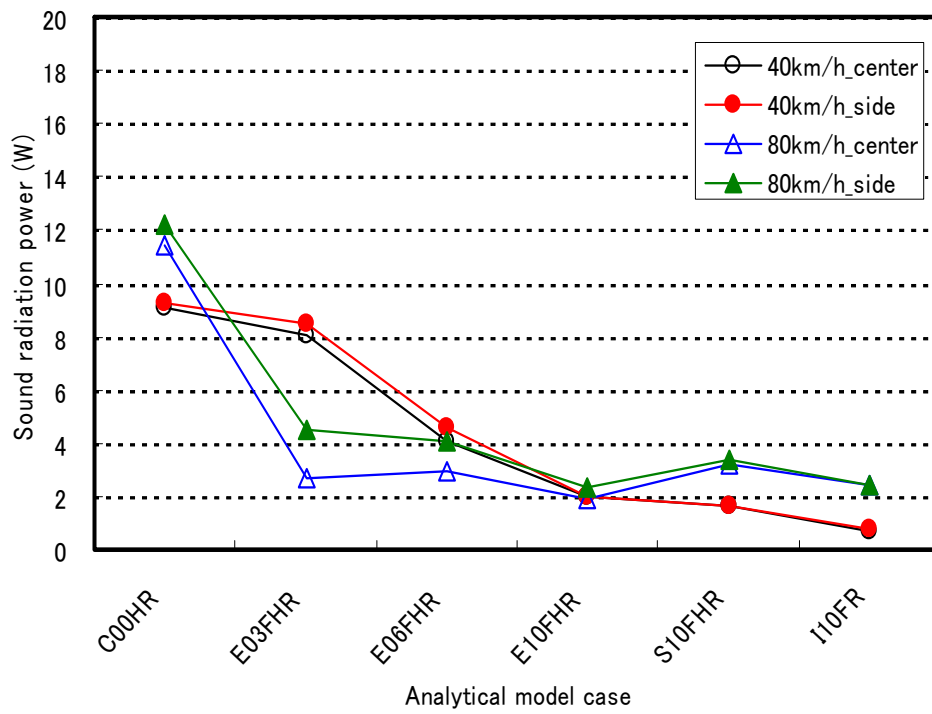


Fig. 5.19: Sound radiation power with rigid foundation models

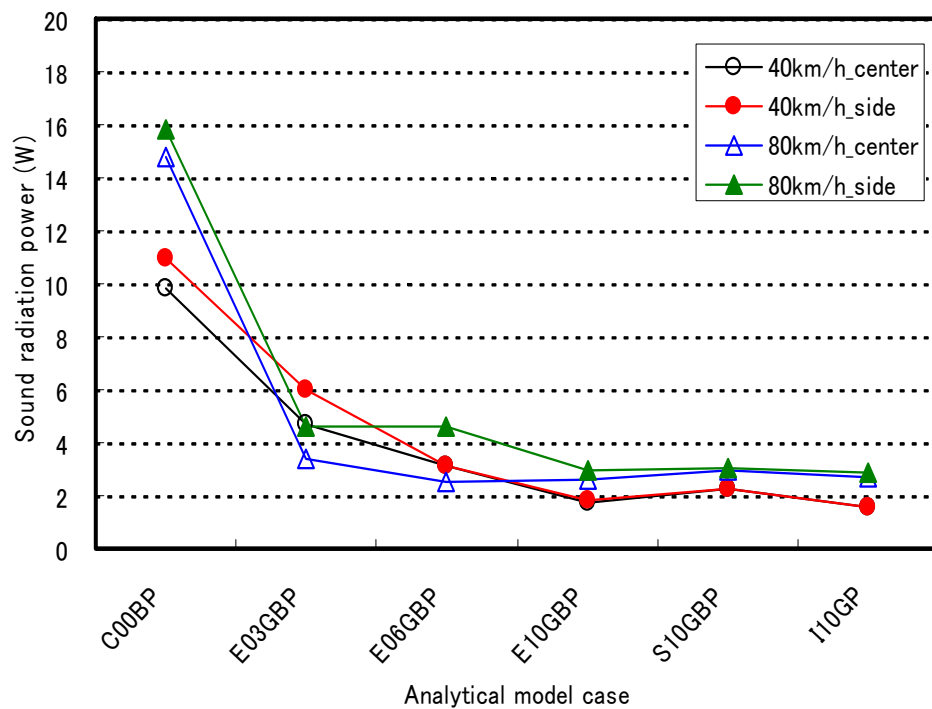


Fig. 5.20: Sound radiation power with soft foundation models

5.7 Dynamic Response Analysis - Ground Vibration -

Ground vibration caused by the interaction between bridge and vehicles sometimes gives an uncomfortable low frequency vibration to the houses and buildings around the bridge. The ground vibration caused by traffic load is evaluated with the dynamic increment factor (DIF) of the reaction. The incremental reaction by dynamic amplification (R_{inc}) is defined by Eq. (5.2):

$$R_{inc} = R_{dynamic} - R_{static} \quad (5.2)$$

where

$R_{dynamic}$: dynamic reaction

R_{static} : static reaction

The DIF of the reaction is defined as follows:

$$DIF = R_{inc} / R_{static} \quad (5.3)$$

The DIF of each model is shown in *Figs 5.21* and *5.22*. The results are as follows:

- The soft foundations (pile foundations on soft ground) give a relatively large DIF for extended deck models.
- The longer extended deck length would not essentially give smaller responses for the interaction between the vehicle and the structure. The vibration modes, driving speed and tracking lane are supposed to interact with each other for the response of ground vibration.
- The higher driving speed generally gives larger responses except for the short extended deck models, though the tendency is a little different in the case of short extended deck models for the interaction of vibration modes between the vehicle and the structure.
- When the length of the extended deck is 6 m or longer, the extended deck models are able to control ground vibration.
- Semi-integral models and integral models are also equally able to control ground vibration.

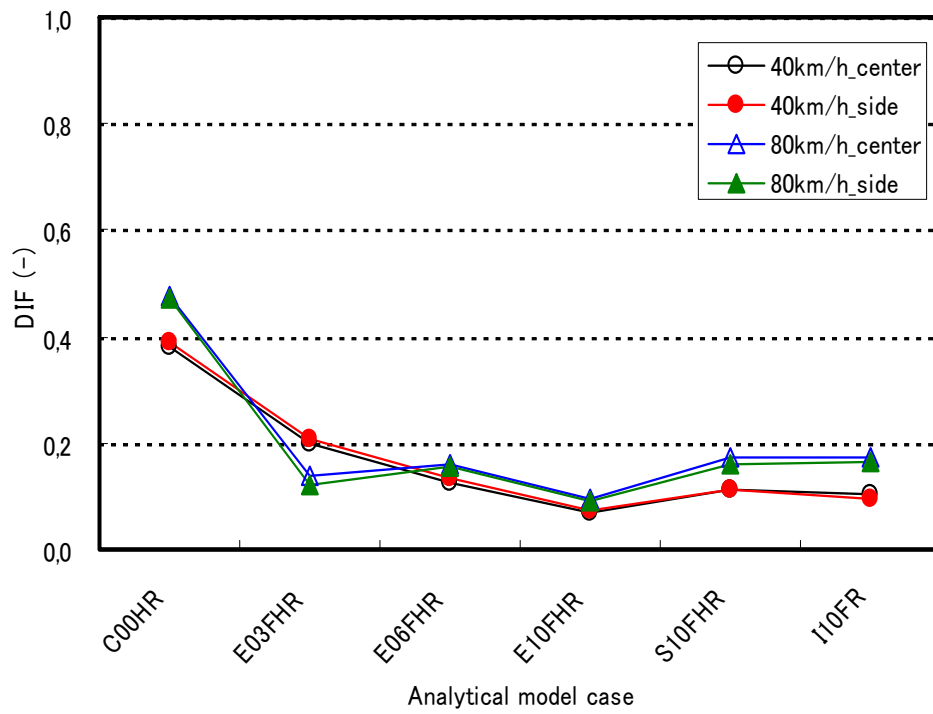


Fig. 5.21: Dynamic increment factor of rigid foundation models

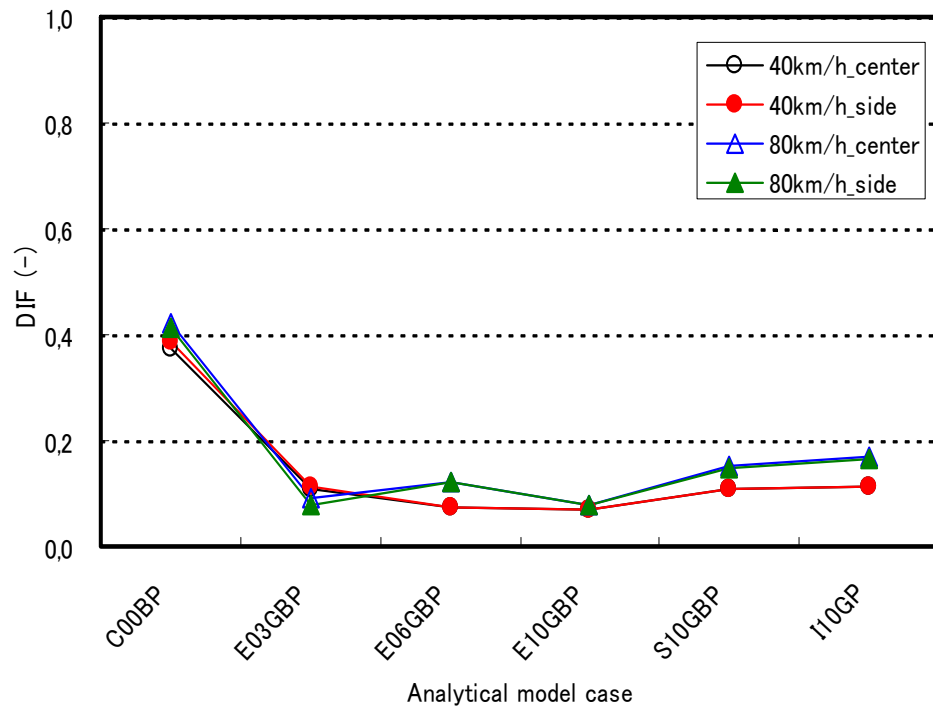


Fig. 5.22: Dynamic increment factor of soft foundation models

5.8 Conclusion

The numerical study was conducted to understand and evaluate the dynamic behaviour and vibrational serviceability of flexible single span bridges with different types of structural systems. The main conclusion of the study can be summarised as follows:

- Integral and semi-integral models provide effective and stable ergonomic bridge serviceability for pedestrians.
- The 10 m long extended deck solution is also effective in improving the serviceability of existing bridges.
- Integral and semi-integral models are effective in controlling infrasound radiation.
- Integral, semi-integral and extended deck models with 6 m and 10 m extended decks are equally effective in controlling ground vibration.
- Conventional simple supported bridge models give the largest responses and stand out among the four alternative solutions in all aspects.
- Regarding the extended deck length, 10 m is recommended for ergonomic bridge serviceability for pedestrians, infrasound radiation and ground vibration.
- Semi-integral models give intermediate results between the extended deck models and integral models.
- Semi-integral bridge system is a widely applicable and effective solution for the vibrational problems, because it can be applicable even if the abutments are too short to employ the integral bridge system.
- Integral bridge system is the best solution for the vibrational problems for pedestrians, infrasound radiation and ground vibration.

The selection of a structural system for bridges should be determined considering vibrational aspects, especially when the bridges are constructed in sensitive environmental areas and/or have sensitive serviceability requirements, because it greatly influences the traffic vibration phenomena. Besides, once undesirable vibration phenomena

appear, vibration control is generally difficult and more costly than applying it at the design phase.

In need, vibrational analysis and study would be of good use for the structural design of the bridges with excellent bridge serviceability.

References

- [5-1] KAJIKAWA, Y., *Traffic Bridge Vibration and Environment*, Journal of Prestressed Concrete, Japan, Vol. 45, No.6, Japan Prestressed Concrete Engineering Association, Tokyo, Japan, pp.37-42, 2003.
- [5-2] IKEDA, K., ETO, S., NAGAI, J., ANDO, R., OBAYASHI, M., *A Measure for Vibration of Plate Girder Steel Bridge*, EXTEC'99.6, Japan Highway Public Corporation, Tokyo, pp. 35-37, Jul. 1999.
- [5-3] Expressway Technology Centre, *Manual of Design and Construction of Extended Deck System (Draft)*, Japan, 2006.
- [5-4] JIN, X., SHAO, X., PENG, W., YAN, B., *A New Category of Semi-integral Abutment in China*, Structural Engineering International, Vol.12, No.3, IABSE, Zurich, pp. 186-188, Aug. 2005.
- [5-5] PRITCHARD, B. ed., *Continuous and Integral Bridges*, E and FN Spon, London, 1993.
- [5-6] ENGLAND, G. L., TSANG, N. C. M., BUSH, D. I., *Integral Bridges*, Thomas Telford, London, 2000.
- [5-7] FUKADA, S., *Studies on the Establishment of the Three Dimensional Analytical Model for the Review of Dynamic Bridge Performance*, dissertation, Kanazawa University, Kanazawa, 1999.
- [5-8] FUKADA, S., USUI, K., KAJIKAWA, Y., HARADA, M. *Simulation of vibration and sound characteristics occurred from extended deck bridges with various skew due to running vehicle*, Journal of Structural Engineering, Vol.53-A, Japan Society of Civil Engineers, Tokyo, pp. 287-298, Mar. 2007.
- [5-9] Bridge Vibration Research Group, KAJIKAWA, Y. eds. et al. *Measurement and Analysis of Bridge Vibration*, Gihodo Shuppan, Tokyo, 1993.
- [5-10] FUKADA, S. *Dynamic Response Analysis of a Test Bridge due to Running Vehicle*, Proceedings of IMAC-XXV Conference, No.046 (CD-ROM), 2007.
- [5-11] FUKADA, S., KAJIKAWA, Y., KITAMURA, Y., HARADA, M., SHIMIZU, H. *Vibration Serviceability of Nielsen System Lohse Girder Bridge due to Running Vehicle*, Journal of Structural Engineering, Vol. 50A, JSCE, Tokyo, pp.421-430, 2004.
- [5-12] HONDA, H., KAJIKAWA, Y., KOBORI, T. *Roughness Characteristics at Expansion Joint on Highway Bridges*, Proceedings of Japan

- Society of Civil Engineers, Vol. 324, JSCE, Tokyo, pp.173-176, Aug. 1982.
- [5-13] KOBORI, T., KAJIKAWA, Y. *Ergonomic Evaluation Methods for Bridge Vibrations*, Proceedings of Japan Society of Civil Engineers, Vol. 230, JSCE, Tokyo, pp. 23-31, Sept. 1974.
- [5-14] KAJIKAWA, Y. *Some Considerations on Ergonomical Serviceability Analysis of Pedestrian Bridge Vibrations*, Proceedings of Japan Society of Civil Engineers, Vol.325, JSCE, Tokyo, pp. 23-33, Sept. 1982.
- [5-15] *ISO2631-5 Mechanical Vibration and Shock - Evaluation of Human Exposure to Whole-Body Vibration - Part 1: General Requirements*, International Organisation for Standardisation, Geneva, 1997.
- [5-16] KOYASU, M., IGARASHI, H., ISHII, K., TOKITA, Y., SEIMIYA, H. *Noise and Vibration*, Vol. 1/2, Corona Publishing, Tokyo, pp. 167-168, 1978.
- [5-17] AKIYAMA, H., FUKADA, S., KAJIKAWA, Y. *Numerical Study on the Vibrational Serviceability of Flexible Single Span Bridges with Different Structural Systems under Traffic Load*, Structural Engineering International, Vol. 17, No.3, International Association for Bridge and Structural Engineering, Zurich, pp. 256-263, Aug. 2007.

Chapter 6 Application of High Performance Lightweight Aggregate Concrete to Integral Bridges

6.1 Introduction

In general, dead load is the major load in design of bridges; especially self-load of deck/girder often takes largest share in all the primary loads. The lightweightisation of self-load gives eminent benefits as follows.

- Less quantity of prestressing steel and reinforcement
- Application to longer spans
- Slenderer superstructure
- Compacter substructures and foundations

Lightweight aggregate concrete is one of the most effective solutions to extend the application of integral bridges, if it can clear the durability and cost requirements. The lightweight aggregate concrete bridges have been rarely constructed in Japan because of its scant frozen-thawed resistance.

However, various developments of lightweight aggregate concrete with high strength and high frozen-thawed resistance have pursued [6-1,6-2], also it was applied to some bridges [6-3, 6-4, 6-5].



Photo 6.1: Shirarika River Bridge, Central Hokkaido Expressway

Among them, Shirarika River Bridge of Hokkaido expressway, 96,2 m long (span:28,5 m + 42,7 m + 24,0 m) three span continuous rigid frame prestressed concrete bridge completed in 2001, is the first application of high performance lightweight aggregate concrete as an integral bridge [6-3].

The author have been researching the lightweight aggregate concrete with low water absorption and high strength which are made from Huang River clay deposits in China to apply to the prestressed concrete structures (*Photo 6.2*).

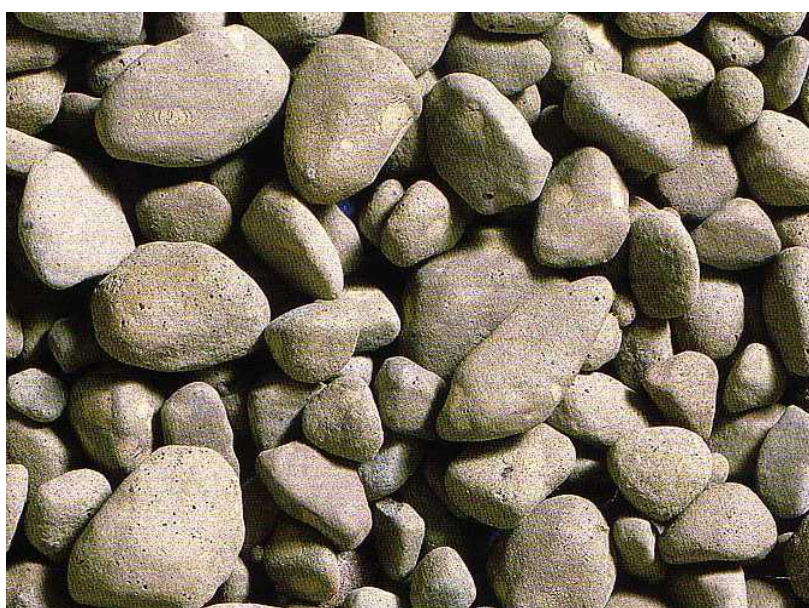


Photo 6.2: High performance lightweight aggregate

Hereinafter "high performance lightweight aggregate" and "high performance lightweight concrete" are respectively called as "HLA" and "HLAC".

Here, high performance lightweight aggregate (HLA) means the lightweight aggregate with high strength and low water absorption. High performance lightweight concrete (HLAC) means the concrete with HLA that has higher frozen-thawed resistance than conventional lightweight aggregate concrete.

In this chapter, the fundamental properties of HLA and HLAC are comprehensively described on material properties, properties of confined concrete and dynamic behaviour for serviceability of the single span bridges with comparison to those of normal concrete.

6.2 Fundamental Properties of HLA and HLAC

6.2.1 Materials

It is essential to clarify the basic properties such as elastic modulus, creep and shrinkage to apply HLAC to the prestressed concrete structures for appropriate evaluation of the prestressing force loss and estimation of the deflection. The standard specification of concrete - structural performance verification - of JSCE, viz., Japan Society of Civil Engineers [6-6] (hereinafter called "JSCE Specification") allows to estimate the creep coefficient as 75 % of that of normal concrete. But, it is known that the property of the creep is largely influenced by the characteristic condition of the concrete, e.g. the properties of aggregate, cement, mix proportion, etc. In addition, the results of creep experiments of high performance lightweight concrete are rarely reported.

That is why the authors have conducted the experimental test of creep and shrinkage of HLAC with rapid hardening cement that is widely employed to the prestressed concrete structures for the improvement of early age strength.

This paper summarises the results of the experiments of creep and shrinkage of HLAC and gives discussion about such basic properties with comparison to that of normal concrete and conventional design codes. The basic properties of HLA are shown in *Table 6.1*.

Table 6.1: Basic properties of high performance lightweight aggregate (HLA)

			Results	JIS
Chemical ingredient	Ignition loss	%	0,04	Equal or less than 1,0
	Calcium oxide (CaO)	%	8,4	-
	Sulfur trioxide (SO ₃)	%	0,00	Equal or less than 0,5
	Chloride quantity (NaCl)	%	0,005	Equal or less than 0,01
Organic impurities	%	Lighter than standard colour	Lighter than standard colour	
Clay clod quantity	%	0,02	Equal or less than 1,0	
Gradation, fineness modulus	FM	6,58	-	
Water absorption	%	1,20	-	
Absolutely dry density	%	1,16	-	
Solid content of	%	64,6	Class A: Equal or more than 60	

The experiment of HLA was performed in accordance with JIS A 5002. The cement employed in the experiments is rapid hardening Portland cement in JIS R 5210 and classified as rapid hardening high strength cement "RS" in CEB-FIB Model Code 1990 (hereinafter called "MC-90") as shown in *Table 6.2*; the compressive strength is larger than the requirement of 52,5 N/mm² in MC-90.

Table: 6.2 Unconfined compressive strength of rapid hardening cement

Material age	Compressive strength (N/mm ²)			
	1day	3days	7days	28days
Strength	28,0	47,0	58,0	68,0

Table 6.3: Mix proportion of HLAG (kg)

Water/Cement ratio	Cement	Water	Coarse aggregate	Fine aggregate		Admixture
W/C	C	W	G	S1	S2	Sp
37,5%	440	165	416	567	254	3,52

Cement(c): Rapid Portland cement ("RS" in CEB-FIP Model Code 1990)

Coarse aggregate(G): HLA(absolute density:1,16)

Fine aggregate (S1): Land sand produced in Hasaki, Ibaraki pref. (finer than S2)

Fine aggregate (S2): Crashed sand produced in Kuzuu, Tochigi pref. (coarser than S1)

Admixture(Sp): High range super plasticizer and air entrainer

The HLA with the 1,16 of absolutely dry density was only employed as coarse aggregate for the specimens, while fine aggregate comprises natural sand. The mix proportion is shown in *Table 6.3* and other conditions are as follows.

- Nominal Strength: 40 N/mm²
- Slump: 15 cm
- Air Content: 4,5 %
- Maximum Diameter of Coarse Aggregate: 20 mm
- Unit Mass: 1845,5 kg/m³

6.2.2 Experiments of Creep and Shrinkage of HLAC

6.2.2.1 Experimental Condition

The experiments were conducted fundamentally based upon "JIS Draft" [6-7] for the experiment of creep and shrinkage among major specifications, e.g. ASTM C 512, RILEM CPC 12 and "JIS Draft". Each item of the experimental condition is shown in *Table 6.4*.

Table 6.4: Experimental condition of creep and shrinkage

Items	JIS draft	Experimental condition
Shape of specimens	Shape: Cylinder ϕ : More than 3 times of maximum diameter of coarse aggregate and more than 10cm H: 2-4 times of diameter (ϕ), 3ϕ is desirable	Cylinder ($\phi 150 \times H300$)
Number of specimens	Creep: 2 (pcs.) Shrinkage: 2 (pcs.) Compressive strength and static elastic modulus: 3 (pcs.)	Creep: 2 (pcs.) $\times 2$ (type) Shrinkage: 2 (pcs.) Compressive strength and static elastic modulus: 3 (pcs.) $\times 2$ (type)
Curing	Keep 24Hrs in formwork after casting, Keep in the water until 7days material age, Keep in the atmosphere of $20^{\circ}\text{C} \pm 1^{\circ}\text{C}$, R. H. $65 \pm 5\%$	
	Sealed curing	-
Loading intensity	25-35% of compressive strength	Around 1/3 of compressive strength
Loading precision	Keep the load within $\pm 2\%$ fluctuation	
Material age at the beginning of loading	Standard: 28days	7days, 28days
Measured length of strain	More than 3 times of maximum diameter of coarse aggregate and more than 10cm	250mm
Position of measurement	2 points of the side of the specimen facing each other	
Precision of strain measurement	More than 10×10^{-6}	More than 10×10^{-6} (measured by contact gauge)
Loading term	Standard: 1 year	1 year
Test equipment	-	Pressure loading test equipment (illustrated in <i>Fig. 6.1</i>)

6.2.2.2 Static Elasticity Test

The static elasticity test was conducted for 2 cases for the material ages at the beginning of loading- 7days and 28days. The results are shown in *Table 6.5* and *Table 6.6*. The unconfined compressive strength tests after 365days creep experiment were also conducted, and then the both results were $61,9 \text{ N/mm}^2$, i.e. 25 % improvement from 7days strength. The results are summarised as follows with comparison to the elastic modulus of normal concrete specified in JSCE Specifications.

- (1) The elastic modulus at the age of 7days is 69,6 % of that of normal concrete that is estimated by JSCE Specifications.
- (2) The elastic modulus at the age of 28days is 71,9 % of that of normal concrete that is estimated by JSCE Specifications.
- (3) These above results, around 70 % of that of normal concrete, is higher than the specified value - 60 % of that of normal concrete in JSCE Specifications.
- (4) The unconfined compressive strength after 365days loading term is $61,9 \text{ N/mm}^2$, 25 % increment from 7days material age strength.

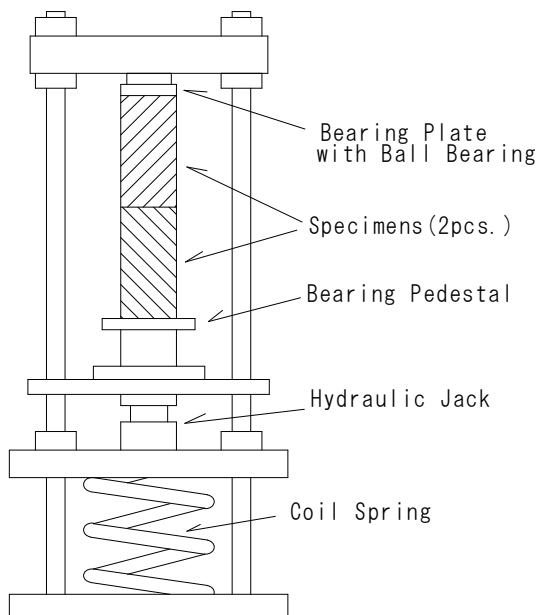


Fig. 6.1: Creep test equipment



Photo 6.3: Creep experiment

Table 6.5: Results of static elasticity test (loading start at 7days)

No. of specimens	Maximum stress	Stress at 50×10^{-6} longitudinal strain	Longitudinal strain at 1/3 of maximum stress	Static elastic modulus
	N/mm ²	N/mm ²	$\times 10^{-6}$	N/mm ²
No. 1	50, 2	1, 2	716	$2,34 \times 10^4$
No. 2	48, 5	1, 3	670	$2,39 \times 10^4$
No. 3	49, 5	1, 6	752	$2,13 \times 10^4$
Average	49, 4	1, 37	712, 7	$2,29 \times 10^4$

Table 6.6: Results of static elasticity test (loading start at 28days)

No. of specimens	Maximum stress	Stress at 50×10^{-6} longitudinal strain	Longitudinal strain at 1/3 of maximum stress	Static elastic modulus
	N/mm ²	N/mm ²	$\times 10^{-6}$	N/mm ²
No. 1	57, 6	1, 2	788	$2,45 \times 10^4$
No. 2	58, 3	1, 3	752	$2,54 \times 10^4$
No. 3	58, 9	1, 6	787	$2,49 \times 10^4$
Average	58, 3	1, 37	775, 7	$2,49 \times 10^4$

6.2.2.3 Results of Creep and Shrinkage Experiments

The results of creep and shrinkage experiments at 365days loading term are shown in *Table 6.7*. The hysteresis curves of the experiments are illustrated in *Figs. 6.2* and *6.3*. The recovered strains immediately after unloading are also shown in *Table 6.7*. Here, the creep strain is calculated from the total strain and elastic strain measured in the creep test, shrinkage strain obtained from the parallel performed shrinkage test in the same environment measured by contact gauge.

Table 6.7: Results of creep experiment (at 365days loading)

Material age at the beginning of loading	Elastic strain	Shrinkage strain	Creep strain	Total strain	Recovered strain immediately after unloading
	$\times 10^{-6}$				
7days	735	489	848	2072	634
28days	760	254	823	1837	613

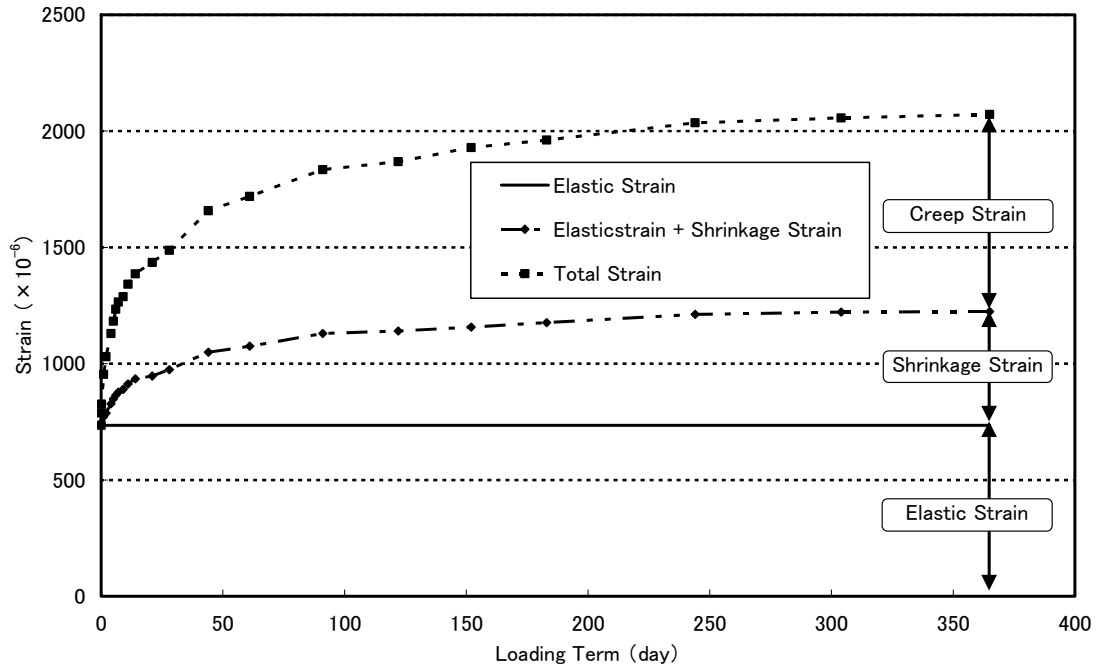


Fig. 6.2: Time dependent strain of HLAC (loading start at the age of 7days)

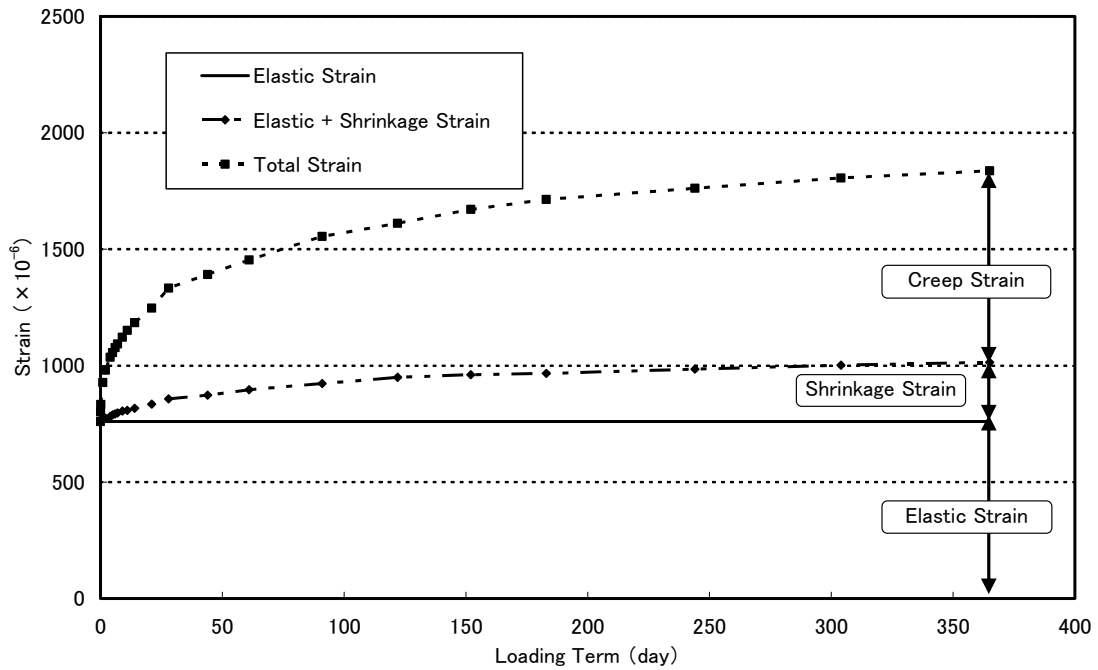


Fig. 6.3: Time dependent strain of HLAC (loading start at the age of 28days)

6.2.3. Comparison to Design Codes

6.2.3.1 Comparison to CEB-FIP Model Code 1990 for Creep

Since the results should be compared with the code that can take into account the influence of the type of cement, hereinafter the results are discussed with comparison to MC-90 [6-8].

As the past reports, e.g. JSCE Specifications, says that the creep coefficient of lightweight aggregate concrete ranges from 60 % to 85 % of that of the normal concrete, the results of the experiments also proves the conventional results. The description of JSCE Specification that allows taking 75 % of the creep coefficient of normal concrete for lightweight concrete gives conservative value to estimate prestressing force loss of HLAC (*Table 6.8*).

6.2.3.2 Behaviour after Unloading

The unloaded behaviour after 365days loading was also monitored to study the behaviour of the recover of the elastic strain, delayed elastic strain and flow strain. The monitoring was separately conducted for 42days and 21days for the specimens which had been begun to load at the material age of 7days and 28days. The results are illustrated in *Figs. 6.4, 6.5* and shown in *Tables 6.9, 6.10*.

The elastic strains immediately after unloading are not equal to the initial applied elastic strains, as shown in *Table 6.7*, which are 86,3 % and 80,7 % of initial applied strains for the specimens of loading age at 7days and 28days. *Tables 6.7, 6.9* and *6.10* say that it needs 2 or 3 weeks for complete recover of initial applied elastic strain.

6.2.3.3 Comparison to CEB-FIP Model Code 1990 for Shrinkage

The shrinkage of HLAC was also measured in the experiments in the same condition as creep test specimens except loading. The results of the shrinkage are shown in *Table 6.11* with comparison to MC-90 that is able to take into account the influence of the kind of cement to calculate the shrinkage strain.

The shrinkage estimation by MC-90 gives about 30 % smaller than the value obtained in the experiments. The reason of the difference is not clear at present. For one thing, the difference would be merely sprung of the variance of the property. On the other hand, autogenous shrinkage would

be a reason for the difference. But, MC-90 does not refer to the autogenous shrinkage in clear sentence.

Here, if the autogenous shrinkage is estimated by Eurocode2 [6-9], the values are 118×10^{-6} (7days) and 119×10^{-6} (28days) for each specimen. These values would be correspondent to the compensation for the difference between estimation by MC-90 and the experimental results, if autogenous shrinkage would be considered besides the "shrinkage" in MC-90, i.e.

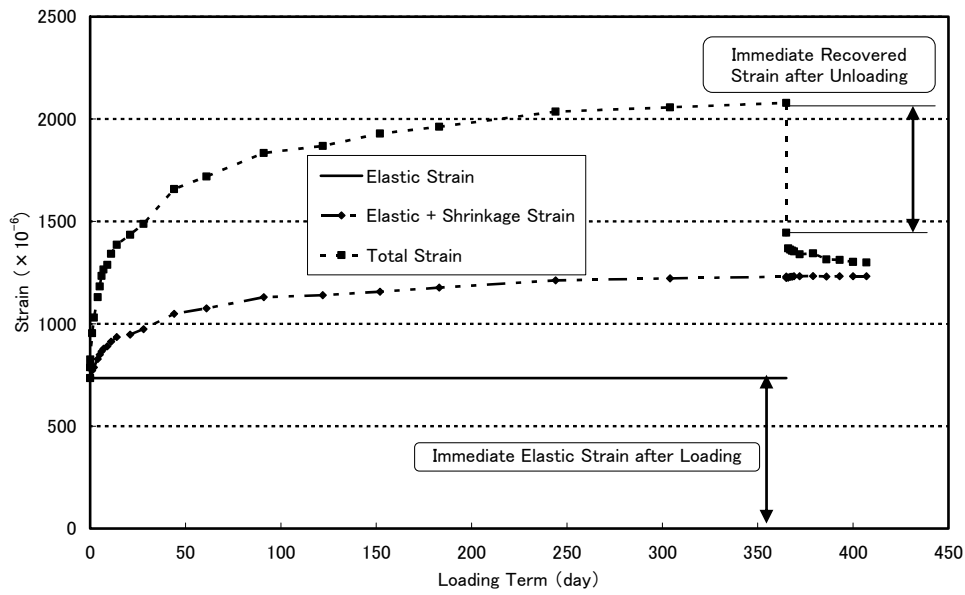


Fig. 6.4: Time dependent strain of HLAC after unloading (loading start at the age of 7days)

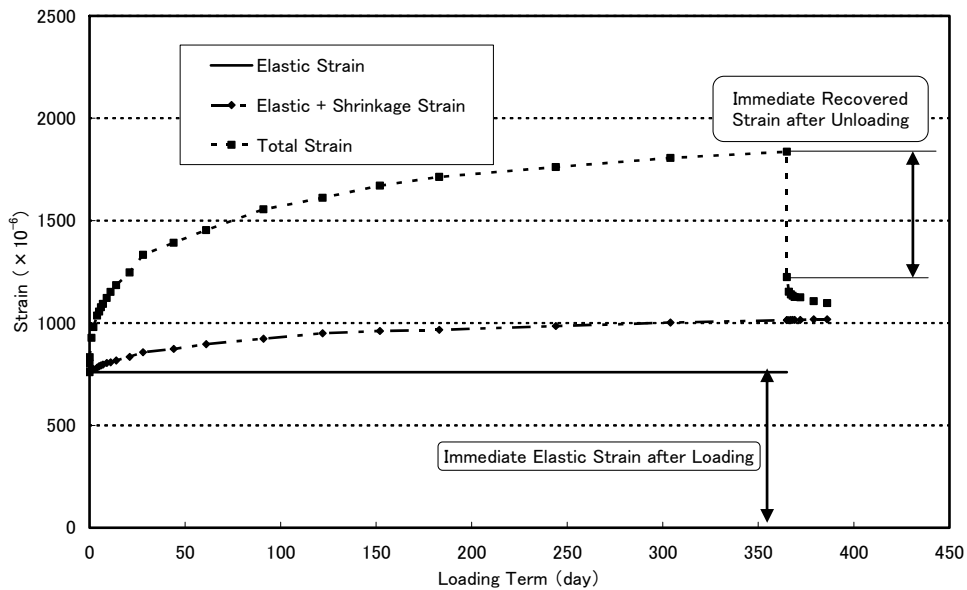


Fig. 6.5: Time dependent strain of HLAC after unloading (loading start at the age of 28days)

with the assumption that the "shrinkage" in MC-90 means drying shrinkage, though the contents of "shrinkage" in MC-90 is not clear.

Table 6.8: Comparison between test results and MC-90

Material age at the beginning of loading	Creep coefficient obtained by experiments	Estimation by MC-90	Experiment/MC-90
7days	1,154	1,813	63,7%
28days	1,083	1,555	69,6%

Table 6.9: Behaviour after unloading (loading start at the age of 7days)

Day	Total	Shrinkage	Residual*
	$\times 10^{-6}$		
0	1438	489	949
1	1368	491	877
2	1362	494	868
3	1357	495	862
4	1354	497	857
7	1339	497	842
14	1344	498	846
21	1314	496	818
28	1312	497	815
35	1302	497	805
42	1300	497	803

* The residual strain contains recovering elastic strain, delayed elastic strain and flow strain.

Table 6.10: Behaviour after unloading (loading start at the age of 28days)

Day	Total	Shrinkage	Residual*
	$\times 10^{-6}$		
0	1224	254	970
1	1153	254	899
2	1140	255	885
3	1133	255	878
4	1127	255	872
7	1125	255	870
14	1107	258	849
21	1097	258	839

* The residual strain contains recovering elastic strain, delayed elastic strain and flow strain.

Table 6.11: Comparison to MC-90 at the material age of 365days

Material age at the beginning of shrinkage	Results of experiments	MC-90	Experiments / MC-90
7days	496×10^{-6}	375×10^{-6}	132, 3%
28days	493×10^{-6}	378×10^{-6}	130, 4%

6.2.4. Conclusions

Following knowledge was obtained through the experiments.

- (1)The unconfined compressive strength of the specimens after 365days loading got 25 % improvement compared with those of the age of 7days.
- (2)The static elastic modulus of HLAC showed around 70 % value of normal concrete.
- (3)The creep coefficient of HLAC was ca. 65 % of those of the normal concrete estimated by MC-90.
- (4)The description to allow assuming the creep coefficient of HLCA as 75 % of normal concrete by JSCE Specification gives conservative value for the estimation of prestressing force loss of prestressed concrete structures.
- (5)The shrinkage strain obtained in the experiments proved larger than the estimation by MC-90 by around 30 %.
- (6)The recovered strains immediately after the unloading were respectively 86 % (loading start at 7days material age) and 81 % (loading start at 28days material age) of initial applied elastic strains.
- (7)The complete recover of the initial applied elastic strain needed 2 or 3 weeks in the experiments.
- (8)The HLA employed in these experiments is supposed to be suitable for prestressed concrete for the higher elastic modulus and the lower creep coefficient as lightweight aggregate that gives less deflection and prestressing force loss at least considered from the results obtained in the experiments.

6.3 Confining Effect of HLAC under Axial Pressure Load

6.3.1 Introduction

Lightweightisation of structures gives significant benefits for seismic design. It leads to less amount of reinforcement, prestressing steel or steel; in addition, it also enables slender superstructure and compacter foundation compared with normal concrete structures.

By the way, lightweight aggregate concrete has lower ductility compared with normal concrete in general. Confining reinforcement is predominant measure to improve the ductility, however the research on confining effect of lightweight concrete is not many. In addition, the properties of lightweight aggregates are supposed to have characteristic properties for each one.

Thus, experimental study of confining effect of HLAC with HLA made from Huang River clay deposits in China was conducted. The axial pressure loading tests were performed; analytical model for stress-strain relationship was also proposed in this study.

6.3.2. Experiment Plan and Specimens

Six specimens were planned as 200×200×500 mm square sectioned short column. The target compressive strength of every specimen was set as 40 N/mm². The mix proportion of HLAC is shown in *Table 6.12*.

The results of tensile test of rebar and unconfined compressive test of HLAC are shown in *Table 6.13*; the stress-strain relationship of rebar is also shown in *Fig. 6.6*.

As confining reinforcement was taken as dominant parameter in this experimental study, all the specimens have same longitudinal reinforcement; eight deformed bars of SD345, D13 were arranged. The longitudinal reinforcement ratio is 2,54 %.

Two types of transverse layouts and confining reinforcement volume ratio were taken as parameters (*Fig. 6.7, Table 6.14*). The confining reinforcement volume ratios were taken as 4,41 %, 2,57 % and 0,05 % for Type A layout specimens, while taken as 4,39 %, 2,64 % for Type B layout specimens. The spacing "S" of confining rebar was taken as 35 mm, 60 mm, and 300 mm for each Type A layout specimen, while taken as 60 mm and 100 mm for Type B specimens (*Table 6.14*).

Two specimens with 300mm confinement spacing and same conditions were

made for unconfined concrete column models, because complete unconfined concrete models had high risks to fail the experiments in inductile failure mode.

Table 6.12: Mix proportion (kg)

Water/Cement ratio	Cement	Water	Coarse aggregate	Fine aggregate	Admixture	Air
W/C	C	W	G	S	Sp	A
40,0%	412	165	418	841	7,42	4,9%

Slump flow: 650mm

Table 6.13: Results of rebar tensile test and unconfined compressive strength of concrete

Rebar			Test results of cylindrical specimens	
Diameter	D10	D13		
σ_y (N/mm ²)	372,3	372,3	Compressive strength (N/mm ²)	38,0
$E \times 10^5$ (N/mm ²)	1,849	1,833	Elastic modulus (10 ⁴ N/mm ²)	1,98
Elongation (%)	16,1	17,6	Unit weight (kN/m ³)	17,0

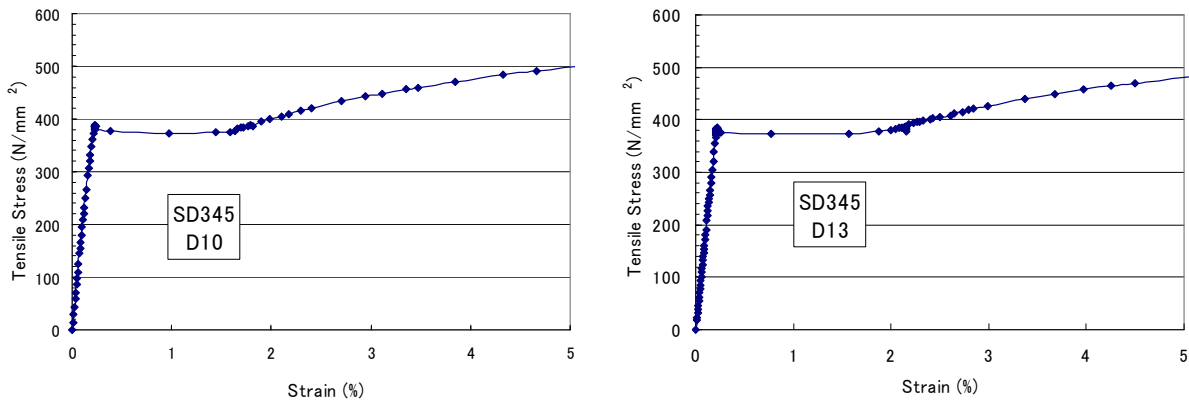
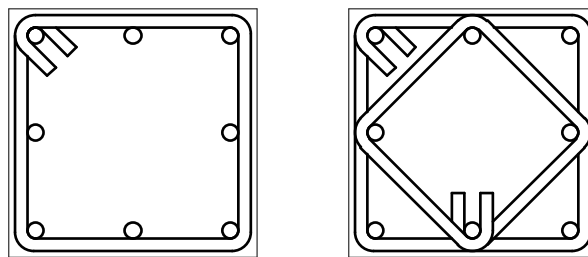


Fig. 6.6: Stress-strain curves of reinforcement



TYPE A

TYPE B

Fig. 6.7: Transverse layouts of confining rebar

Table 6.14: Specimens details

Specimen	f_c' (N/mm ²)	ρ_l (%)	f_{sy} (N/mm ²)	Confinement layout and details				
				TYPE	Diameter	Spacing (mm)	ρ_h (%)	f_{yh}' (N/mm ²)
A-S35	38, 0	2, 54	372, 3	A	D10	35	4, 41	372, 3
A-S60						60	2, 57	
A-S300*						300	0, 05	
B-S60				B		60	4, 39	
B-S100				100		2, 64		

f_c' : Unconfined compressive strength
 ρ_l : Longitudinal reinforcement ratio
 f_{sy} : Yield strength of longitudinal rebar
 ρ_h : Confining reinforcement volume ratio
 f_{yh}' : Yield strength of confinement rebar

* A-S300: 2 pcs. of specimens were made to simulate unconfined concrete model

6.3.3 Loading and Measure Equipments

Monotonic loading was conducted by 5000 kN hydraulic loading equipments. The longitudinal displacement was measured by eight displacement gauges attached at four sides; two gauges were attached at each side (Fig. 6.8). The measurement length of each gauge was 340 mm. The strain of confining rebar was measured by strain gauge attached at the surface of rebar (Fig. 6.9).

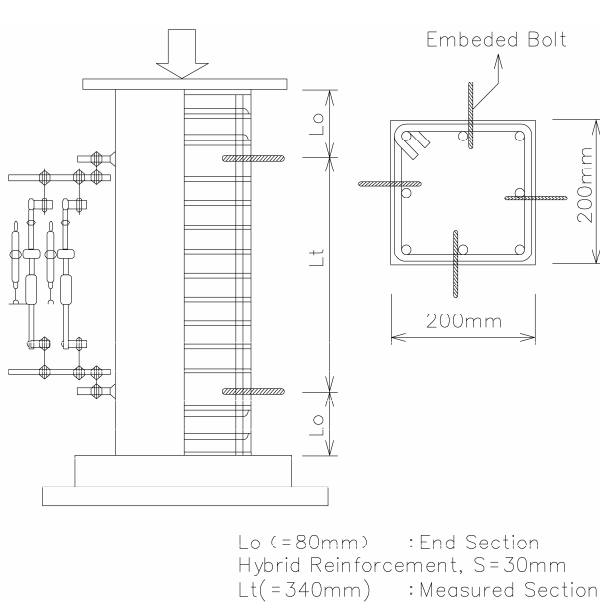


Fig. 6.8: Loading and measure equipments

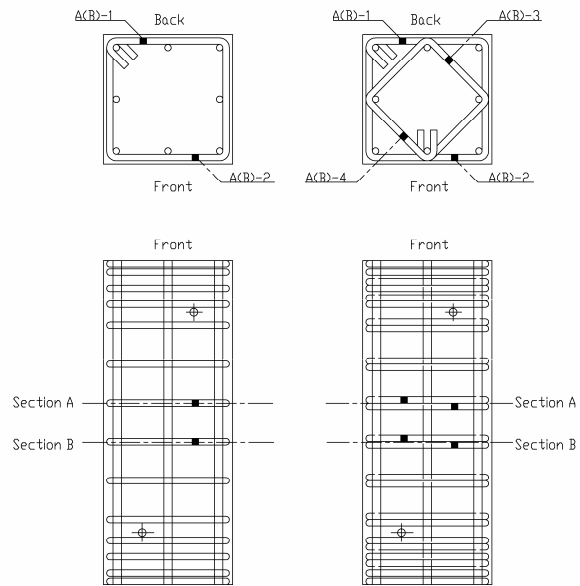


Fig. 6.9: Strain gauges of confinements

6.3.4 Results and Discussion

6.3.4.1 Stress-Strain Relationship of Confined Concrete

The states of experiment and specimens after loading are shown in *Photo 6.4*. The longitudinal strain of confined concrete ε_c is calculated from longitudinal displacement measured by displacement gauges attached at each side with dividing by measured length (=340 mm).

The evaluation of cover concrete is important for calculation of compressive stress σ_c of confined concrete.

The cover concrete peel off commenced when longitudinal strain came to 0,15 % - 0,20 % in the experiment.

The peel off of cover concrete was completed when longitudinal rebar strain came to 0,35 % - 0,75 %.

The confined compressive stress of HLAC σ_c is calculated as follows with consideration of obtained results from the experiment.



- (1) At the stage of *Photo 6.4: View of experiment and specimens after loading* cover concrete peel off commencement:

The confined concrete stress σ_c is calculated by share axial load of concrete divided by the area of total section; share axial load of concrete is calculated from total load minus longitudinal rebar share load.

- (2) At the stage of cover concrete peel off completion:

The confined concrete stress σ_c is calculated by share axial load of confined concrete divided by the area of core concrete. The area of core concrete is calculated by total area minus cover concrete area.

(3) At the stage from cover concrete peel off commencement through the state when the column loses axial load resistance:

The confined concrete stress σ_c is calculated by interpolation with three dimensional curvature.

The stress strain curves of HLAC obtained by above described way are shown in *Figs. 6.10, 6.11 and 6.12.*

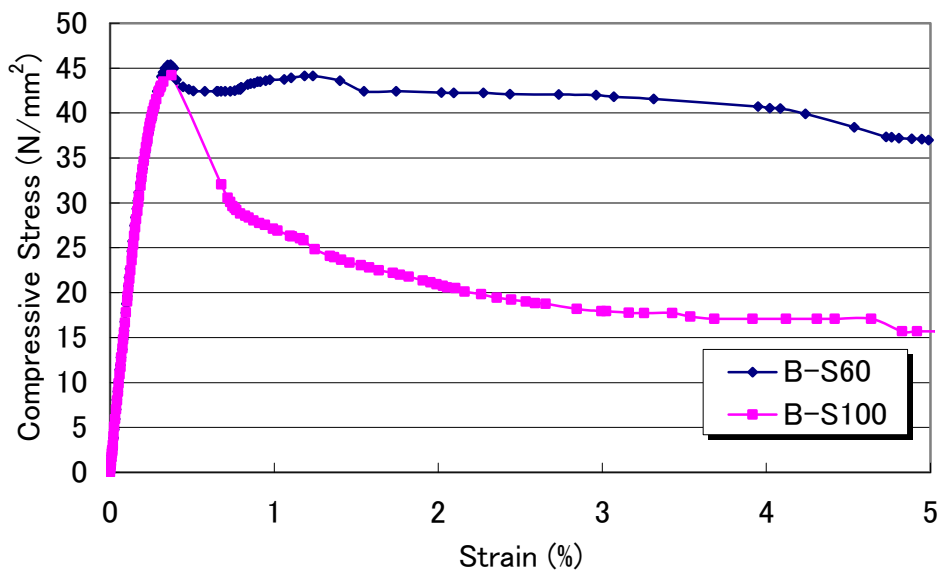
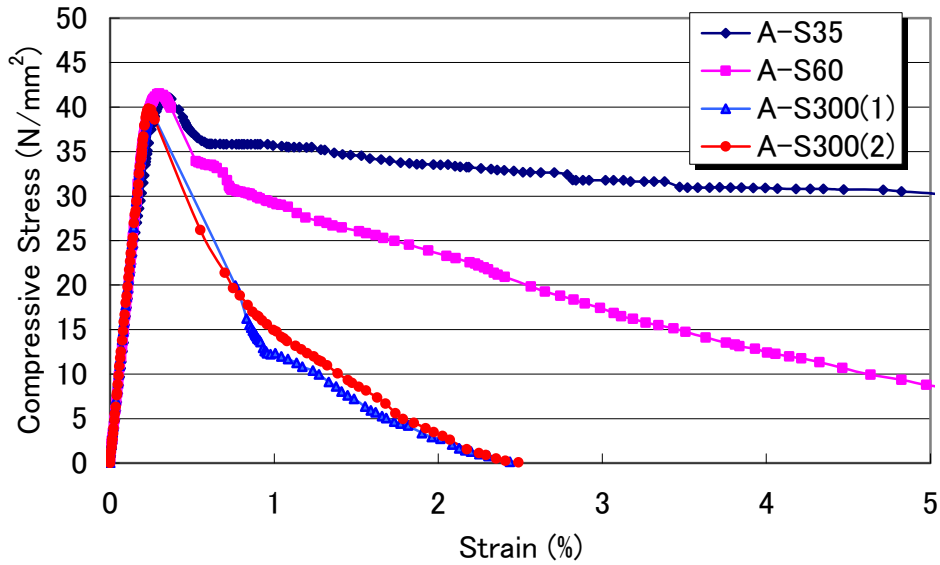


*Fig. 6.10: Measured stress strain relationship
(Same type rebar layout with different confining reinforcement volume ratio)*

Fig. 6.10 is the comparison between the specimens with same type of confinement layout and different confining reinforcement volume ratio. The increased confinement gives gentler post peak slope. Although peak stress of confined concrete is larger than that of unconfined concrete, the influence of confinement is slight. However confinement gives distinctly higher ductility with comparison between confined specimens and unconfined specimens.

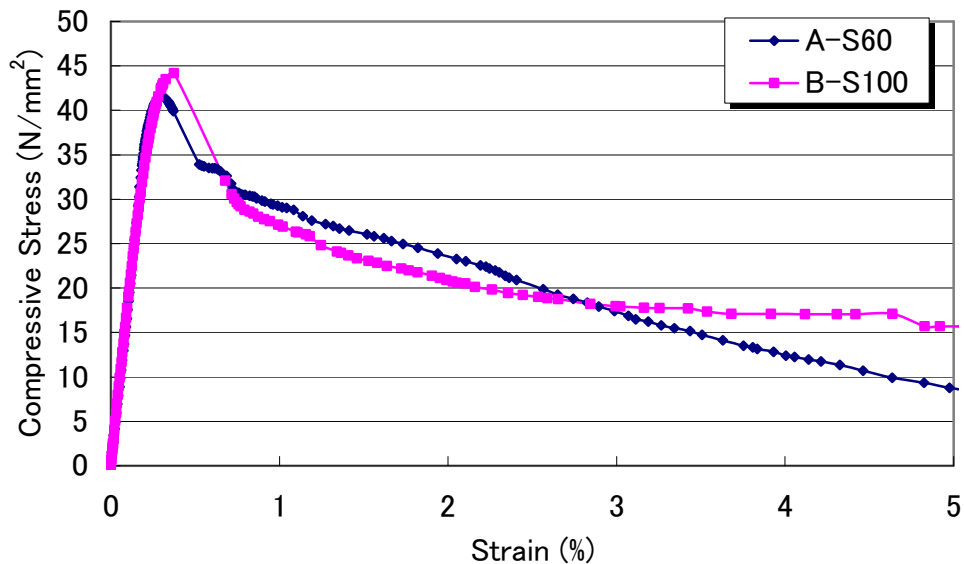
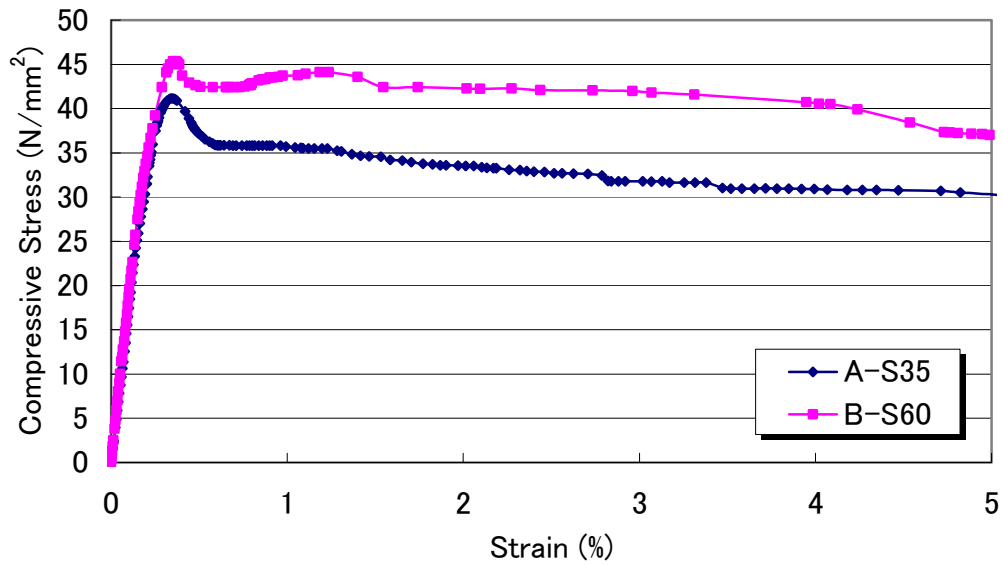


Fig. 6.11: Measured stress strain relationship
(Same confining reinforcement volume ratio with different type rebar layout)

Fig. 6.11 is the comparison between specimens with same confining reinforcement volume ratio and different types of confining rebar layout. Type B layout gives higher peak stress and ductility.

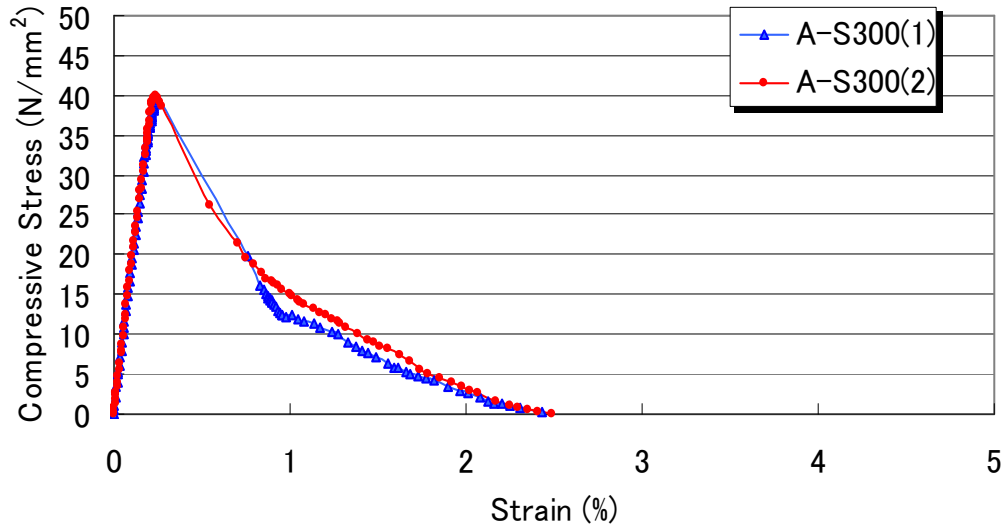


Fig. 6.12: Measured stress strain relationship (Unconfined specimens)

Table 6.15: Confining rebar strain and tensile stress of specimens at peak stress of confined concrete

Specimen	Items	Symbols of strain gauges							
		A-1	A-2	A-3	A-4	B-1	B-2	B-3	B-4
A-S35	Strain (%)	0,0516	0,0688	—	—	0,0625	0,1030	—	—
	Stress (N/mm ²)	94,3	127,2	—	—	115,6	190,4	—	—
A-S60	Strain (%)	0,0577	0,1923	—	—	0,1031	0,2246	—	—
	Stress (N/mm ²)	106,7	355,6	—	—	190,6	372,3	—	—
B-S60	Strain (%)	0,0577	0,1357	0,0701	0,0954	0,0420	0,1536	0,0600	0,0858
	Stress (N/mm ²)	106,7	250,9	129,6	176,4	77,7	284,0	110,9	158,6
B-S100	Strain (%)	0,1302	0,2926	0,2139	0,1794	0,2807	0,2432	0,2679	0,7803
	Stress (N/mm ²)	240,7	372,3	372,3	331,7	372,3	372,3	372,3	372,3

Fig. 6.12 shows the results of unconfined specimens. The decrease of stiffness after peak stress is prominent compared with confined concrete specimens; this shows the inductile behaviour of unconfined concrete specimens.

6.3.4.2 Strain of Confining Reinforcement

The strain of confining reinforcement measured by strain gauges attached at the confining reinforcement is shown in Fig. 6.13. The strain and stress of confining reinforcement at the maximum compressive stress of confined

concrete are shown in *Table 6.15*.

The majority of confining rebars are not yielded when compressive stress of confined concrete is at peak stress.

However the confining rebars of B-S100 were yielded at six gauges.

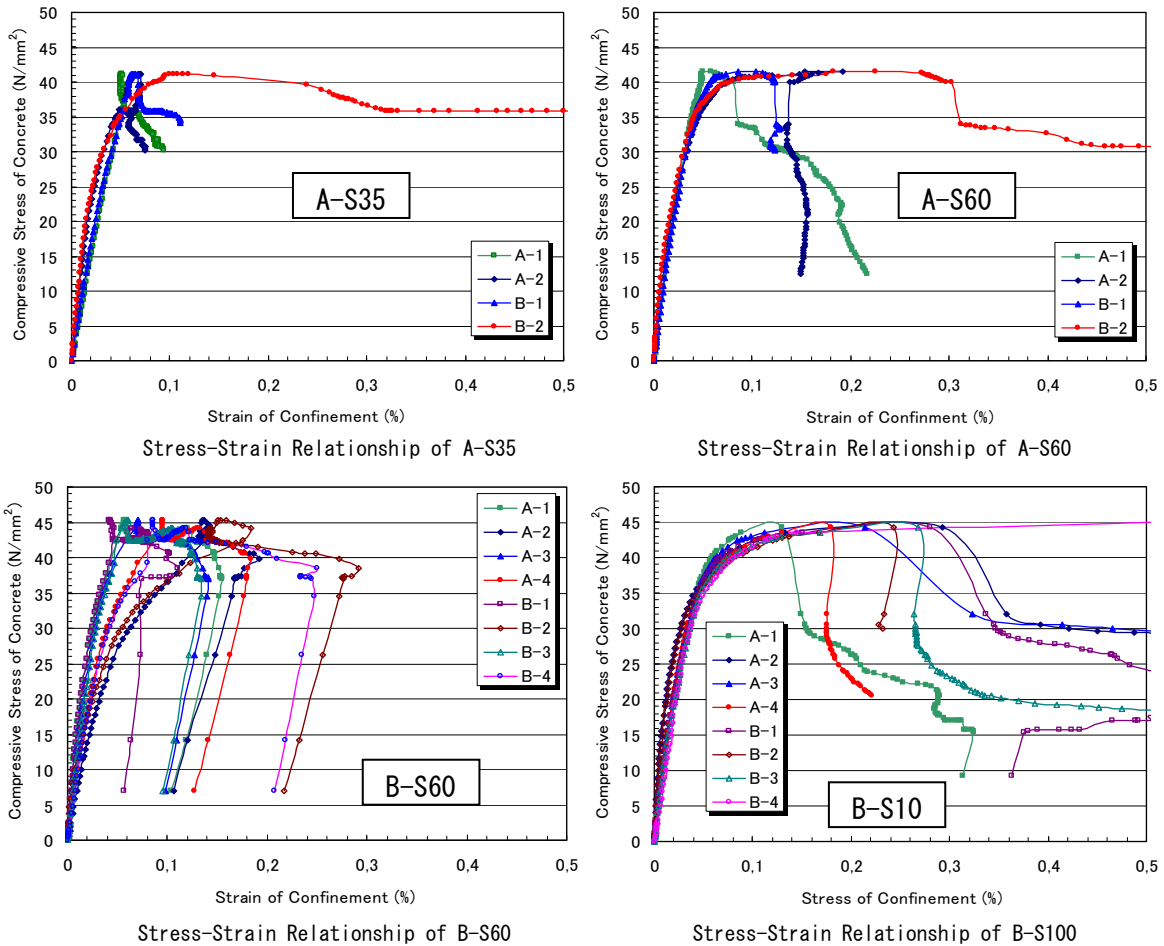


Fig. 6.13: Strain of confining reinforcement

6.3.4.5 Evaluation for Confining Effect on Stress-Strain Relationship

Not a few numerical models of stress-strain relationship are proposed for normal concrete, however only a few models are presented for lightweight concrete; particularly the research on the HLA employed in this research is not reported. As statistical analysis is not suitable to evaluate the confining effect of HLAC for its scant number of experimental test as of the state of today, modified model for stress-strain relationship from normal concrete is presented as follows. The comparison between proposed calculation model and experiment is shown in *Fig. 6.14*.

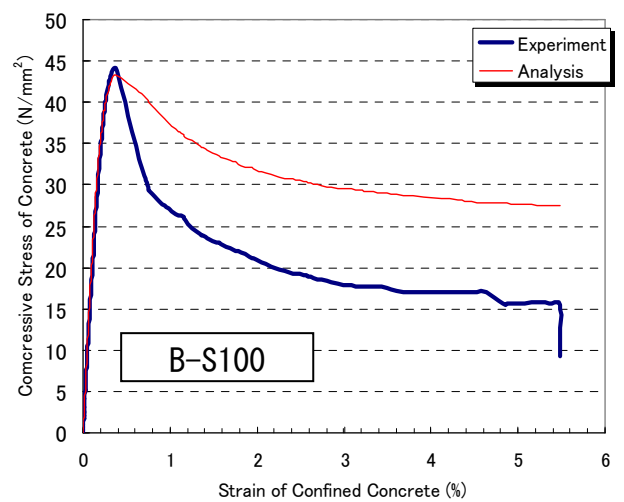
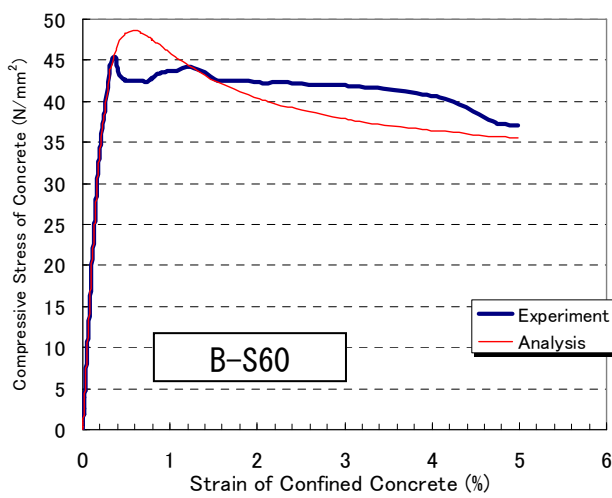
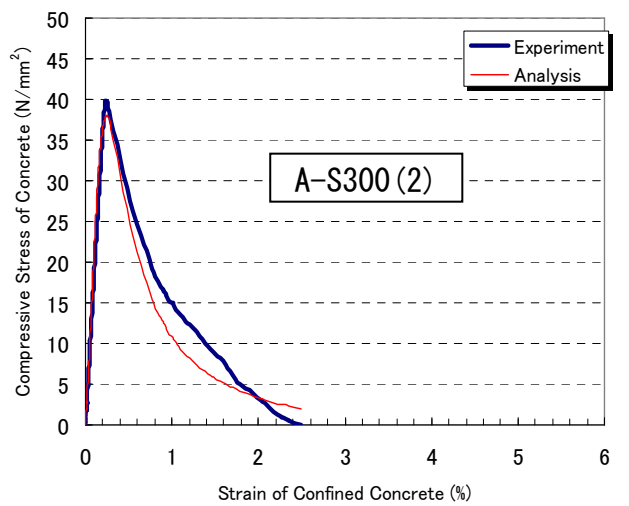
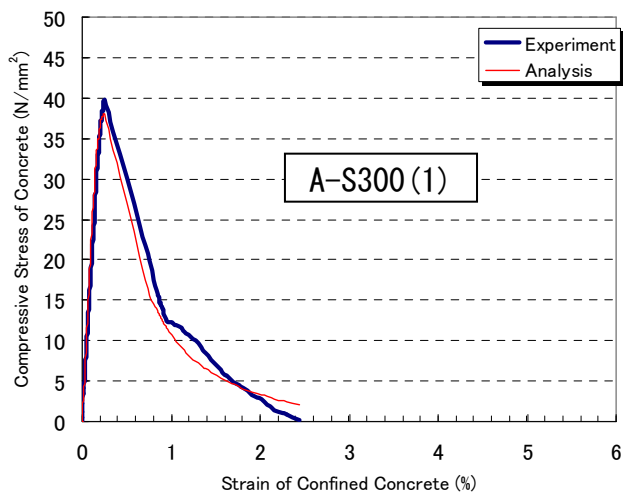
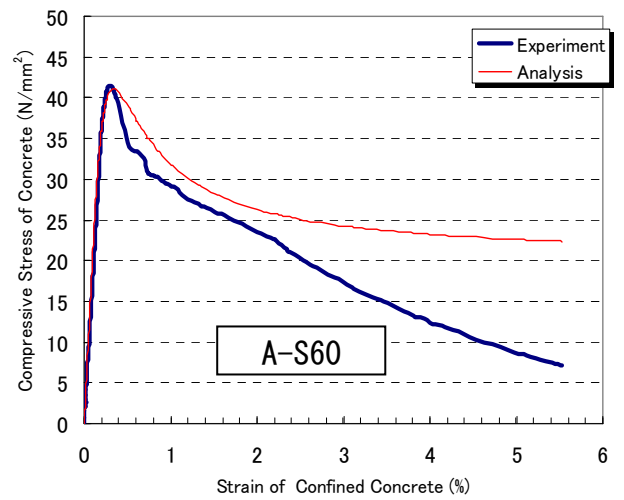
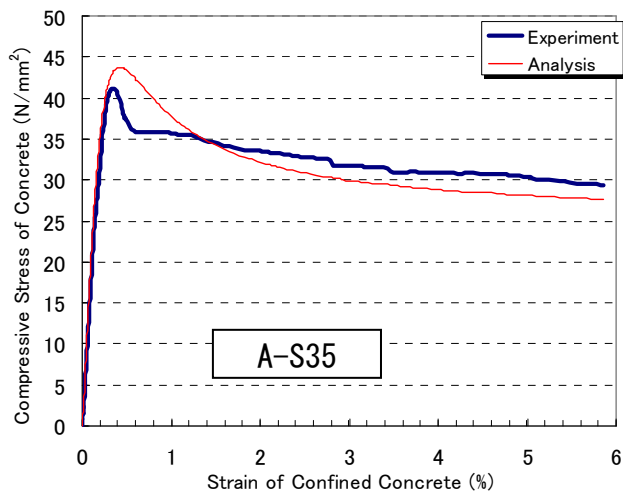


Fig. 6. 14: Comparison between experiment and analysis

$$Y = \frac{AX + (D-1)X^2}{1 + (A-2)X + DX^2} \quad (6.1)$$

where

$$Y = f_c / f_{cc}' \quad , \quad X = \varepsilon_c / \varepsilon_{co} \quad (6.2)$$

$$K = f_{cc}' / f_c' = 1 + 6 \frac{\rho_h f_{yh}}{f_c'} \left(\frac{d''}{C} \right) \left(1 - \frac{s}{2D_c} \right) \quad (6.3)$$

$$A = E_c \varepsilon_{co} / f_{cc}' \quad (6.4)$$

$$E_c = 0,3 \sqrt{f_c'} \times 10^4 \quad (6.5)$$

$$\frac{\varepsilon_{co}}{\varepsilon_o} = \begin{cases} 1 + 4,7(K-1) & , \quad K \leq 1,5 \\ 3,35 + 20(K-1,5) & , \quad K > 1,5 \end{cases} \quad (6.6)$$

$$\varepsilon_o = (f_c')^{1/4} \times 10^{-3} \quad (6.7)$$

$$D = 1,50 - 0,017 f_c' + 3 \sqrt{(K-1) f_c' / 23} \quad (6.8)$$

with

- f_{cc}' : Compressive strength of confined concrete (N/mm²)
- f_c' : Unconfined compressive strength of concrete (N/mm²)
- ρ_h : Confining reinforcement volume ratio (%)
- f_{yh} : Yield strength of confining rebar (N/mm²)
- C : Effective length of confining reinforcement (mm)
- d'' : Diameter of confining reinforcement (mm)
- s : Spacing of confining reinforcement (mm)
- D_c : Side length of hoop reinforcement (mm)

As shown in *Fig. 6.14*, proposed numerical model makes good fitting with experiment in the pre-peak area of stress-strain curve. It also shows effectively good fitting in the post-peak area of stress-strain curve. The test results of four of six specimens show the good fitting with analytical model, however there is no telling to assure the propriety with confidence for scant experimental data.

6.3.5 Conclusion

Experiment of HLAC short columns with HLA made from Huang River clay deposits in China was conducted to research the confining effect. The analytical model modified from that of normal concrete is proposed in this study. Conclusion is summarised as follows.

- (1) The post-peak slope of stress-strain curve is significantly improved by increase of confining reinforcement volume ratio, however the contribution for peak stress by confinement is slight.
- (2) Type B confinement rebar layout gives better confining effect for peak stress and ductility than that of type A layout (*i.e.* gentle slope of post-peak area of stress-strain curve).
- (3) Unconfined specimens showed inductile failure with significant decline of compressive stress of concrete after peak stress.
- (4) The analytical model proposed in this study makes effectively good fitting with the results of experiment. However, further experimental studies are expected to obtain reliable number of data to evaluate the validity of the proposed analytical model.

conducted with lightweight concrete, the vibrational serviceability is supposed to get worse. This clause discusses the vibrational serviceability of single span bridges similarly to chapter 5.

The structural models are same as those described in chapter 5 (Fig. 6.15). Cross section of the structural model is also shown in Fig. 6.16. The unit weight and elastic modulus are shown in Table 6.16. The parameters of analytical cases and symbols are shown in Table 6.17. Substructures of all the models are assumed as normal concrete; HLAC is only applied to superstructure.

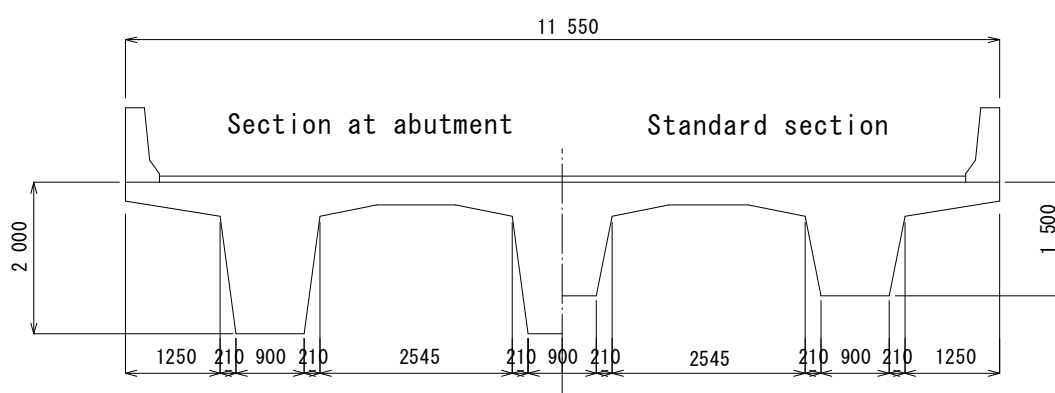


Fig. 6.16: Cross section of super structure

6.4.2 Static Analysis

Static deflection diagrams by truck driving are shown in Figs. 6.17 and 6.18. The deflections are merely proportional to the elastic modulus; other tendencies are same for all the models.

Table 6.16: Material properties

Material classification		Normal concrete model	HLAC model
Superstructure concrete	f_{ck}	40 N/mm ²	
	E_c	$3,10 \times 10^4$ N/mm ²	$2,49 \times 10^4$ N/mm ²
	W	24,5 kN/m ³	20,0 kN/m ³
Substructure concrete	f_{ck}	30 N/mm ²	
	E_c	$2,80 \times 10^4$ N/mm ²	
	W	24,5 kN/m ³	

f_{ck} : Characteristic value of unconfined compressive strength

E_c : Elastic modulus

W : Unit weight

Table 6.17: Analytical cases

		Conventional	Extended Deck	Semi-Integral Bridge	Integral Bridge
		C	E	S	I
Approach Length	0m	00	—	—	—
	3m	—	03	—	—
	6m	—	06	—	—
	10m	—	10	10	10
Stiffness of Approach Slabs Bed	Nominal	—	G	G	G
	Fix	—	F	F	F
Stiffness of Bearings	Nominal	B	B	B	—
	20 times	H	H	H	—
Stiffness of Foundations	Nominal	P	P	P	P
	Rigid	R	R	R	R
Tracking Lane	Central	C	C	C	C
	Side	S	S	S	S
Speed	40km/hour	40	40	40	40
	80km/hour	80	80	80	80
Concrete Type	Normal	N	N	N	N
	Lightweight	L	L	L	L

example : The case name “I10FPC80L” means the following.
 Integral model, 10m approach, Fixed approach slab bed, nominal pile foundation stiffness, Central tracking, 80km/hour, Lightweight concrete

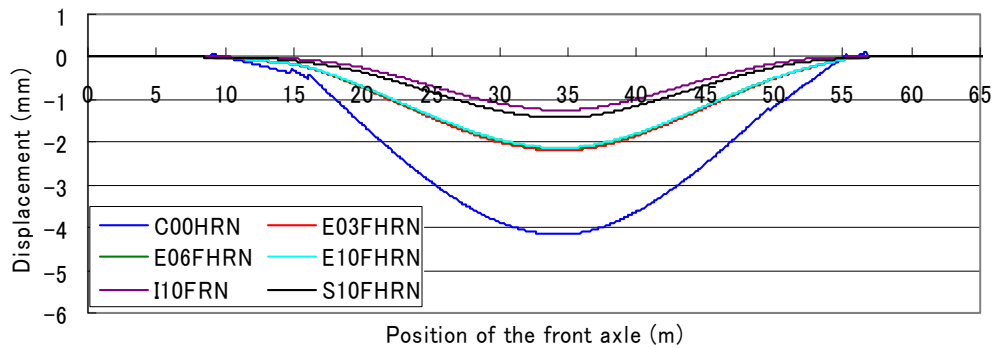


Fig. 6.17: Static deflection of mid-Span (Normal concrete)

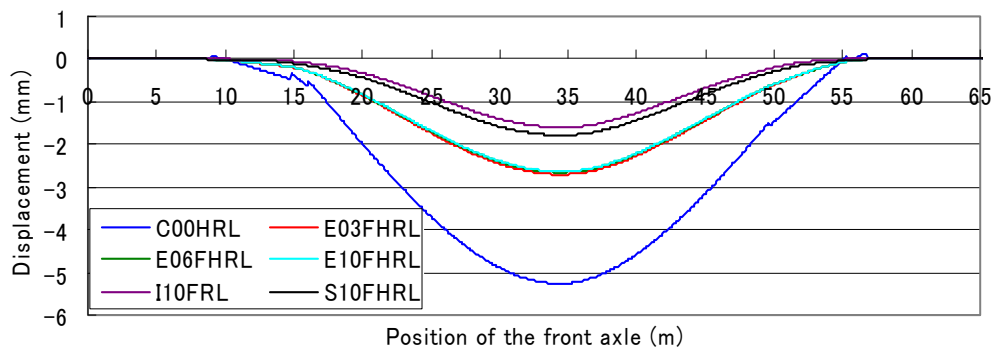


Fig. 6.18: Static deflection of mid-span (HLAC)

6.4.3 Eigen-value Analysis

Eigen-value analysis was conducted to grasp the fundamental vibrational properties of each model. The major vibration modes of the integral model are shown in *Fig. 6.19*. The natural frequencies of primary vibration modes are shown in *Figs. 6.20* and *6.21*. The strain energy share of members for damping of each model is shown in *Fig. 6.22*. The results are summarised as follows:

- The tendencies among structural systems (*i.e.* conventional model, extended deck model, semi-integral model and integral model) are similar between normal concrete models and HLAC models.
- The frequencies of HLAC models are slightly less than those of normal concrete models.
- There are almost no differences appeared between normal concrete models and HLAC models; structural system is dominant for the strain energy share of members for damping regardless of concrete material.

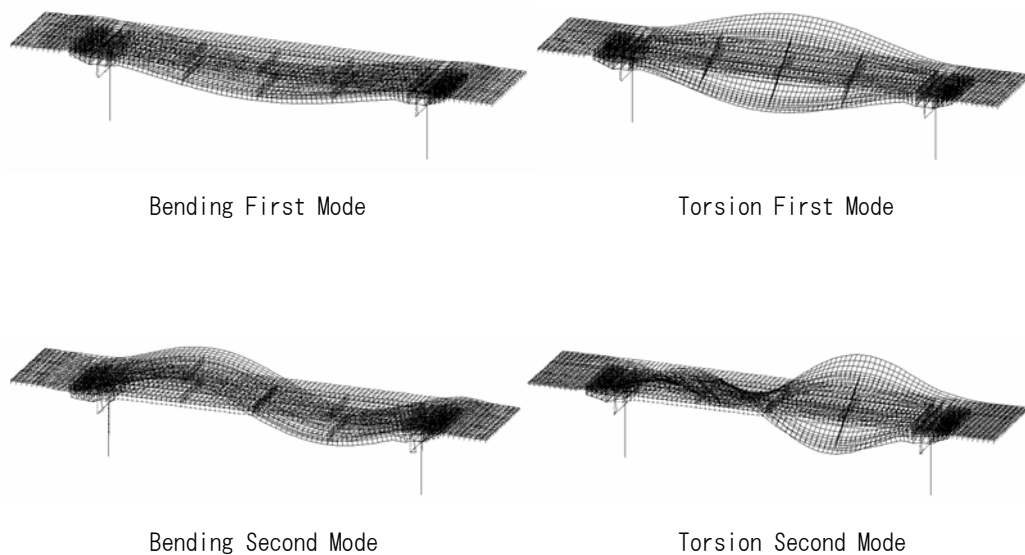


Fig. 6.19: Vibration modes of integral bridge model

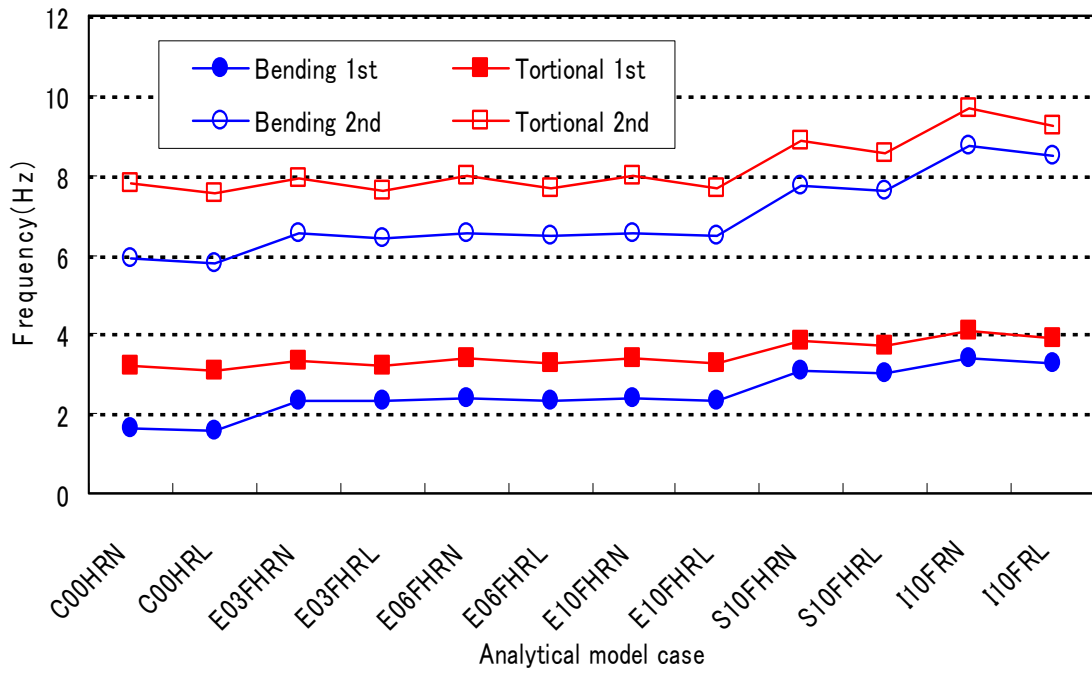


Fig. 6.20: Frequencies of rigid foundation models (Normal vs. HLAC)

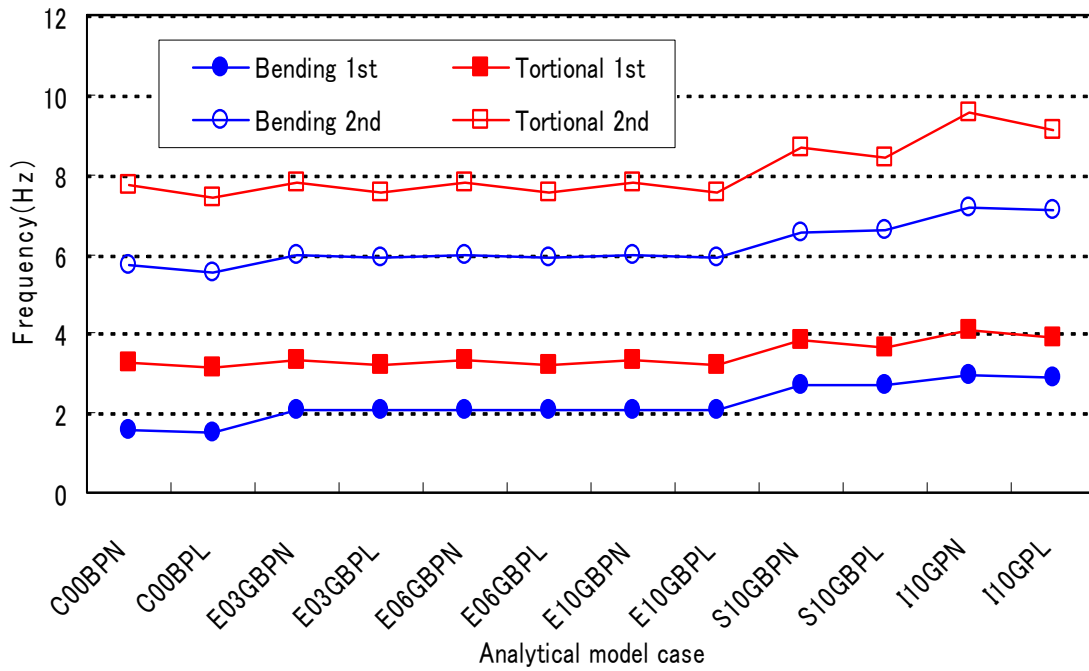


Fig. 6.21: Frequencies of pile foundation models (Normal vs. HLAC)

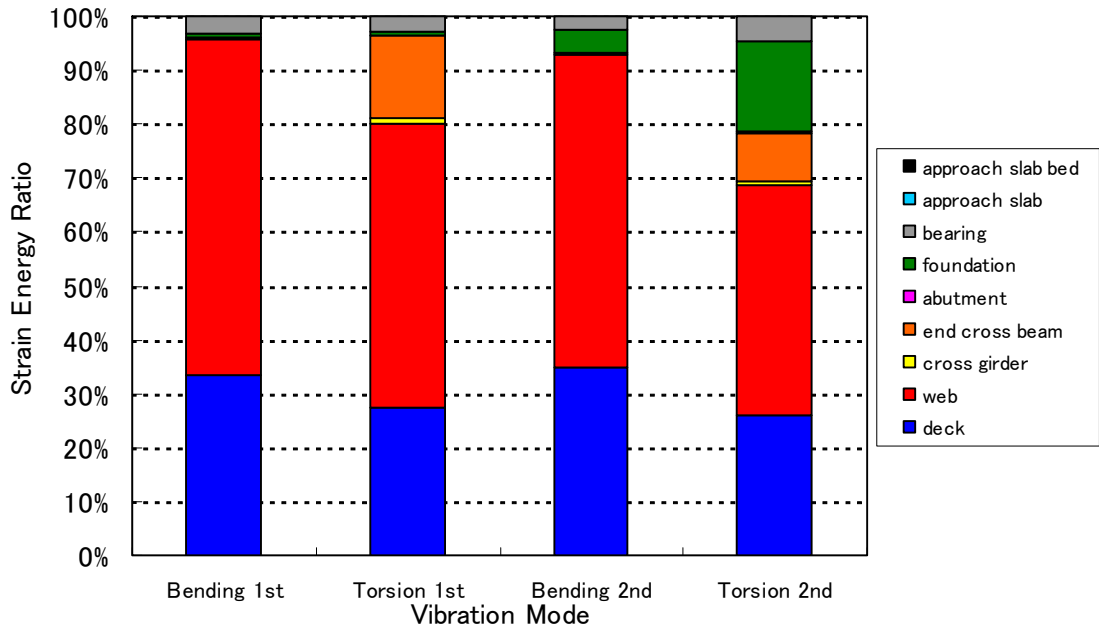


Fig. 6.22(A-1): Strain energy share of members for damping, Conventional model with normal concrete (COOBPN)

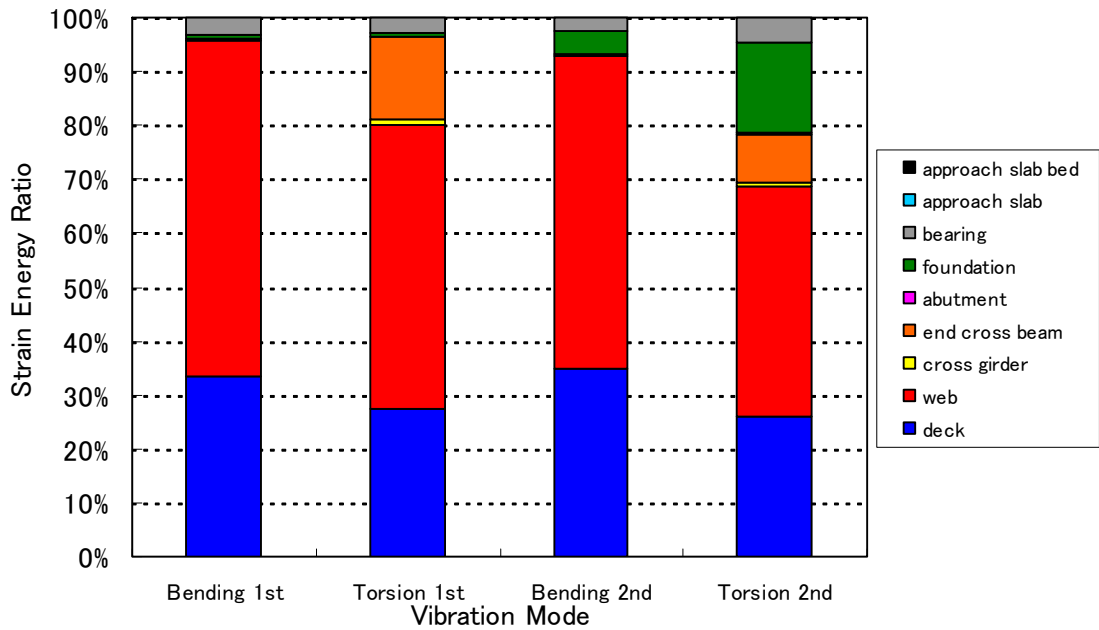


Fig. 6.22(A-2): Strain energy share of members for damping, Conventional model with HLAC (COOBPL)

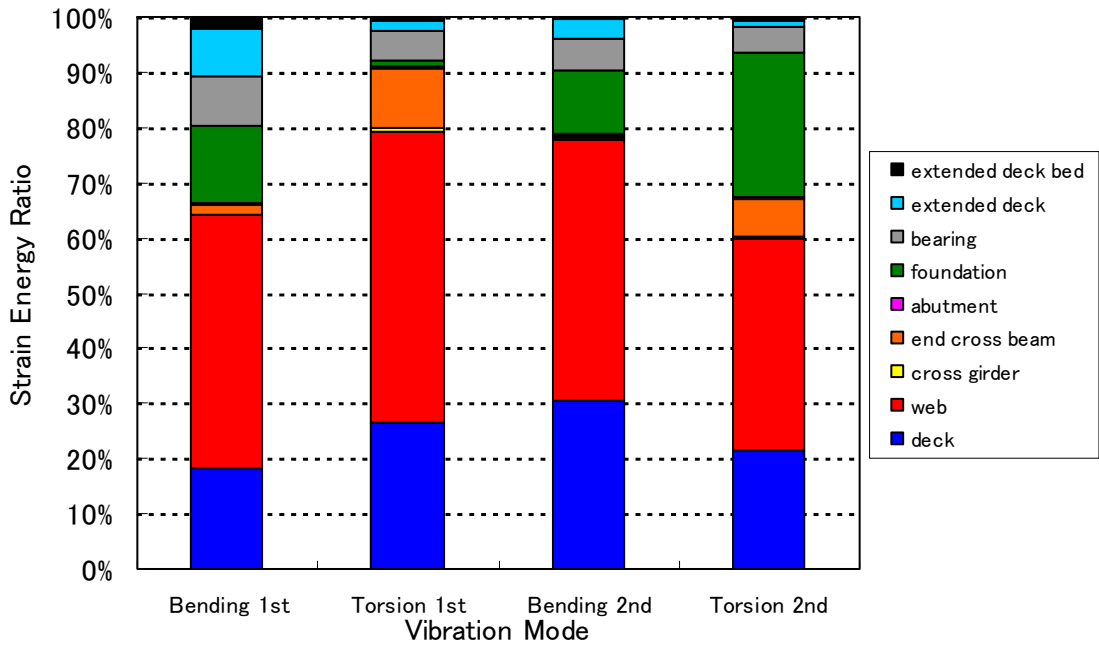


Fig. 6.22(B-1): Strain energy share of members for damping, Extended deck model with normal concrete (E10GBPN)

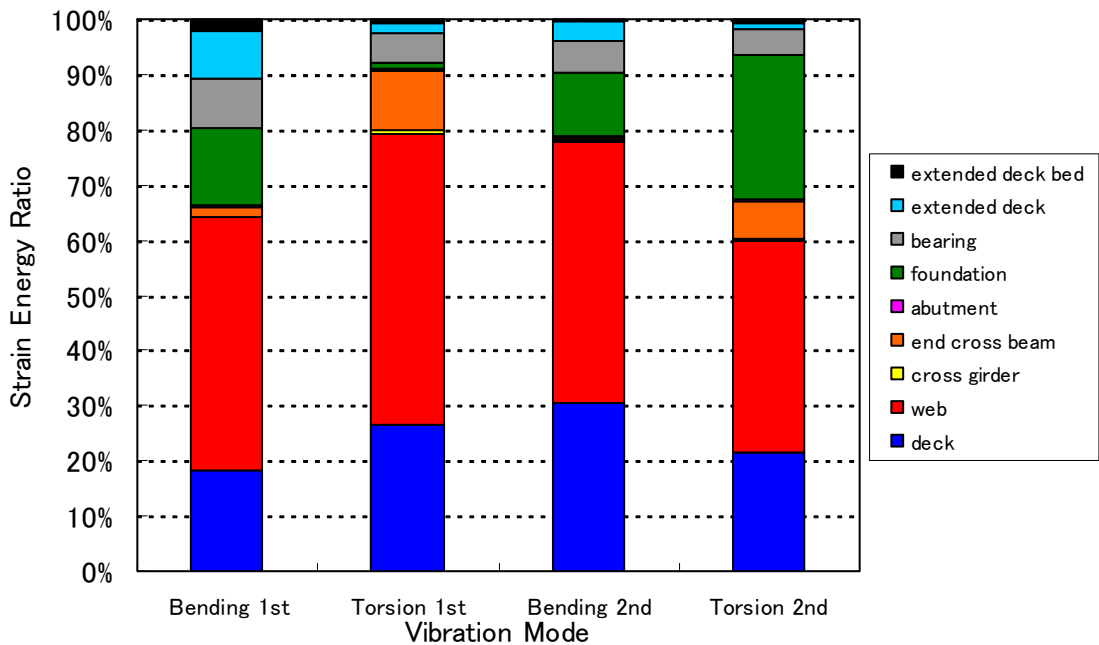


Fig. 6.22(B-2): Strain energy share of members for damping, Extended deck model with HLAC (E10GBPL)

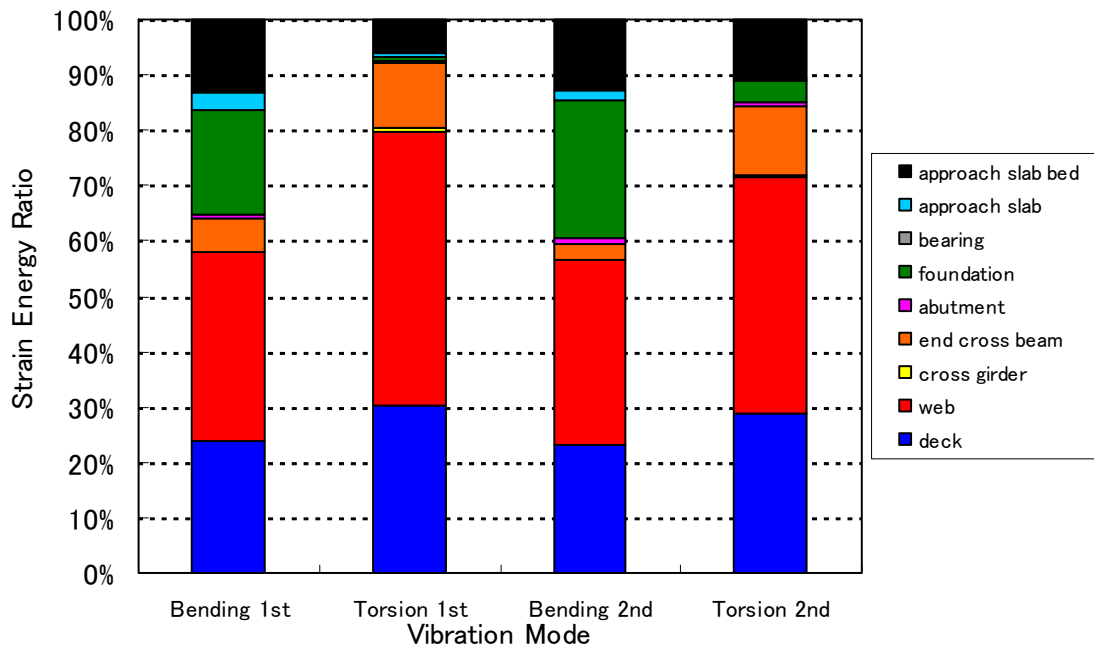


Fig. 6.22 (C-1): Strain energy share of members for damping, Semi integral model with normal concrete (S10GBPN)

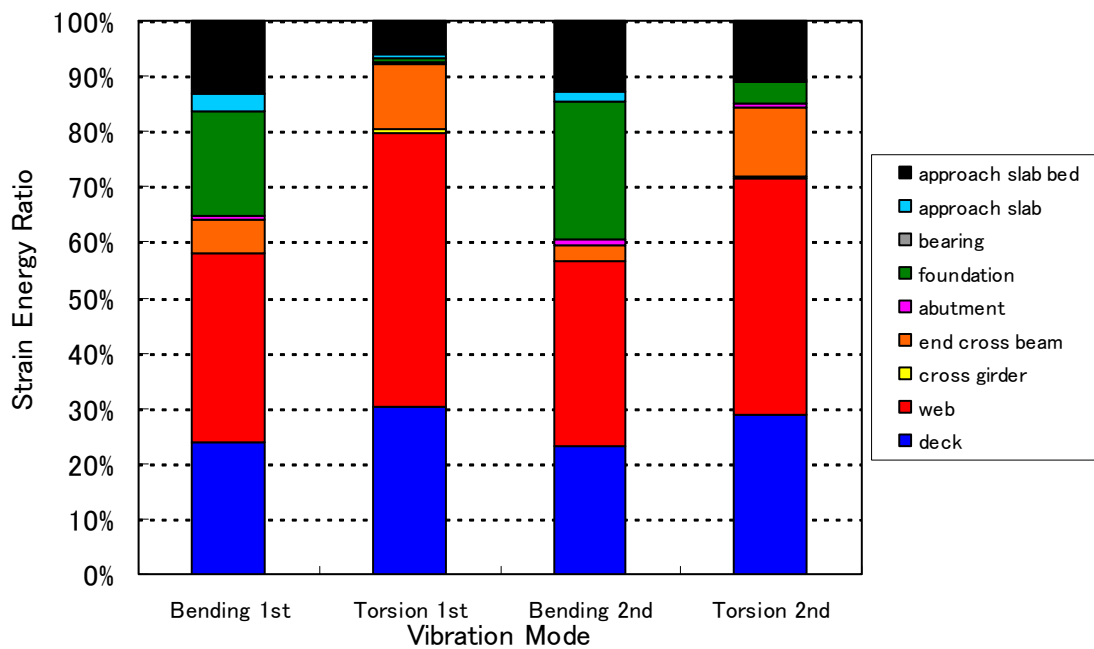


Fig. 6.22 (C-2): Strain energy share of members for damping, Semi integral model with HLAC (S10GBPL)

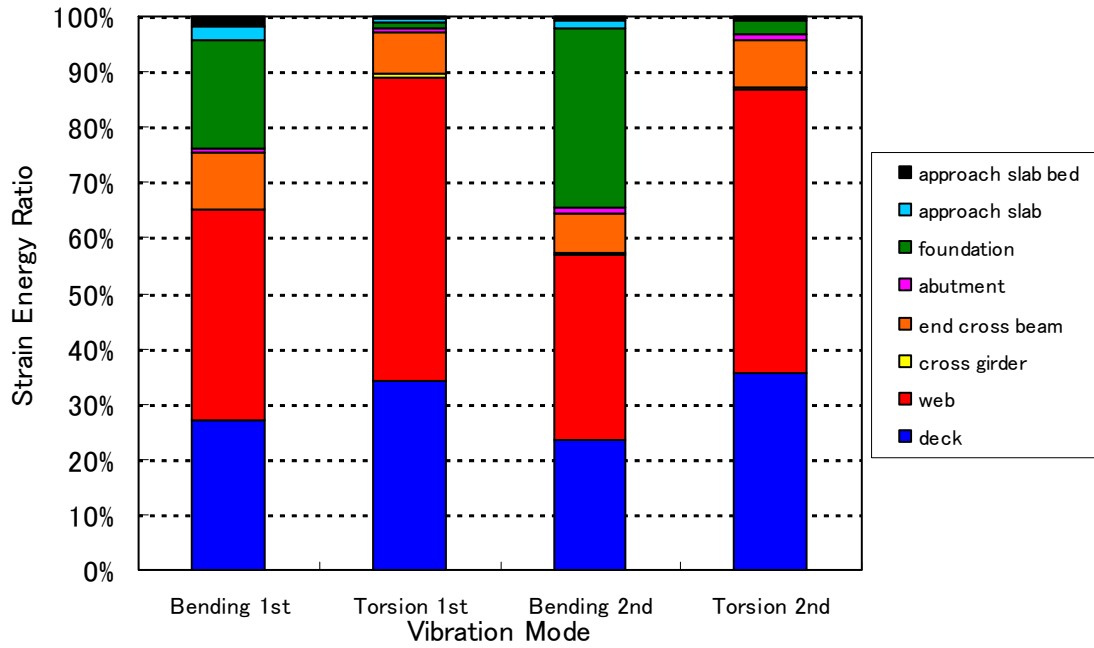


Fig. 6.22(D-1): Strain energy share of members for damping, Integral model with normal concrete (110GBPN)

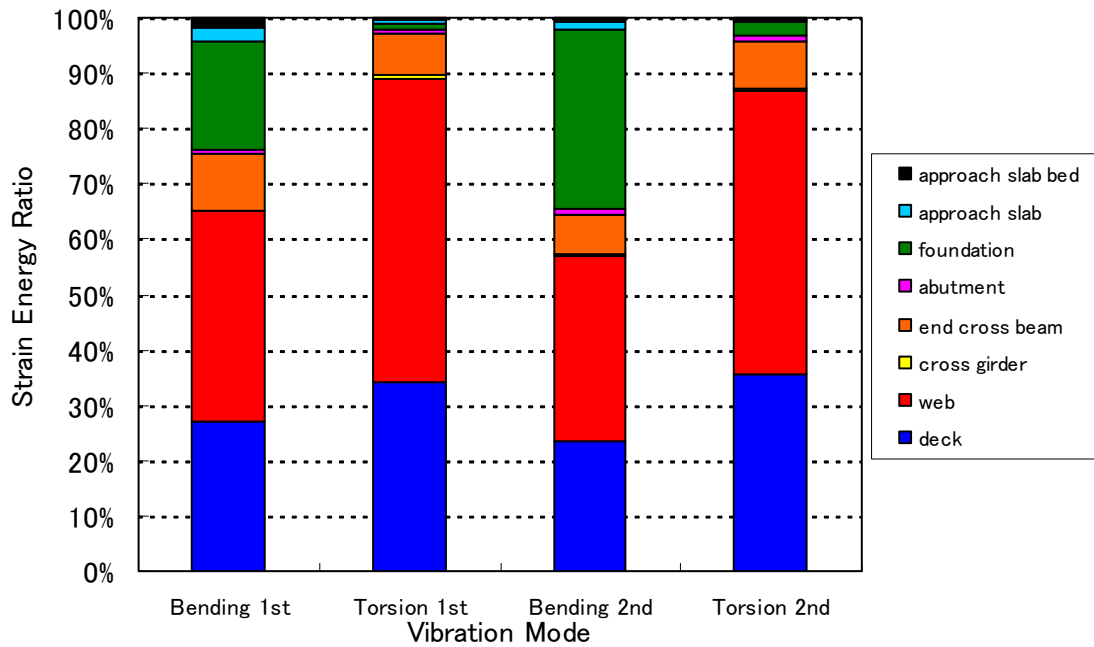


Fig. 6.22(D-2): Strain energy share of members for damping, Integral model with HLAC (110GBPL)

Fig. 6.22: Strain Energy Share of Members for Damping

6.4.4 Dynamic Response Analysis - Serviceability for Pedestrians -

The ergonomic serviceability of the bridge with respect to the vibration for pedestrians of HLAC bridges is also studied by numerical analyses with comparison to normal concrete ones.

The damping ratios of HLAC bridge models are taken as same values of normal concrete bridge models from the results of eigen-value analyses. The conditions of truck modelling and roughness are same as the assumptions described in chapter 5.

The evaluation is also conducted with effective value of response velocity, *i.e.* the maximum of root mean square (RMS) of the response velocity. The results of dynamic response analyses are shown in *Figs. 6.23* and summarised are as follows.

- The qualitative tendencies (*e.g.* the influences of type of structural system, tracking lane, driving speed and type of foundation) are effectively same as the results of normal concrete models and HLAC models.
- The responses of HLAC models are larger than those of normal concrete models in all the cases.
- The average increment of RMS of the response velocity of HLAC models is 22% of normal concrete models. The increment ratio (HLAC/Normal) ranges from 15% to 25%.
- The responses of integral models, semi integral models and extended deck models with 10m extension remain low level even HLAC is employed.
- Integral models gain the lowest responses in all the cases. However, semi-integral models come close in response to the integral models. Extended deck models with 10m extension also makes good control for serviceability for pedestrians.

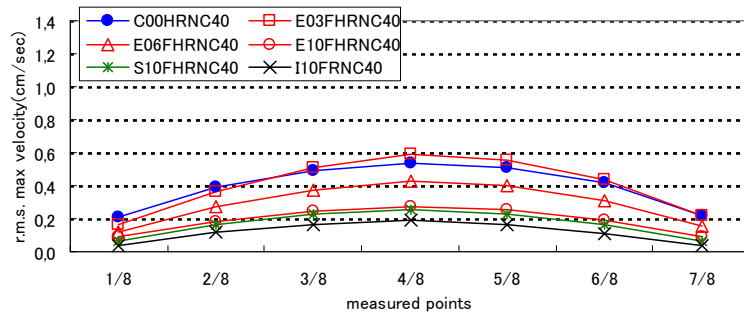


Fig. 6.23(A-1): Maximum R.M.S. of velocity of side girder of rigid foundation models in 40km/hour driving of central tracking lane (Normal concrete)

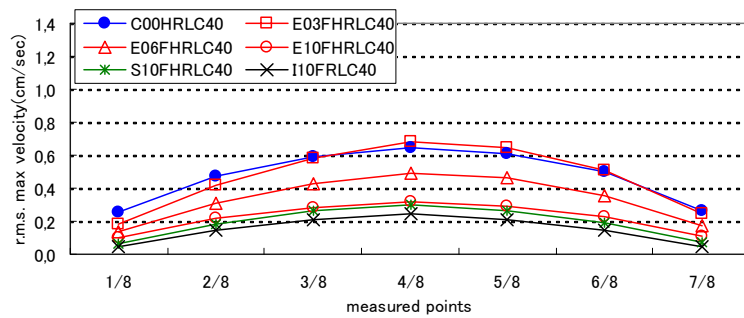


Fig. 6.23(A-2): Maximum R.M.S. of velocity of side girder of rigid foundation models in 40km/hour driving of central tracking lane (HLAC)

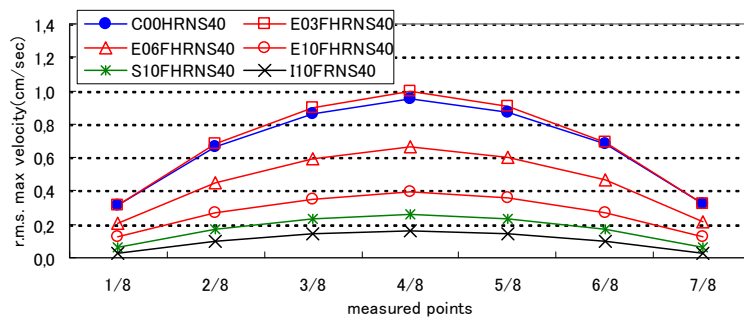


Fig. 6.23(B-1): Maximum R.M.S. of velocity of side girder of rigid foundation models in 40km/hour driving of side tracking lane (Normal concrete)

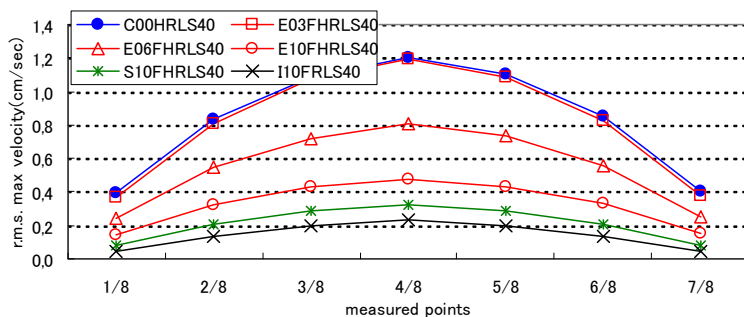


Fig. 6.23(B-2): Maximum R.M.S. of velocity of side girder of Rigid foundation models in 40km/hour driving of side tracking lane (HLAC)

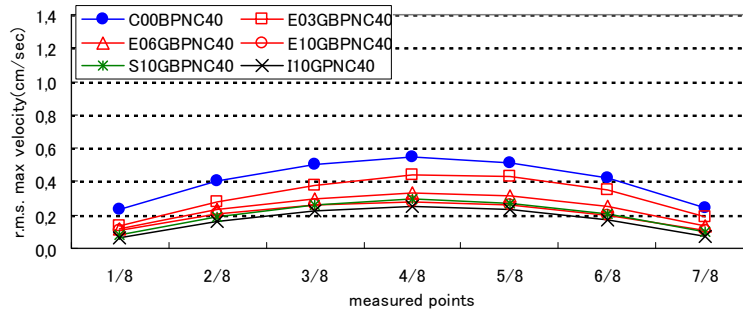


Fig. 6.23(C-1): Maximum R.M.S. of velocity of side girder of soft foundation models in 40km/hour driving of central tracking lane (Normal concrete)

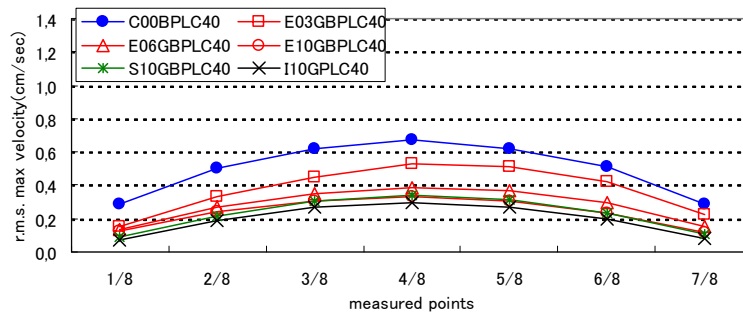


Fig. 6.23(C-2): Maximum R.M.S. of velocity of side girder of soft foundation models in 40km/hour driving of central tracking lane (HLAC)

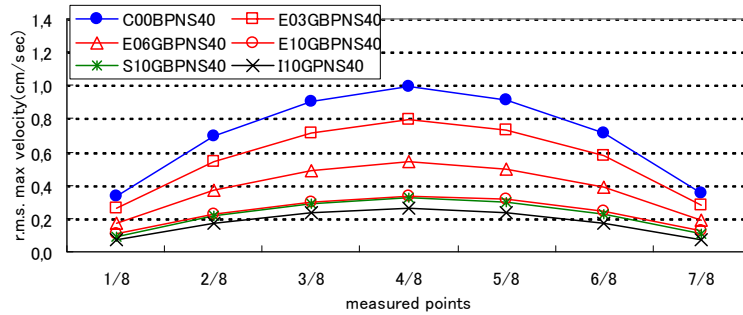


Fig. 6.23(D-1): Maximum R.M.S. of velocity of side girder of soft foundation models in 40km/hour driving of side tracking lane (Normal concrete)

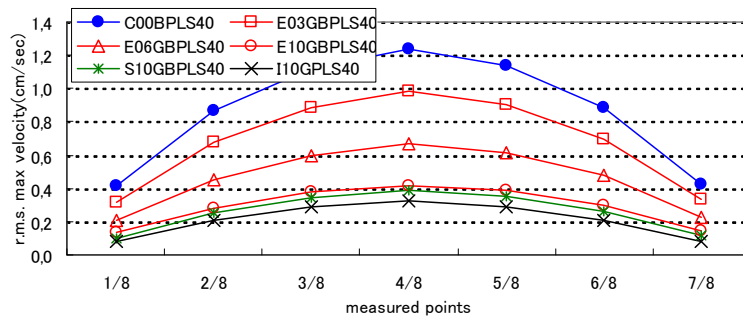


Fig. 6.23(D-2): Maximum R.M.S. of velocity of side girder of soft foundation models in 40km/hour driving of side tracking lane (HLAC)

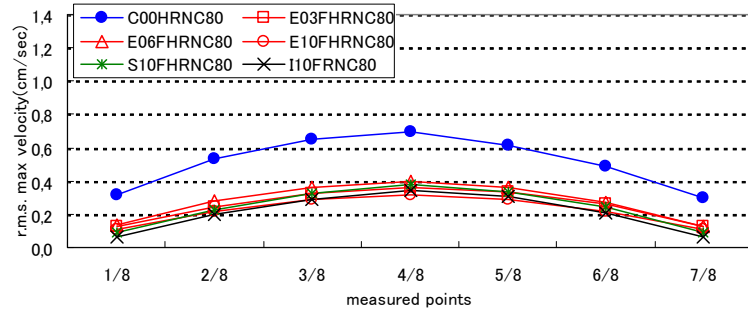


Fig. 6.23(E-1): Maximum R.M.S. of velocity of side girder of rigid foundation models in 80km/hour driving of central tracking lane (Normal concrete)

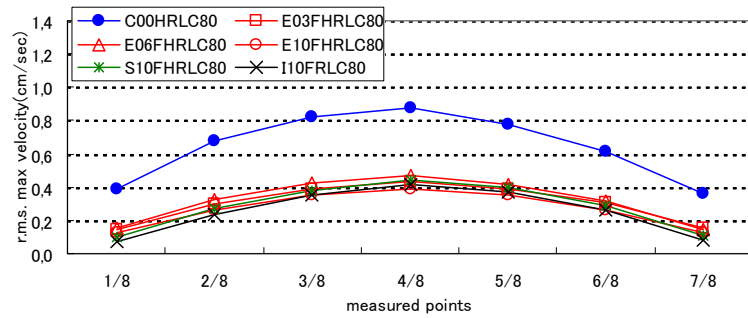


Fig. 6.23(E-2): Maximum R.M.S. of velocity of side girder of rigid foundation models in 80km/hour driving of central tracking lane (HLAC)

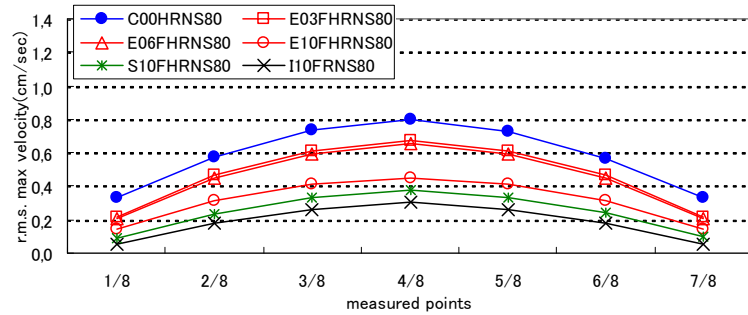


Fig. 6.23(F-1): Maximum R.M.S. of velocity of side girder of rigid foundation models in 80km/hour driving of side tracking lane (Normal concrete)

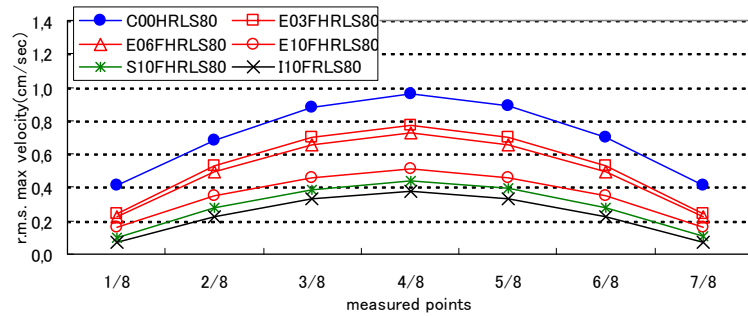


Fig. 6.23(F-2): Maximum R.M.S. of velocity of side girder of rigid foundation models in 80km/hour driving of side tracking lane (HLAC)

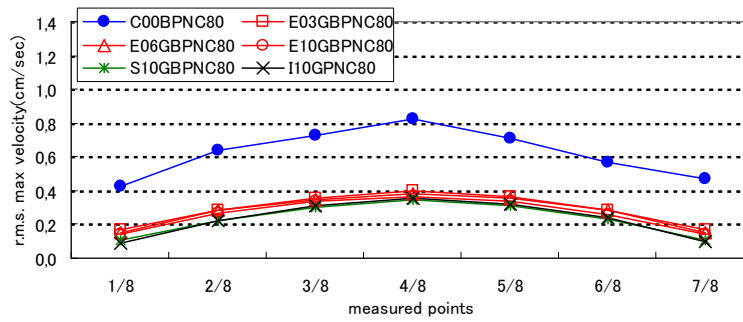


Fig. 6.23(G-1): Maximum R.M.S. of velocity of side girder of soft foundation models in 80km/hour driving of central tracking lane (Normal concrete)

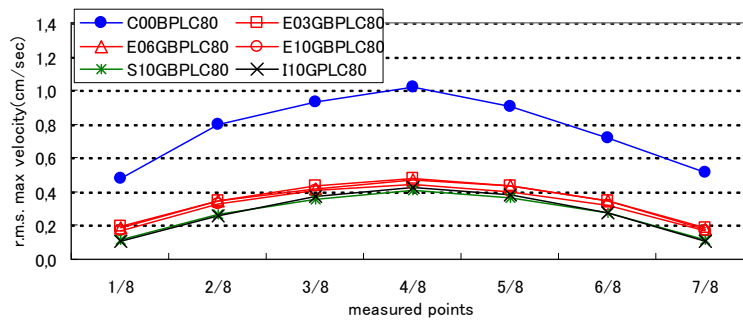


Fig. 6.23(G-2): Maximum R.M.S. of velocity of side girder of soft foundation models in 80km/hour driving of central tracking lane (HLAC)

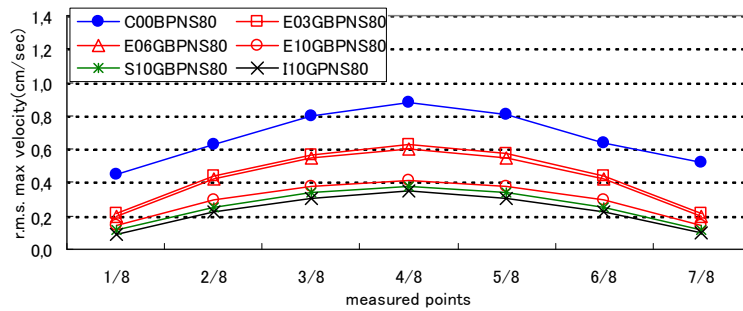


Fig. 6.23(H-1): Maximum R.M.S. of velocity of side girder of soft foundation models in 80km/hour driving of side tracking lane (Normal concrete)

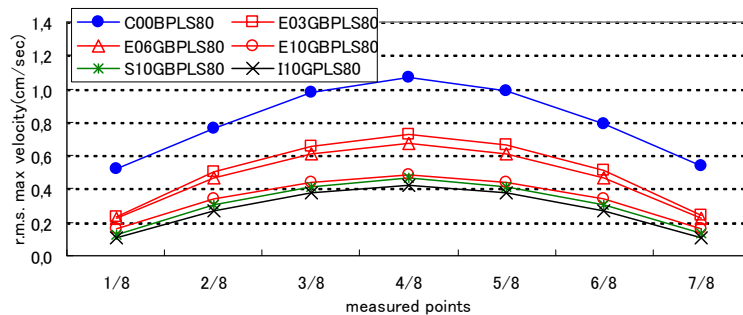


Fig. 6.23(H-2): Maximum R.M.S. of velocity of side girder of soft foundation models in 80km/hour driving of side tracking lane (HLAC)

Fig. 6.23: Maximum R.M.S. of velocity of side girder of normal concrete models and HLAC models

6.4.5 Dynamic Response Analysis - Infrasound -

The infrasound of the deck of HLAC bridge model was also studied with comparison to normal concrete bridge model.

The evaluation of infrasound is conducted by the same method as described in chapter 5 with sound radiation power estimated by equation (5.1).

The results of the maximum sound radiation power are shown in *Figs. 6.24* with comparison between normal concrete models and HLAC models.

The results are summarised as follows.

- The qualitative tendencies on infrasound radiation power (e.g. the influences of type of structural system, tracking lane, driving speed and type of foundation) are effectively same as the results of normal concrete models and HLAC models.
- The sound radiation power of HLAC models are larger than those of normal concrete models in all the cases.
- The average increment ratio of sound radiation power of HLAC models is 44% with comparison to normal concrete models; it ranges from 28% to 61%.
- The responses of integral models, semi integral models and extended deck models with 10m extension remain low level even HLAC is employed.
- Integral models gain the lowest responses in all the cases. However, semi-integral models and extended deck model with 10m extension come close in response to the integral models.

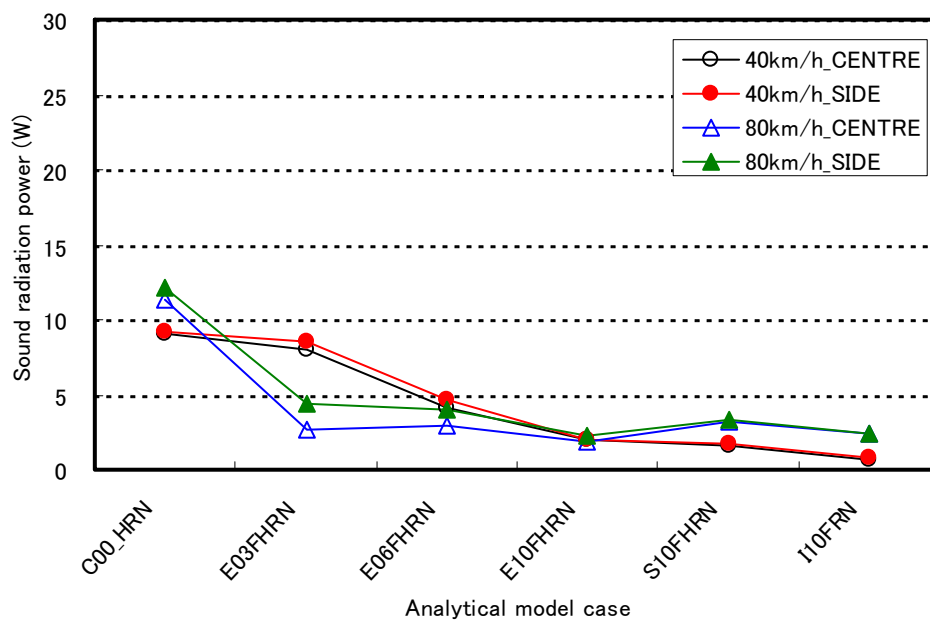


Fig. 6.24(A-1): Sound radiation power with rigid foundation models (Normal concrete models)

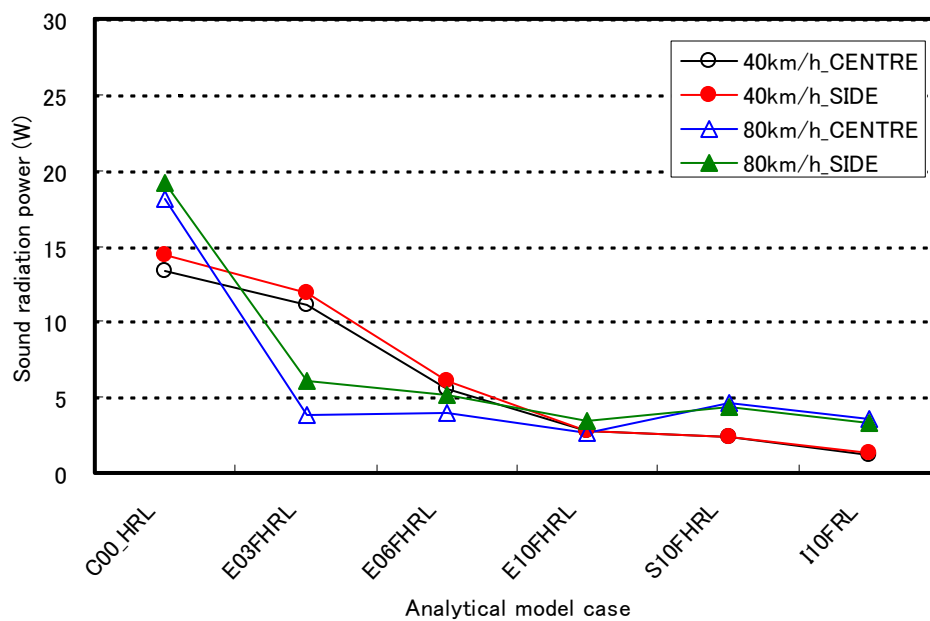


Fig. 6.24(A-2): Sound radiation power with rigid foundation models (HLAC models)

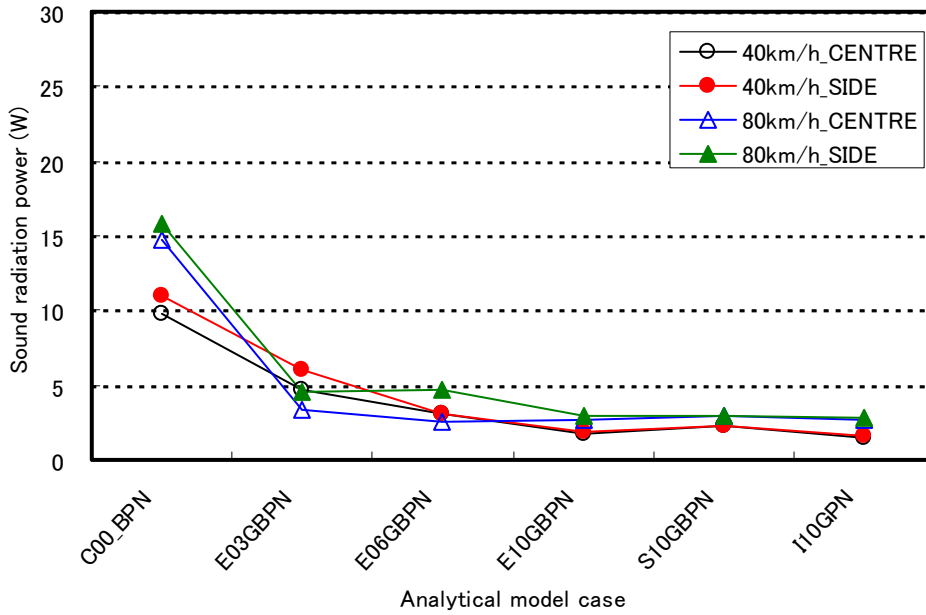


Fig. 6.24(B-1): Sound radiation power with pile foundation models (Normal concrete models)

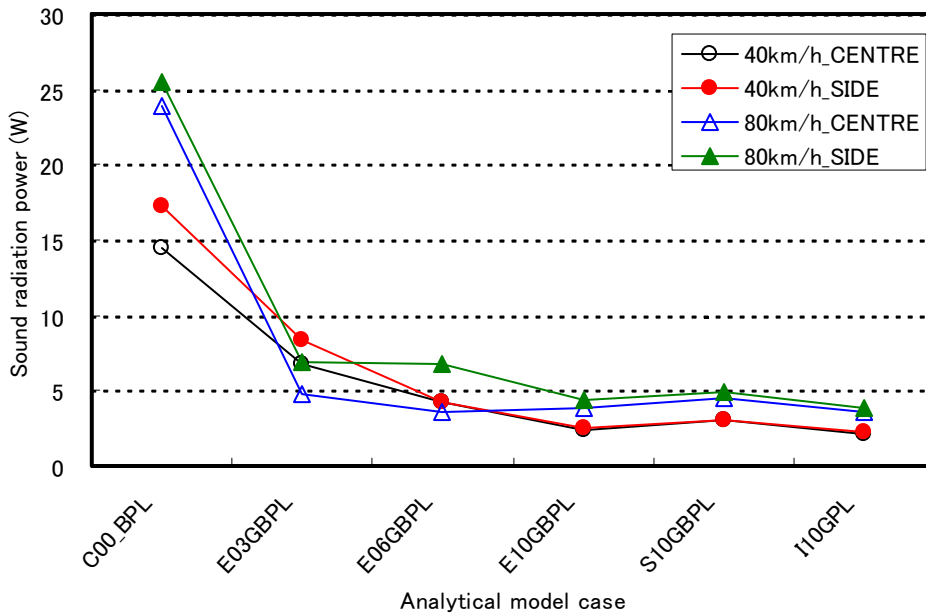


Fig. 6.24(B-2): Sound radiation power with pile foundation model (HLAC models)

Fig. 6.24: Sound radiation power of normal concrete models and HLAC models

6.4.6 Dynamic Response Analysis - Ground Vibration -

The ground vibration of HLAC bridge models were also studied with comparison to normal concrete bridge models.

The evaluation of ground vibration is conducted by the same method as described in chapter 5 with dynamic increment factor (DIF) of the reaction estimated by equation (5.2).

The results of dynamic increment factor (DIF) are shown in *Figs. 6.25* with comparison between normal concrete models and HLAC models.

The results are summarised as follows.

- The qualitative tendencies on infrasound radiation power (e.g. the influences of type of structural system, tracking lane, driving speed and type of foundation) are effectively same between the results of normal concrete models and HLAC models.
- The dynamic increment factors of HLAC models are almost equal to those of normal concrete models and slightly less than those of normal concrete.
- The average increment ratio of sound radiation power of HLAC models is -5% with comparison to normal concrete models; it ranges from -8% to +9%.
- The responses of integral models, semi integral models and extended deck models with 10m extension remain low level even HLAC is employed. Extended deck models with 10m extension showed the best control for ground vibration.
- In general, the influence of types of concrete materials for ground vibration is slight. Structural system is dominant factor for ground vibration.

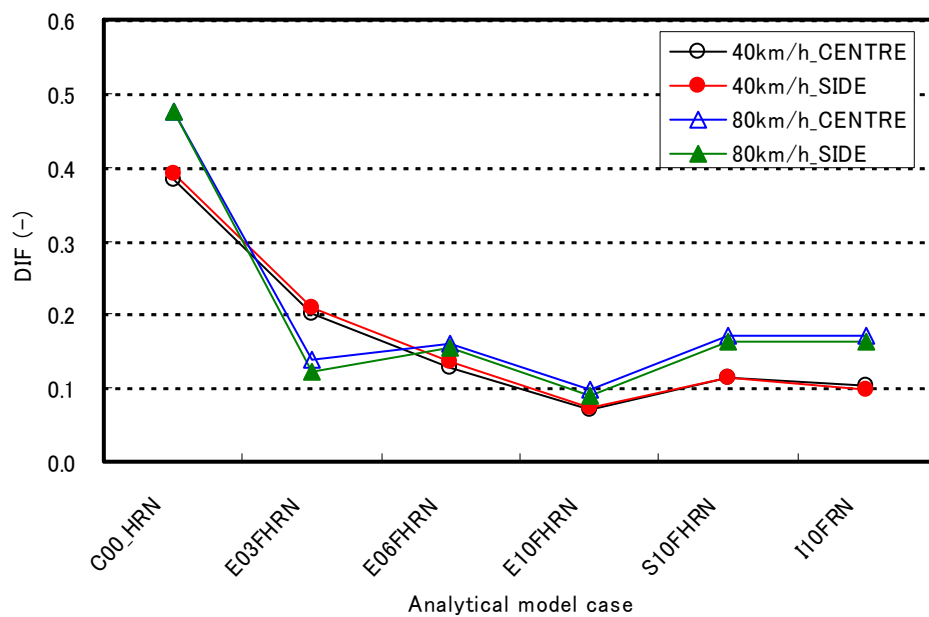


Fig. 6.25(A-1): Dynamic increment factor of rigid foundation models (Normal concrete models)

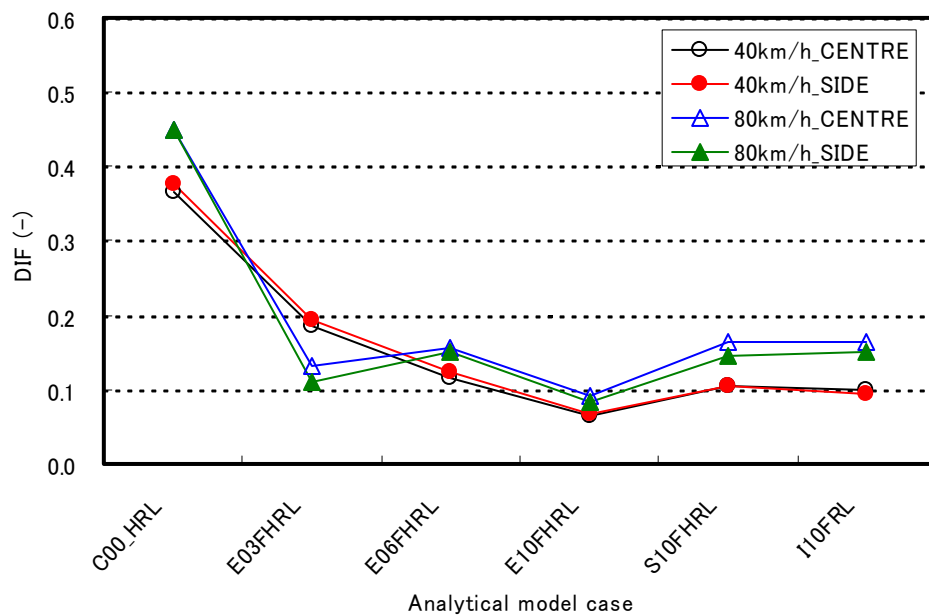


Fig. 6.25(A-2): Dynamic increment factor of rigid foundation models (HLAC models)

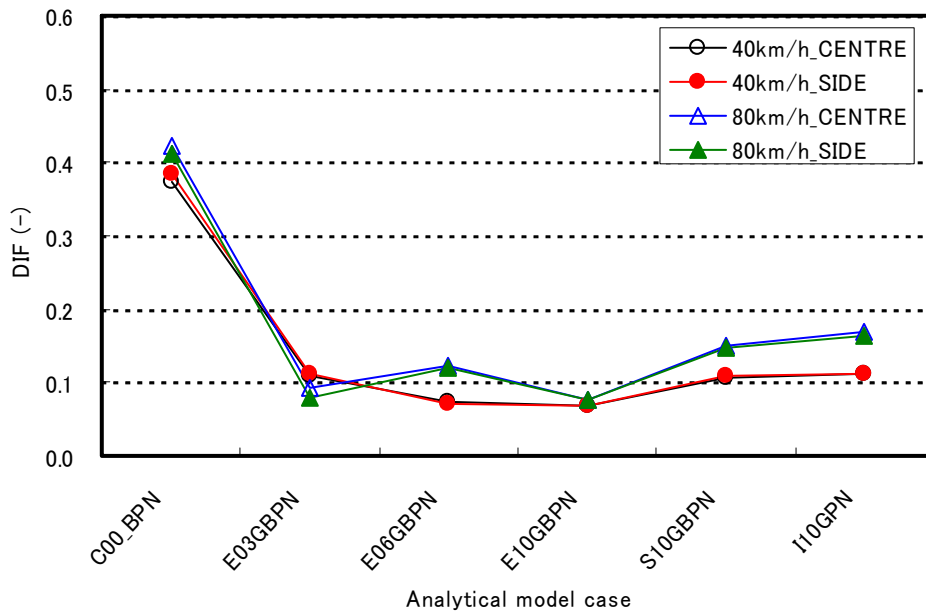


Fig. 6.25(B-1): Dynamic increment factor of pile foundation models (Normal concrete models)

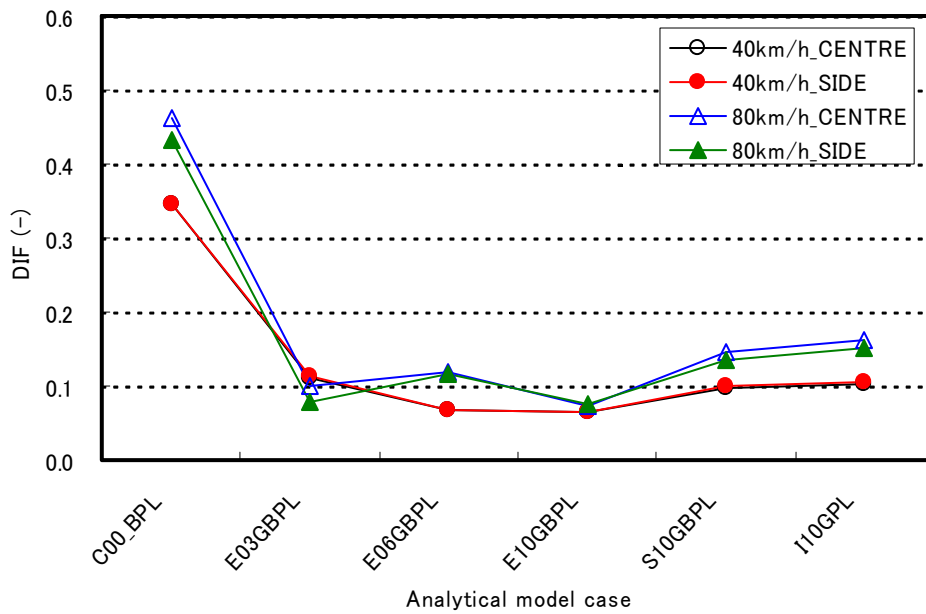


Fig. 6.25(B-2): Dynamic increment factor of pile foundation models (HLAC models)

Fig. 6.25: Dynamic increment factors of normal concrete models and HLAC models

6.4.5 Conclusion

The studies on the application of HLAC for integral bridges are comprehensively performed on basic material properties, confining effect of reinforce concrete column and vibrational serviceability. Summarised Conclusion is as follows.

(1) Basic Material Properties

- The static elastic modulus of HLAC showed around 70 % value of normal concrete.
- The creep coefficient of HLAC was *ca.* 65 % of those of the normal concrete estimated by MC-90.
- The description to allow assuming the creep coefficient of HLCA as 75 % of normal concrete by JSCE Specification gives conservative value for the estimation of prestressing force loss of prestressed concrete structures and overestimation for deflection.
- The HLA employed in the experimental study is supposed to be suitable for prestressed concrete for the higher elastic modulus and the lower creep coefficient as lightweight aggregate that gives less deflection and prestressing force loss at least considered from the results obtained in the experiments.

(2) Confining Effect

- The post-peak slope of stress-strain curve is significantly improved by increase of confining reinforcement volume ratio, however the contribution for peak stress by confinement is slight.
- Type B confinement rebar layout gives better confining effect for peak stress and ductility (*i.e.* gentle slope of post-peak area of stress-strain curve) than type A layout.
- Unconfined specimens showed inductile failure with significant decline of compressive stress of concrete after peak stress.
- The analytical model proposed in this study makes effectively good fitting with the results of experiment. However, further experimental studies are expected to obtain reliable number of data to evaluate the validity of the proposed analytical model

(3) Vibrational Serviceability

- The type of concrete gives almost no difference for fundamental vibrational behaviour (*i.e.* natural periods, damping, etc.).
- The influence of type of concrete for serviceability for pedestrian is evaluated with RMS of the response velocity. The average increment of RMS of the response velocity of HLAC models is 22 % of normal concrete models.
- The influence of type of concrete showed 44 % increment for infrasound radiation; appropriate structural system should be selected for the control of infrasound.
- The influence of types of concrete is slight for ground vibration.
- Integral model, semi integral model and extended deck model with 10m extension give excellent structural systems for vibrational serviceability in all the aspects; they are excellent structural systems for vibrational control.

As a whole, HLAC has valid properties that are suitable for longer span prestressed concrete structure as follows.

- Lighter unit weight than normal concrete
- Low water absorption
- Higher elastic modulus than conventional lightweight concrete
- Lower creep coefficient than conventional lightweight concrete

The smaller elastic modulus and lighter weight gives more easiness to vibrate by traffic load, however the numerical analysis proved that appropriate selection of structural system as integral bridge can settle the vibrational problems.

Therefore, integral bridge concept including semi integral bridge concept is of good use for further extension of bridge length by lightweight aggregate concrete.

References

- [6-1] YAMAHANA, Y., OTSUKA, H., HOSHI, M., AKIYAMA, H. *A Study on the Application of High Performance Lightweight Concrete for Arch Bridges*, Journal of Structural Engineering, Vol.49-A, Japan Society of Civil Engineers, Tokyo, pp.971-977, Mar. 2003.
- [6-2] AKIYAMA, H., YAMAHANA, Y., FUNAHASHI, M., HAMADA, Y. *A Study on the Creep and Shrinkage of High Performance Lightweight Aggregate Concrete*, Proceedings of the Japan Concrete Institute, Vol.27, Japan Concrete Institute, Tokyo, pp. 1363-1368, June 2005.
- [6-3] YAMAZAKI, M., HIGASHIDA, N., NAKAMURA, H., TAKEMOTO, S. *Design and Construction of APC Box Girder Bridge of High Performance Lightweight Aggregate Concrete - Hokkaido Expressway Shirarika River Bridge -*, Journal of Japan Prestressed Concrete Engineering Association, Vol.44, No.3, Japan Prestressed Concrete Engineering Association, Tokyo, pp.33-40, May 2002.
- [6-4] SAKAKI, T., TANIGUCHI, S., YODA, S., YANAI, S. *Application of Lightweight Aggregate Concrete for Numakunai Bridge*, Concrete Journal, Vol.40, No.2, Japan Concrete Institute, Tokyo, pp.28-37, Mar. 2002.
- [6-5] KOBAYASHI, H., FURUYAMA, S., IWATA, M., GOTO, K., OBA, M. *Design and Construction of the Panel-stayed Bridge using Lightweight Concrete - Sukawa Bridge -*, Bridge and Foundation Engineering, Vol.38, No.6, Kensetsu Tosho, Tokyo, pp.25-32, June 2004.
- [6-6] *Standard Specifications of Concrete - Structural Performance Review -*, Japan Society of Civil Engineers, Tokyo, pp.28-37, Mar. 2002.
- [6-7] *JIS DRAFT of Compressive Creep Test Method of Concrete*, Japan Concrete Institute, Japan Concrete Institute Journal of JCI, Vol.23, No.3, Tokyo, pp.55-56, Mar. 1985.
- [6-8] CEB-FIP MODEL CODE 1990, CEB-FIP, pp.51-58, 1990
- [6-9] *European Standard EN 1992, Eurocode2: Design of Concrete Structures (Final Draft)*, Oct. 2001.
- [6-10] RUSCH, H., JUNGWIRTH, D. (translated by Momoshima, S.) *Berücksichtigung der Einflüsse von Kriechen und Schwinden auf das Verhalten der Tragwerke (Japanese version)*, 1976.
- [6-11] GHALI, A., FAVRE, R., (translated by Kawakami, M., et al.)

Concrete Structures: Stress and Deformations (Japanese version), Gihodo Shuppan, Tokyo, 1994.

- [6-12] *Committee Report of Time Dependent Deformation of Concrete Structures Caused by Creep and Shrinkage*, Committee Report of Japan Concrete Institute, Tokyo, Jul. 2001.
- [6-13] AKIYAMA, H., YAMAHANA, Y., FUNAHASHI, M., HAMADA, Y. *A Study on the Creep and Shrinkage of High Performance Lightweight Aggregate Concrete*, Proceedings of the Japan Concrete Institute, Vol.27, Japan Concrete Institute, Tokyo, pp. 1363-1368, 2005.
- [6-14] AKIYAMA, H., FUKADA, S., KAJIKAWA, Y. *Numerical Study on the Vibrational Serviceability of Flexible Single Span Bridges with Different Structural Systems under Traffic Load*, *Structural Engineering International*, Vol. 17, No.3, International Association for Bridge and Structural Engineering, Zurich, pp. 256-263, Aug. 2007.

Chapter 7 Conclusion

7.1 Conclusion

The fundamentally structural characteristics of integral bridges are comprehensively discussed in this thesis.

Chapter 1 covers the concepts of integral bridge and overall scope of the studies.

Chapter 2 provides states of art of integral bridges in Japan and foreign countries. The findings and summary of the conclusion of the chapter is as follows.

- More than 100m long span integral bridges have been constructed with cement treated soil for abutment backfill in expressway bridges recent years in Japan; multiple span integral bridges are also employed.
- Integral bridge is widely taken as a first choice of bridge form for the bridge under ca. 60m overall length in the U.K. and states and provinces of U.S.A and Canada.
- Integral bridge is focused in European countries, too. The research on integral bridge is keenly conducted in Europe, the U.K. and North America.
- Integral bridges are positively evaluated in the U.K. and North America.

The basic characteristics on static primary loads for integral bridge are discussed in Chapter 3. The characteristics of long single span integral bridge and curved multiple span integral bridge is also discussed. The conclusion is as follows.

- The influence of stiffness of pile foundation upon post tension prestressing efficiency of post tensioning to integral bridge is not prominent. Thus, pile foundation would provide wide feasibility to post tensioned integral bridges in respect of the prestressing efficiency.
- Spread footing is not feasible as post tensioned integral bridge foundation in respect of prestressing efficiency.
- Partially prestressed concrete structure is preferred to be selected to curved integral bridge for its lower constraint stress to fully prestressed concrete structure.

The seismic design toward displacement based design is discussed with case study in Chapter 4. The case study between Japan-U.S.A. (California) design codes and material standards resulted in fairly different confining rebar layouts. In particular, the rebar strain at tensile strength is influential upon the required confining rebar amount. Chapter 5 provides practical simulations to evaluate vibrational serviceability of single span bridges with comparison to four different forms of bridge systems. The following is summarised conclusion.

- Integral bridge and semi-integral bridge shows excellent control against traffic vibration for bridge serviceability for pedestrians, infrasound and ground vibration.
- Extended deck bridge with 10m extension also provides good vibrational control almost to equal to integral and semi-integral bridges.

The application of high performance lightweight aggregate concrete (HLAC) is studied to extend the range of integral bridge by lightweightisation in Chapter 6. The following is summarised conclusion.

- The elastic modulus of HLAC is *ca.* 70% of that of normal concrete.
- Creep coefficient of HLAC is *ca.* 65% of that of normal concrete.
- Novel equation to estimate stress-strain relationship of confined HLAC is proposed that shows effectively good fitting with experiment; however, moreover experimental study is still necessary to obtain sufficiently reliable results for only six specimens were tested.
- The comparison between HLAC and normal concrete bridge is conducted to verify the vibrational serviceability. The types of concrete make little differences to natural frequencies and damping ratios.
- The serviceability of HLAC bridges for pedestrians and infrasound showed lower performance than those of normal concrete. However appropriate selection of structural system, *e.g.* integral bridge, semi-integral bridge and extended deck bridge with 10m extension, gives good control for vibrational serviceability.
- The types of concrete give little differences to ground vibration regardless the types of structural systems.

7.2 Vista

The cost and effort to maintain the infrastructure will increase with the stock accumulation along with ageing society with declining birthrate. In these circumstances, low maintenance structures are highly expected.

Integral bridge solution is applicable to short and middle span bridges at least up to ca. 60 m over all bridge length considering foreign experiences and recent domestic practices. In particular, integral bridge should be considered as an alternative of structural system for short and middle long bridges (at least up to ca. 60 m long) in planning phase.

The study on the vibrational serviceability proved the excellent performance of integral bridge including semi-integral bridge to control the vibration by traffic load. The utilisation of integral bridge system as a countermeasure for vibration by traffic load would also give new frontier in bridge engineering.

7.3 Feature Assignment

The following is expected as feature assignment of integral bridges.

- Long time monitoring of integral bridges are highly expected, since integral bridge applications are limited over recent years in Japan. The monitoring would serve as valuable data to feedback themselves to the integral bridge plan, design, construction and maintenance; it would also enable the extension of the range of integral bridge application.
- The interaction between abutment and backfill soil should be studied with monitoring to grasp the behaviour for cyclic thermal effects under domestic conditions.
- Displacement based design should be established for integral bridge seismic design. In the procedure of displacement based design establishment, code calibration with rebar strain at tensile strength should be conducted to enable the application of various kinds of materials rationally.
- In addition, serviceability limit state in damaged condition after earthquake should be established besides research on structural characteristics of integral bridge itself to secure safety for

bridge users, especially for highway drivers and passengers. It is rational for the limit state to be given in displacement dimension.

- The study on refurbishment of existing simply supported bridge into integral bridge is expected, for it is of good use for bridge retrofiting projects.
- As semi-integral bridge is relatively new concept of bridge system, the research on it is highly expected; for semi-integral bridge is widely applicable form of bridge system than fully integral bridge.

EPILOGUE

Although integral bridge is the simplest structural system without bearing, expansion joint and seismic failsafe device, it has excellent structural characteristics.

- Maintenance friendliness
- Higher redundancy for breaking loads
- Higher redundancy for seismic performance
- Excellent vibrational serviceability

The diffusion and development of integral bridge are highly expected with recognition of above described benefits. In a sense, integral bridge is a form of supreme structural systems. The following passage seems to express the quintessence of structural design.

Il semble que la perfection soit atteinte non quand il n'y a plus rien à ajouter, mais quand il n'y a plus rien à retrancher.

Terre des Hommes (1939)
Antoine de Saint-Exupéry

Perfection is achieved in design, not when there is nothing more to add, but when there is nothing left to take away.

Wind, Sand and Stars (1939)
Antoine de Saint Exupéry

ACKNOWLEDGEMENT

This Dissertation is the fruit of the studies through my professional carrier as a bridge engineer in The Zenitaka Corporation and 3 years study in doctorate program in division of environmental science and engineering of postgraduate school of natural science and technology of Kanazawa University.

The accomplishment greatly owes to the most considerate and pregnant instructions by Prof. Yasuo KAJIKAWA. His great achievement in bridge vibration upon serviceability extended my study toward vibrational serviceability of bridges and resulted in the paper of the journal of IABSE - Structural Engineering International.

The author would like to pay my best respect to Prof. Hisanori OOTSUKA in Kyushu University for the long time interview for the review of the dissertation and courteous advices in spite of his busy schedule.

The author sincerely thanks Dr. Saiji FUKADA for his great contribution to the numerical study on the vibrational serviceability of various types of bridges and valuable discussions.

The tender discussions and instructions on materials and structural design of bridges by Prof. Kazuyuki TORII and Prof. Hiroshi MASUYA are greatly acknowledged.

The generous gifts of photographs by Mr. Takashi OOURA and Mr. Mitsuhiro TOKUNO were essentially to my dissertation; they made me pay great thanks and respect to them.

The author sincerely expresses the most cordial gratitude to Mr. Kazuyoshi ZENITAKA, the president of The Zenitaka Corporation, for the favour and grant to my doctoral research program.

Helps, advices and understanding given to my study by Dr. Yutaka YAMAHANA, Dr. Kazuyuki MIZUTORI and colleagues are also largely acknowledged.

The author cannot thank enough for the continuing encouragement and interest by Dr. Masahiko HARADA, Dr. Meguru TSUNOMOTO and Dr. Yoshihiro TACHIBANA who are the seniors of the laboratory in Kanazawa University. Among the contents of the dissertation, the fruit on vibrational serviceability of bridges is ripened by the greatest achievement of the studies upon the field of Kanazawa University accomplished by Prof. KAJIKAWA, Dr. FUKADA and numerous people concerned with the research.

It has been my great pleasure and honour to have been engaged in the study and practical engineering with above estimable people.

Finally, the author would like to dedicate the dissertation to my family and the memory of my grand mother to express my most cordial gratitude from all my heart.